GENETIC AND PHYSICAL MAPPING OF THE RAT *AGU* LOCUS

Nicola Jane Craig

Institute of Biomedical and Life Sciences

Division of Molecular Genetics

University of Glasgow

April 1998

For John

With Love Always

Preface

The work presented in this thesis was entirely my own work, except as acknowledged. I declare that this thesis is not substantially the same as any that I have submitted for any other degree at any other University. I also state that no part of this thesis has already been or is currently being submitted for any other degree or qualification.

Nicola J. Craig
April, 1998

Acknowledgements

I would like to thank Dr. R. G. Sutcliffe and Professor R. W. Davies for allowing me to carry out this work in both of their laboratories and for there advice given on writing a thesis. I would also like to thank Mary Gardiner, Lynn Loughlin and Irene Houghton for the excellent technical support I received during my PhD.

I am eternally grateful to Dr. T.A. Glencorse (Dora) for all her help and advice given freely about research and the writing of this thesis.

I indebted to the all members of Team Scotland who supported me throughout my PhD and made New Orleans a great memory. Especially to Brett and Lynn for keeping me company through all those "Miller Nights", which kept me sane. Thanks also to all the members of Waynes World for advice and support.

I would also like to express my deepest gratitude to Mum and Dad who have supported me without question through all my years at University.

My biggest thanks must go to John, without whom I couldn't have made it through the last three years. You were always there when I needed you and have been a constant source of support, hope and affection. You have always believed in me, even when I doubted myself and I will always be grateful.

Table of Contents

List of Figures

List of Tables

Abbreviations

AS	Albino Swiss
bp	base pair
cDNA	Complementary Deoxyribonucleic Acid
CHEF	contour-clamped homogenous field electrophoresis
CNS	Central Nervous System
cM	centimorgan
BAC	bacterial artificial chromosome
BN	Brown Norway
DA	dopamine
DNA	Deoxyribonucleic Acid
DOPAC	3,4 - dihydroxyphenylacetic acid
HVA	homovanillic acid
kb	kilobase pair
MAO	monoamine oxidase
Mb	mega base
MGD	Mouse Genome Database
MPTP	1-methyl - 4 - phenyl-1,2,3,6 - tetrahydropyridine
NSF	*N*-ethylmaleimide-sensitive ATPase
PAC	P1-artificial chromosome
PCR	Polymerase Chain Reaction
PD	Parkinson's disease
PNK	Polynucleotide kinase
RNA	Ribonucleic Acid
SSCP	Single Strand Conformation Polymorphism
SSLP	Simple Sequence Length Polymorphism
SSR	Simple Sequence Repeat
SN	substantia nigra
SNpc	substantia nigra pars compacta
SV	synaptic vesicle
Sxtb2	Syntaxin binding protein 2
3'UTR	3' Untranslated Region
VMAT	vesicular monamine transporter
YAC	Yeast Artificial Chromosome

Summary

Rats homozygous for a mutation in the *agu* gene display reduced ability to initiate movement and slow movement. The phenotype of these rats is of particular interest as they display the closest available non-human phenotype to Parkinson's Disease and other neurodegenerative diseases. The rats show rigidity of the hindlimbs resulting in a staggering gait and a tendency to fall over every few steps. The major characteristic of the disorder, which is progressive, is difficulty in initiating movement. The mutation leading to this phenotype is a recessive mutation in single autosomal gene, and displays full penetrance in backcross progeny. AS/AGU rats have a 30-35% reduction of neostriatal dopamine when compared to control AS rats. These animals respond well to L-Dopa treatment. This thesis presents progress towards the positional cloning of the *agu* gene. Since few informative markers were available in the region where *agu* is found to map in rat, new microsatellite markers were isolated from P1 clones identified to contain rat genes from the interval or from regions of synteny in mouse and man. These novel microsatellite markers were used to refine the genetic interval containing *agu*. The 3' UTR of rat genes mapped to the interval containing the *agu* locus were also investigated for SSCPs. Microsatellite markers from the region of synteny in mouse were also investigated for strain differences between the rat strains used, to allow mapping. Novel markers identified from the P1 clones were used in conjunction with published markers to position the *agu* gene within a region of approximately 10 cM. A marker was identified which maps less than 0.1 cM from the *agu* locus. This marker was identified within the 3' UTR of a rat gene and was used in a screen of rat genomic P1 and YAC libraries. Another probe designed to the 5' UTR of this gene was also used in a screen of a rat PAC library. One P1 clone, seven YAC and three PAC clones were isolated in this initial screen using the closest marker. The cloned end sequences of one of these PACs were then used in a further screen of the PAC library, resulting in seven PAC clones. All of these clones have been used to establish a genomic contig spanning at least 750 kb, thought to contain the *agu* gene.

Chapter 1

Introduction

1.1 Introduction

In this thesis I present work that has resulted in the definition and cloning of a region of the rat genome less than 1 Mb in length, that is very likely to contain the *agu* gene. Rats homozygous for a mutation in this gene have an interesting phenotype, with similarities to human Parkinson's disease (PD). These rats display reduced ability to initiate movement and slow movement. They also display rigidity of the hindlimbs resulting in a staggering gait and a tendency to fall over every few steps. This interesting mutation could prove useful in the investigation of human Parkinson's disease and other neurodegenerative disorders and the identification of the mutation is vital.

1.2 Parkinson's disease

Parkinson's disease (PD) was first described in 1817 by James Parkinson in *An Essay on the Shaking Palsy* and to date the primary cause or causes of this debilitating disorder remains an enigma. PD affects one in 500 of the population in general and while the incidence is lower than that of other neurodegenerative diseases, such as Alzheimer's disease, it remains an illness of socio-economic importance (Jenner, 1992). In the UK, PD afflicts 100,000 individuals; it usually strikes in mid- to late life and has a duration which varies from 5-40 years. Parkinson's disease is characterised by three classical symptoms; muscle rigidity, movement disorders (akinesia and bradykinesia) and gait abnormality. The primary pathology of the disorder is the degeneration of pigmented dopamine-containing cells within the zona compacta of the substantia nigra, although many other neuronal systems in the brain are also affected. Cell death is accompanied by the appearance of eosinophilic inclusions termed "Lewy bodies". While dopamine replacement therapy with L-Dopa or dopamine agonist drugs is initially effective in relieving the symptoms of PD in the early stages of the illness, there is, at present, no means of preventing the progression of pathology There is no cure for PD and the underlying cause of neuronal death remains unknown.

1.2.1 Pathology of the nervous system in PD.

All cases of PD show moderately severe cell loss in the substantia nigra pars compacta associated with Lewy bodies in a portion of the remaining cells. Lewy bodies are intracellular cytoplasmic inclusions which are mostly eosinophilic. Lewy bodies always signify neuronal degeneration, and nerve cell loss in PD does not occur without them being found in some of the degenerating nerve cells. They appear at an early stage of the process, and because of their distinctive appearance, they can be readily found before significant cell loss is apparent (Gibb, 1992). The classical appearance of a Lewy body is

of one or several spherical bodies with a dense core and a peripheral halo in the cytoplasm of a pigmented nerve cell (Forno, 1996).

Lewy bodies are not unique to PD, but are seen in a wide variety of other neurodegenerative disorders e.g. Alzheimer's disease. This suggests that Lewy bodies might simply be a final common pathway in the neurodegenerative process. They are so characteristic of PD, however, that they may provide an insight into the pathogenesis of the disease.

The tight link between Lewy bodies and nerve cell degeneration means that their distribution in the nervous system maps out the territories involved in the degeneration. In addition to the substantia nigra, these sites are the locus coeruleus, ventral tegmental area, nucleus basalis of Meynert, raphe nuclei, thalamus, cerebral cortex, and the entire autonomic nervous system. All of these areas appear to be affected shortly after the onset of the disease process, and spread of Lewy bodies does not occur in new areas (Gibb, 1992). As a rule, Lewy bodies are located in the cytoplasm of neurons in the substantia nigra, the locus coeruleus, the raphe nuclei and the cerebral cortex, and as elongated forms in nerve cell processes in the nucleus basalis of Meynert, the hypothalamic dorsal motor nucleus of the vagus and autonomic ganglia, but both forms can be found in any of these anatomical areas (Forno, 1996).

In most cases of PD, the inclusions are numerous, easy to find and are usually present in one unilateral 7-μm section cut horizontally through the midbrain. The most important element which all Lewy bodies have in common is the filamentous cytoskeletal component, now considered to consist of neurofilaments which have undergone a number of alterations, including phosphorylation, ubiquitination, proteolysis, and cross-linking (Pollanen *et.al.*, 1992). The exact mechanism leading to the formation of the Lewy body is unknown, but it is thought that they are formed in three over-lapping steps involving self-assembly and aggregation of protein, followed by posttranslational phosphorylation and, last, ubiquitination. Proteolysis is felt to be the last step. They are not known to contain abnormal proteins, as in the paired-helical filament of the Alzheimer tangle, and consequently they may result simply from the structural degradation of abnormal accumulations of the cytoskeleton. These accumulations could reflect deranged energy-dependent processes responsible for the normal transport of the cytoskeleton within the neurone. The Lewy body also contains neuromelanin, lipofuscin, mitochondria, dense core vesicles, and other organelles as well as electron dense granular or amorphous material, as observed by electron microscopy (EM) (Forno, 1996).

A second type of nerve cell inclusion seen in PD is the pale body. It often lies close by or contiguous with the Lewy body and is restricted to the substantia nigra and locus

coeruleus. It has a featureless ultrastructure comprising a mixed loose accumulation of granules, vesicles, and sparse filaments.

In Parkinson's disease (PD) neuronal loss within the substantia nigra shows a characteristic pattern with preferential degeneration of lightly melanised cells forming a ventral tier of the pars compacta and relative preservation of heavily melanised cells forming a dorsal tier, a marked difference to that seen in normal ageing (Gibb, 1992). The anatomical and functional significance of this division of the pars compacta is unknown.

1.2.2 Dopamine and Parkinson's Disease.

Parkinson's disease (PD) is an age-related disease, the primary cause of which is the degeneration of dopamine producing neurons within the substantia nigra pars compacta (SNpc) of the basal ganglia, giving rise to the characteristic disruption of normal movement. Since the discovery in 1960 that the primary neurotransmitter loss in PD was dopamine and the region of the brain most affected the substantia nigra, much research has been focused on the production and metabolism of dopamine and it's role in the function of the normal brain.

Synthesis of dopamine.

Tyrosine is usually considered to be the starting point in the biosynthesis of dopamine and this amino acid is abundant in dietary proteins. Blood-borne tyrosine is taken up into the brain by a low-affinity amino acid transport system and subsequently from brain extracellular fluid into dopaminergic neurons by high- and low-affinity amino acid transporters. Once tyrosine has entered the neuron, it's conversion to dihydroxyphenylalanine (L-Dopa), driven by the cytosolic enzyme tyrosine hydroxylase, is normally the rate-limiting step in dopamine biosynthesis (Figure 1.1).

Tyrosine availability does not influence the rate of tyrosine hydroxylation *in vivo* under normal conditions (Elsworth and Roth, 1997). Short-term activation of tyrosine hydroxylase involves feedback inhibition, phosphorylation of the regulatory domain by protein kinases and possibly also alternate splicing. For example, in man the single tyrosine hydroxylase gene generates four different mRNA species through alternative splicing events, TH-1 and TH-2 being the predominant forms in the locus coeruleus and the substantia nigra. An additional residue in TH-2 for phosphorylation, generated through alternative splicing, leads to an increase in enzyme activity by giving rise to an increase in its affinity for the cofactor (Le Bourdellès *et.al.*, 1991). The activated form of tyrosine hydroxylase is thought to have a lower Km for its cofactor, and a higher Ki for dopamine, which effectively reduces end-product inhibition. In primates, rodents and

Drosophila, multiple tyrosine hydroxylase mRNAs are produced through alternative mRNA splicing from a single primary transcript, and it has been speculated that different isoforms of TH may occur in different brain regions or be expressed differentially during development (Lanièce *et.al.*, 1996).

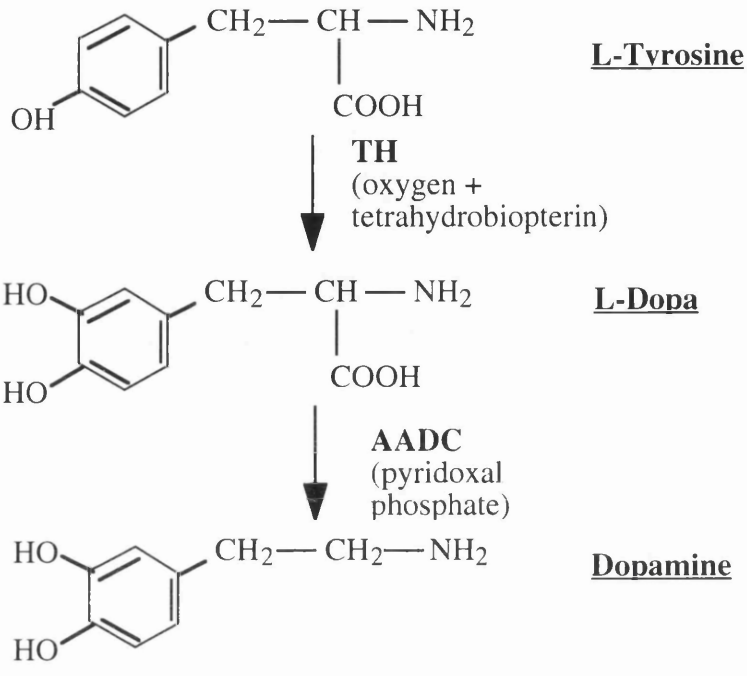

Figure 1.1 The production of dopamine from tyrosine within the dopaminergic neuron. Adapted from Elsworth and Roth, 1997. TH=tyrosine hydroxylase, AADC=dopa decarboxylase. The enzyme cofactors are shown in brackets below each enzyme.

Aromatic amino acid decarboxylase (AADC, dopa decarboxylase) is the enzyme responsible for the cytosolic conversion of L-Dopa to dopamine. This enzyme so avidly decarboxylates L-Dopa that the levels of this amino acid in brain are very low under normal conditions (Elsworth and Roth, 1997).

Storage

In dopaminergic neurons, dopamine is transported from the cytoplasm into specialised storage vesicles. This is carried out by the vesicular monoamine transporter (VMAT) , which differs from the plasma membrane transporter (DAT) located on the outer membrane of the dopamine neuron and transports dopamine in an ATP-dependent and H^+-driven manner. It appears that many of these vesicles are transported empty down the axon, gradually filling with neurotransmitter on their journey, as demonstrated by nerve ligature (Bradford, 1986). These particles accumulate on the proximal side of the ligature.

Release

Upon arrival of an action potential, a change in membrane protein conformation allows the influx of calcium ions, which is a key part of the stimulus responsible for the fusion of vesicles with the neuronal membrane. By the process of exocytosis, the vesicles discharge their soluble contents into the synapse. Exocytosis is a carefully controlled and complicated process. The exocytosis/release of dopamine, or indeed any neurotransmitter, involves at least four key steps (Südhof, 1995) (Figure 1.2) :

1) Docking. Synaptic vesicles (SV) that are filled with neurotransmitter are predocked at a specialised area of the presynaptic membrane called the active zone. Docking is defined as the initial contact between the SV and the presynaptic membrane and occurs only at the active zone opposite to the synaptic cleft, indicating a targeting process.

2) Priming. After docking, SVs go through a maturation process that makes them competent for fast Ca^{2+}-triggered membrane fusion. Such a priming step is suggested by three observations: first, the speed of Ca^{2+}-triggered SV exocytosis occurs too fast for a complex multistep reaction; second, most of the docked SVs cannot be triggered to fuse by Ca^{2+} immediately and therefore appear to be not yet competent to fuse (Rastaad *et.al.*, 1992; Hessier *et.al.*, 1993 and Rosenmund *et.al.*, 1993); and third, during extensive repetitive stimulation, SV exocytosis slows down before the number of docked SVs declines. These results suggest that docking is not rate limiting and that SVs are not immediately competent to fuse after docking and need to go through a rate-limiting priming step. Priming may initiate exocytosis by executing a partial fusion process. At this point SVs arrest, awaiting a Ca^{2+} signal.

3) Fusion/Exocytosis. Primed SVs are stimulated for rapid fusion/exocytosis by a Ca^{2+} spike during an action potential.

4) Endocytosis. Empty SV membranes are rapidly internalised, probably by way of clathrin-coated pits which become coated vesicles.

As anticipated for a highly regulated, multistep pathway, the concerted action of a large number of gene products is required for neurosecretion. Mutated forms of these proteins are being studied in model organisms such as *Drosophila*, *C. elegans* and mouse, all of which allow the thorough investigation of the mutant phenotype. Some examples of these proteins are given in Table 1.1. A short example is then given of some of these proteins and the evidence for their action.

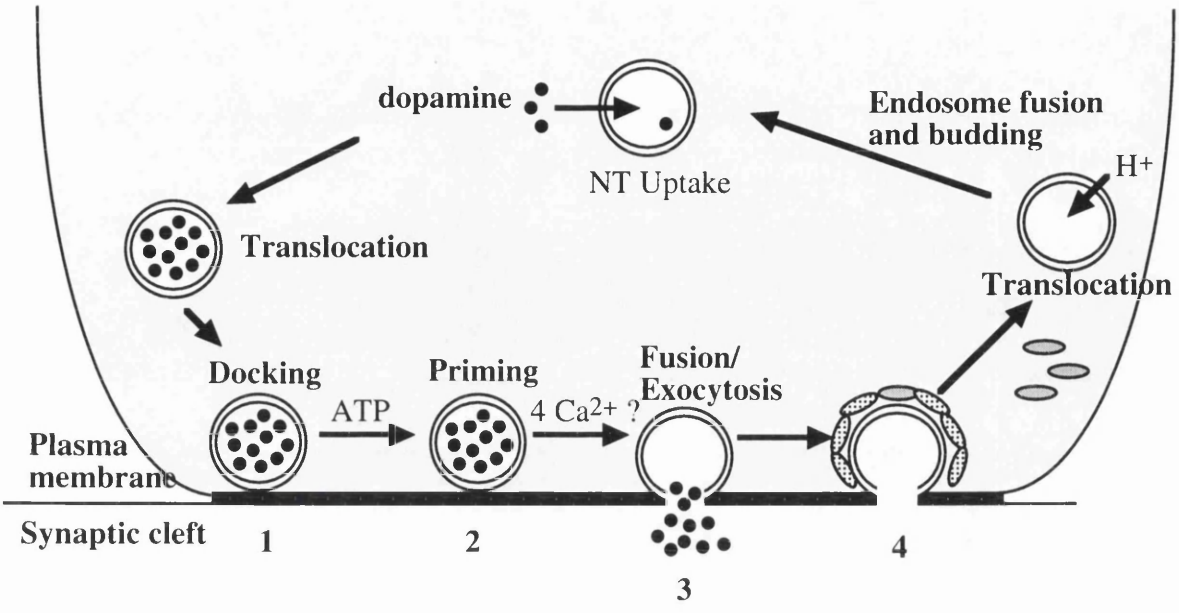

- Dopamine molecule
- Clathrin molecule on coated pit.

Figure 1.2 The synaptic vesicle cycle in the presynaptic nerve terminal. Adapted from (Sudhof, 1995). The four stages of vesicle exocytosis are described in Section 1.1.3 - dopamine release.

Vesicle movement control.	Priming.	Late stages prior to fusion.	Uncharacterised roles/sites of action.
kinesins,myosin II,synapsins,rab3s,rabphillin,actin.	phosphotidylinositol transfer proteins (PEP3), NSF's, α/β/γ-SNAP.	synaptobrevins, CAPS, SNAP-25s,synaptotagmins syntaxins	annexins,neurexins, Rab3s,rabphillin, RabGDI,,GAP-43 VAP33,rop.

Table 1.1 Examples of proteins identified to be involved in synaptic vesicle release. The proteins are grouped by the stage at which they are thought to act in exocytosis.

Results from biochemical and genetic studies allows formulation of a model which although, incomplete, may approximate the molecular events in synaptic vesicle exocytosis. According to this model, SVs dock and then proceed through a partial fusion reaction, priming, to make them competent for the final Ca^{2+}-triggered step. During priming, a complex called the core complex is assembled by three abundant synaptic proteins, two from the plasma membrane (syntaxin and SNAP-25) and one from the SV (synaptobrevin). The core complex forms the anchor for a cascade of protein-protein interactions required for exocytosis to occur.

Syntaxin and SNAP-25 bind tightly to each other and form a high-affinity binding site for synaptobrevin. Under steady-state conditions, most syntaxin, synaptobrevin and SNAP-25 in the nerve terminal are not assembled together. Synaptobrevin is largely bound to synaptophysin, another SV protein. At least some of the syntaxin is bound to munc 18 over the entire plasma membrane. Syntaxin binding protein 2 (Sxtb2) is the mammalian homologue of the proteins encoded by the *C.elegans unc-18* and the *Drosophila* rop genes, mutations in which lead to severe synaptic defects, suggesting an essential function in SV exocytosis. One of the functions of the Sxtb2/syntaxin and the synaptophysin/synaptobrevin interactions may be to inhibit the formation of the synaptic core complex which would otherwise assemble spontaneously and indiscriminately outside the active zone (Südhof, 1995). Binding of Sxtb2 to syntaxin inhibits its interaction with SNAP-25, and the interaction of synaptophysin with synaptobrevin is incompatible with the binding of synaptobrevin to the SNAP-25/syntaxin complex. This suggests that synaptophysin and Sxtb2 have to dissociate from synaptobrevin and syntaxin, respectively, before the core complex can assemble.

After SV docking, Sxtb2 probably dissociates from syntaxin, and synaptophysin from synaptobrevin, this allows assembly of the synaptic core complex. Sxtb2 may collaborate

with rab3 and/or other rab proteins to ensure that the synaptic core complex is assembled only at the active zone (Südhof, 1995). Once the trimeric core complex has assembled, it serves as a receptor for SNAP and NSF. NSF is a *N*-ethylmaleimide-sensitive ATPase with a universal function in membrane fusion. α-, β-, and γ-SNAPs are soluble NSF-attachment proteins that are not related to SNAP-25. Synaptobrevin, syntaxin and SNAP-25 were affinity purified on immobilised α-SNAP, but individually bind only weakly to α-SNAP. Only their assembly into the core complex results in the formation of a high-affinity binding site for α-SNAP which in turn creates a receptor site for NSF. As a trimer, NSF then probably multermerises core complexes and disrupts them under ATP hydrolysis. Thus an ordered sequence of protein-protein interactions leads to the assembly of a multimeric complex that is then disrupted by the enzymatic activity of NSF (Südhof, 1995).

Synaptotagmins

SVs are docked close to Ca^{2+} channels at the active zone. This arrangement facilitates rapid exocytosis by high local concentrations of Ca^{2+} during an action potential. However, signal transduction leading to exocytosis is inefficient. To trigger the final stage of the fusion reaction, a Ca^{2+} sensor is required at the site of exocytosis. This sensor must bind Ca^{2+} co-operatively and undergo a Ca^{2+}-dependent conformational change. If this Ca^{2+} sensor could be identified, it would give the first mechanistic clue to the regulation of the fusion reaction. Five lines of evidence suggest that synaptotagmins function as such sensors in the final fusion step. 1) Biochemically, synaptotagmins are SV proteins that bind Ca^{2+} co-operatively and undergo a Ca^{2+}-dependant conformational change. 2) In synaptotagmin-I knockout mice, Ca^{2+}-dependent neurotransmitter release is severely impaired. The fast, synchronous component of Ca^{2+}-triggered release is inhibited, but the slow, asynchronous component is unimpaired. 3) In the synaptotagmin-I knockouts, release can still be triggered normally by agents that act by Ca^{2+}-independent mechanisms, such as hypertonic sucrose or α-latrotoxin. However, in nerve terminals poisoned by tetanus and botulinum A toxins, the response to hypertonic sucrose is blocked. This suggests that synaptotagmin I acts after the core complex that is inhibited by these toxins. 4) In squid nerve terminals injected with synaptotagmin peptides, release is inhibited and SVs accumulate at the active zone. This presumably results from competition by the peptides for synaptotagmin effectors. 5) Synaptotagmin mutants in *Drosophila* show a severe but incomplete block of neurotransmission with an altered Ca^{2+} dependence in some mutants. Similar changes are also observed with manipulations of synaptic transmission that are unrelated to the Ca^{2+} sensor, making an interpretation of such changes difficult.

Re-uptake

Dopaminergic terminals possess Na^+/Cl^--dependent transporter molecules (the dopamine transporter: DAT) that are critical in terminating transmitter action and in maintaining transmitter homeostasis (Lesch *et.al.*, 1997). Under normal conditions, the transporter recycles dopamine that has been released into the synaptic cleft by actively pumping extracellular dopamine back into the nerve terminal. After its retrieval dopamine is either repackaged into synaptic vesicles or metabolised by mitochondria-associated monoamine oxidase (MAO) (Lesch *et.al.*, 1997).

Vesicular and plasma membrane uptake of dopamine both play important roles in the neurotoxicity of 1-methyl-4-phenyl-1,2,3,6-tetrahydropyridine (MPTP), a drug that produces parkinsonism by inducing damage to dopaminergic nigrostriatal neurones (Langston *et.al.*, 1983). While the vesicular uptake mechanism (through VMAT) can protect the cell from MPTP-induced toxicity, by sequestering the toxic species, MPP^+, in vesicles, uptake of MPP^+ by the plasma membrane uptake mechanism (through DAT) is actually a necessary step in the toxicity of MPTP. It is the relative expression of these transporters which make substantia nigra neurons more susceptible to MPTP toxicity.

Metabolism

The main pathways involved in dopamine metabolism are shown in Figure 1.3. As the relative abundance and activity of the enzymes vary according to the cell type, brain region, and species examined, these factors determine the relative concentration of a particular metabolite present in a given situation. The principal locations of these metabolising enzymes are given in Table 1.2 and it appears that it is possible for 3,4-dihydroxyphenylacetic acid (DOPAC) to be formed either intraneuronally or extraneuronally with respect to the dopamine terminal, whereas, because of the location of catechol-*O*-methyltransferase (COMT), homovanillic acid (HVA) is formed extraneuronally. In brain, dopamine is metabolised mainly to acidic (DOPAC, HVA) metabolites, with less formation of alcoholic metabolites (DOPET, MOPET). The major end product of dopamine metabolism in primate brain is unconjugated homovanillic acid (HVA), whereas in rat brain it is DOPAC, and a significant proportion of DOPAC in the rat brain is sulfate-conjugated. DOPAC sulfate is not a substrate for monoamine oxidase (MAO) or COMT, so that, once formed, it cannot be further metabolised by these enzymes (Elsworth and Roth, 1997).

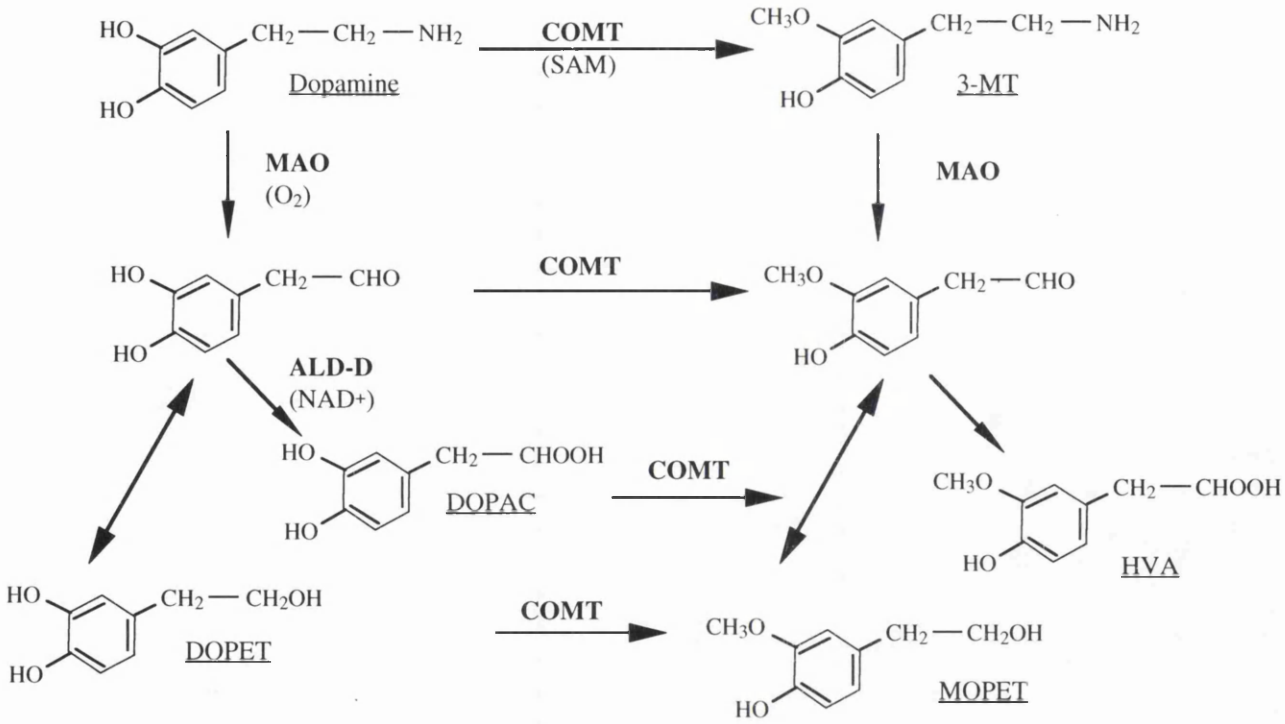

Figure 1.3 The principal pathways involved in dopamine metabolism.

The enzymes involved are MAO = monoamine oxidase, COMT = catechol-*O*-methyltransferase, ALD-D = aldehyde dehdrogenase, ALR = aldehyde reductase, ADH = alcohol dehydrogenase. The metabolites are 3-MT = 3-methoxytryamine, DOPAC = 3,4-dihydroxyphenylacetic acid, HVA = homovanillic acid, DOPET = 3,4-dihydroxyphenyethanol and MOPET = 3-methoxy-4-hydroxyphenylethanol. The figure was adapted from Elsworth and Roth, 1997.

Enzyme	Subtype	Cellular location	Subcellular location
MAO	A	Dopamine and norepinephrine neurons	Mitochondria
MAO	B	Glia, serotonin neurons	Mitochondria
COMT	high Km	Glia	Soluble
COMT	low Km	Postsynaptic to dopamine neuron	Membrane bound
PST	M	Postsynaptic to dopamine neuron	Cytosolic

Table 1.2 Location of the major dopamine metabolising enzymes in the striatum. For abbreviations see text. Table taken from Elsworth and Roth, 1997.

Autoreceptors

A receptor which is sensitive to the transmitter that is secreted from the neuron on which the receptor is located is referred to as an autoreceptor. Activation of autoreceptors by released dopamine is thought to be one of the principal mechanisms responsible for regulation of dopaminergic neuronal function. Autoreceptors are present on the nerve terminals of dopamine neurons. Stimulation of dopamine autoreceptors in the nerve terminals results in an inhibition of dopamine synthesis and/or release (release- and synthesis-regulating autoreceptors). Thus, nerve terminal autoreceptors work to exert feedback regulatory effects on dopaminergic transmission. In general, all dopamine autoreceptors can be classified as D_2-like dopamine receptors. Dopamine autoreceptors are more sensitive to the effects of dopamine than postsynaptic dopamine receptors (Elsworth and Roth, 1997).

Postsynaptic Receptors

There are now known to be at least six different forms of the dopamine receptor. The D_1 class of dopamine receptor has been divided into D_1 and D_5 receptor subtypes, and the D_2 class comprises D_{2short} and D_{2long}, D_3 and D_4 receptor subtypes. When activated, the D_1-like receptor subtypes stimulate adenylate cyclase activity, whereas the D_2-like receptor subtypes inhibit adenylate cyclase activity. The pharmacological profile and regional distribution in the brain of each subtype is different, with the exception of D_{2short} and D_{2long}, which appear identical in these respects (Seeman and Vantol, 1994).

It is now established that D_1 and D_2 dopamine receptors act synergistically in the expression of certain behaviours and in certain electrophysiological and biochemical models. It appears that striatal D_1 receptors are principally located on the striatonigral

projecting neurones ("direct pathway"), while D_2 receptors are mainly located on striatopallidal neurones ("indirect pathway").

1.2.3 The action of dopamine in the basal ganglia.

While there is heterogeneity of dopamine loss within the nigrostriatal dopamine system, overt parkinsonism does not present until approximately 80% of dopamine loss has occurred. The basal ganglia appear to be able to suffer this loss because there is normally a large reserve of nigrostriatal dopamine neurons, which may be linked to the natural age-related loss of these neurons and/or the apparent susceptibility of nigrostriatal dopamine neurons to damage from various insults. However, surviving nigrostriatal dopamine neurons mount a compensatory response by increasing the rate of synthesis and release of dopamine.

Akinesia and slowed movement execution (bradykinesia) are the principal symptoms of PD. These motor deficits of PD result from dysfunction of the nigrostriatal dopaminergic pathway within the basal ganglia. The basal ganglia are several closely grouped neuronal nuclei situated below and on each side of the cerebral cortex; and they are concerned with movement control (Bradford, 1986). They include the neostriatum, consisting of the caudate nucleus and putamen, the two shells of the globus pallidus and the subthalamic nucleus. The substantia nigra, although more caudal in position and situated in the region of the brain stem, is included as a basal ganglion structure because of its close functional and anatomical relationships with the neostriatum. The pars compacta of the inner substantia nigra consists largely of dopamine-containing cell bodies whose dendrites penetrate into the outer, pars reticulata, layer of this nucleus (Bradford, 1986).

A working model of the functional organisation of the basal ganglia is based on the concept of disinhibitory mechanisms regulating the GABAergic output neurons of the basal ganglia (Figure 1.4). According this scheme, SNR (i.e. Gpi) neurons are tonically active, providing a tonic inhibition to their target areas in the thalamus, superior colliculus, and pedunculopontine nucleus. Cortical activity results in activity in the striatonigral pathway, which is inhibitory and results in phasic pauses in the output of nigral neurons. That such disinhibition is responsible for specific movements was elegantly demonstrated by Hikosaka and Wurtz (1983), who demonstrated that phasic pauses in nigral neurons are directly correlated with eye movements, generated by activity in the superior colliculus. Similar findings are reported for activity of the internal segment of the globus pallidus in primates related to arm movements. Here the disinhibitory mechanisms are suggested to modulated thalamocortical feedback loops to premotor and motor cortical areas. The basal ganglia thus appear to affect motor behaviour by way of cortically generated activity of

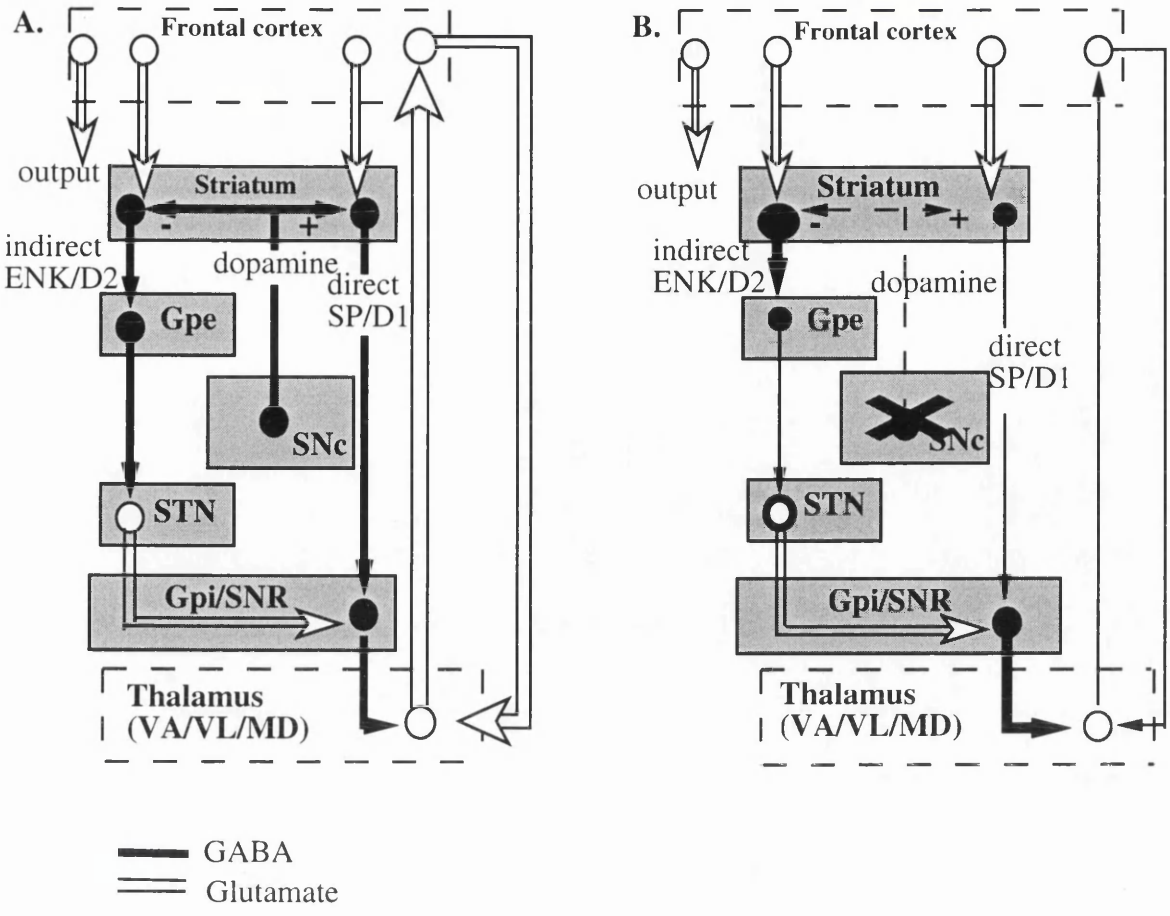

Figure 1.4 Schematic representation of the main connections in a basal ganglia-thalamocortical circuit. **A**. Normal status: The two output routes ("indirect" and "direct") are in balance at the level of the output structures. **B**. Presumed disturbances in Parkinson's disease: Depletion of dopamine in the striatum leads to an imbalance in the two output routes and a suppresion of thalamocortical activity. The large black cross indicates the depletion of the dopamine neurons in the substantia nigra.

ENK = enkephalin, GP = globus pallidus, GPE = external segment of GP, GPI = internal segement of the GP, MD = mediodorsal thalamic nucleus, SNR = pars reticulata of the substantia nigra, SNC = pars compacta of the substantia nigra, SP = substance P, STN = subthalamic nucleus, VA/VL = ventral anterial/ventral lateral thalamic nuclei.

striatal output pathways that regulate the activity of neurons in the substantia nigra (and the internal segment of the globus pallidus) (Gerfen and Engber, 1992).

There are two major output pathways from the striatum, the direct and the indirect, which are responsible for smooth and well co-ordinated movement. The two pathways, which converge in the internal segment of the globus pallidus and in the substantia nigra, have opposing effects: the direct pathway causes disinhibition of the thalamocortical neurons while the indirect pathway causes inhibition of these neurons. Since the glutamatergic thalamocortical neurons facilitate the stimulation of movement via the cortex, the net result of the indirect pathway is to reduce movement while the direct pathway increases it (Gerfen, 1992).

The pars compacta of the substantia nigra (SN_{pc}) projects to the striatum (caudate putamen) using dopamine as a neurotransmitter. At least two dopaminergic receptor types exist within the striatum that respond differently when presented with dopamine. Striatal neurons projecting directly to the internal segment of the globus pallidus (Gpi) contain receptors (D_1 type) that cause net excitation (the "direct" pathway), and striatal neurons projecting to the external segment of the globus pallidus (Gpe) contain receptors (D_2 type) that cause net inhibition when dopamine is present the "indirect pathway"). Activation of the direct pathway results in inhibition of Gpi, whereas activation of the indirect pathway leads to excitation of the Gpi. The Gpi is the major outflow structure of the basal ganglia related to movement control, and it exerts tonic inhibitory influence on the thalamus (Watts *et.al.*, 1992).

Depletion of dopamine in the striatum results in increased activity of the striatopallidal pathway and decreased activity in the striatonigral pathway (Figure 1.4). The functional consequence of the alteration in the balance in activity in the striatal output systems that occurs in the dopamine deafferented striatum results from the disinhibition of the subthalamic nucleus, which coupled with decreased activity in the striatonigral pathway results in increased tonic activity of the GABAergic neurons of the output nuclei of the basal ganglia, the substantia nigra , and the internal segment of the globus pallidus (Gerfen and Engber, 1992). The bradykinesia of PD has been suggested to result from an increase in the inhibitory outputs of these nuclei (Albin *et.al.*, 1989).

The striatal neurons of these pathways constitute over 90% of all neurons in the striatum and are characterised by their medium size (a diameter of approximately 10μm) and spiny dendrites. These are the major output neurons of the striatum and although both groups of neurons (i.e. those of the direct and the indirect pathways) release GABA, they can be distinguished by the neuropeptides they express: the striato-Gpe neurons of the indirect

pathway contain enkephalin while the striato-Gpi/nigral neurons of the direct pathway contain substance P and dynorphin. These striatal neurons, which receive massive excitatory inputs from the cortex and thalamus, are controlled by inhibitory feedback from recurrent collatral axons. Other influences on these neurons include dopamine (released from the nigrostriatal neurons that die in PD) and modulators intrinsic to the striatum including acetylcholine (ACh), which is released from a group of striatal interneurons.

1.2.4 Aetiology of PD.

The cause of the degeneration of dopamine-containing cells and the appearance of Lewy bodies in the zona compacta of the substantia nigra in patients with Parkinson's disease remains unknown. At present little can be done to prevent or slow the progression of the pathological changes because the nature of the degenerative process involved also remains unsolved. The theories postulated on the mechanism leading to this disorder are numerous. In the early twentieth century much weight was given to the theory of a causative environmental agent, mainly due to a pandemic of postencephalitic parkinsonism which occurred between 1918 and 1920 and which appeared to indicate a viral cause of the disease. While it is now clear that postencephalitic parkinsonism is different from idiopathic PD, the possibility that the idiopathic disease might have a viral origin has continued to interest researchers right to the present time. Another discovery which indicated an external factor in the cause of PD was the discovery that 1-methyl-4-phenyl-1,2,3,6-tetrahydropyridine (MPTP), a contaminant of a synthetic pethidine analogue sold as a street drug, produced a condition resembling Parkinson's disease (Langston *et.al.*, 1983). The idea that little or no genetic factors contributed to PD was strengthened by a series of twin studies during the 1980's (Duvoisin *et.al.*, 1981; Ward *et.al.*, 1983; Marttila *et.al.*, 1988) that failed to demonstrate increased concordance rates for PD in monozygotic versus dizygotic twins.

However, in recent years there has been a re-emergence of interest in the genetic causes of idiopathic PD. As a result, there is currently much more research investigating the role of hereditary factors and gene-environment interactions in causing PD.

MPTP induced Parkinsonism.

MPTP was shown to cause a selective destruction of nigrostriatal dopaminergic neurons in primates and some other animal species, and this stimulated a great deal of work on the mechanisms involved in its neurotoxic effects and their possible relationships to idiopathic PD. The selective toxicity of 1-methyl-4-phenyl-1,2,3,6-tetrahydropyridine (MPTP) toward nigral dopamine-containing cells in humans (Langston *et.al.*, 1983) provided the first substantial evidence for toxin involvement in Parkinson's disease. The compound

enters the brain where it is converted by the action of the B form of monoamine oxidase (MAO B) to the 1-methyl-4-phenylpyridinium ion (MPP^+), which is the effective neurotoxin (Heikkila *et.al.*, 1984; Javitch *et.al.*, 1985). Since MAO B is not present within dopaminergic neurons but within glia, MPTP must be oxidised to MPP^+ within glia and not within the dopamine neuron, itself. MPP^+ is a substrate for the presynaptic dopamine uptake system (dopamine transporter, DAT) and the toxicity of MPP^+ and MPTP can be prevented by prior administration of inhibitors of presynaptic dopamine uptake. In contrast, MPP^+ is a poorer substrate for the noradrenergic and serotonergic presynaptic uptake carriers and the selectivity of MPTP as a toxin to dopaminergic neurons can be explained by this energy-dependent concentration within these neurons. This local concentration effect is the critical process for toxicity and is enhanced further by the binding of MPP^+ to neuromelanin. Melanised dopaminergic neurones have been shown to be more susceptible to neurodegeneration in PD and MPTP neurotoxicity.

MPP^+ is a potent inhibitor of mitochondrial oxidation of NAD^+-linked substrates. The cessation of respiration brought about by this blockade leads to rapid depletion of ATP and consequent loss of membrane potential, which in turn, leads to nigrostriatal nerve cell death by mechanisms that may involve altered calcium homeostasis, and perhaps, free radical formation (Tipton and Singer, 1993). The inhibition of mitochondrial respiration is the result of a chain of events, starting with the rapid and extensive accumulation of MPP^+ inside the mitochondrial matrix, driven by the electrochemical potential of the membrane. MPP^+ must be concentrated within the mitochondria in order to be effective (Tipton and Singer, 1993), and this accumulation appears not to be mediated by a carrier because the initial rate is non-saturable (Davey *et.al.*, 1992). The concentration within the mitochondria is followed by a gradual penetration of the compound into a hydrophobic binding region. As a consequence, reducing equivalents from NADH dehydrogenase do not reach ubiquinone [coenzyme Q(CoQ)] and, thus, oxidative phosphorylation is halted. Direct intrastriatal injection of the complex I inhibitor rotenone also results in neurotoxicity, demonstrating that the inhibition of mitochondrial NADH oxidation is sufficient, on its own, to cause nigrostriatal cell death.

Because the inhibitory effects of MPP^+ on mitochondria are not organ-specific, affecting that organelle in all mammalian cells, the selective neurotoxic action may be the result of the specific ability of the nigrostriatal dopaminergic nerve terminals to take up MPP^+ and retain it at sufficiently high concentrations to cause neuronal cell death. The selectivity of the toxic effects may be enhanced further by the binding of MPP^+ by neuromelanin associated with the dopaminergic neurons (Tipton and Singer, 1993).

The involvement of MPTP in producing a parkinsonian syndrome lead researchers to believe that there was an environmental toxin which produced PD. However, this toxin

would have to be world wide as the disease shows no localisation to any distinct areas, also recent evidence indicates that there may be some genetic contribution to the risk of PD (see section Genetic factors influencing PD). Such a genetic factor may affect the activity of one or more of the enzymes involved in drug detoxification.

Several lines of evidence have been interpreted as indicating the involvement of an environmental factor in the development of PD, but the data are confusing and often apparently contradictory (Tanner, 1989). The structural resemblance of paraquat to MPTP might suggest an involvement, as it is widely used in agriculture. However, the toxic actions of paraquat are restricted to the periphery, because, like MPP^+, it does not penetrate the brain. Also paraquat is a relatively new chemical, predated by PD. It has been suggested that tetrahydroisoquinoline or its derivatives may be endogenous compounds giving rise to PD by a mechanism similar to MPTP. Several groups have reported tetrahydroisoquinoline and its 1,3-dimethyl derivative induce a condition resembling PD (Booth *et.al.*, 1989; Makowski and Ordonez, 1981). They have been shown be present in human brain caudate and frontal lobe (Makino *et.al.*, 1990) but there were no significant differences between its concentrations in normal and parkinsonian brains.

Oxidative stress and the pathogenesis of PD.

Another current concept of the cause of PD is that dopamine cell death is due to the excessive formation of oxygen radical species. Oxidative stress refers to the cytologic consequences of a mismatch between the production of free radicals (a free radical is any molecular species with an unpaired electron) and the ability of the cell to defend against them. Powerful oxidising agents cause extensive injury and even cell death through multiple mechanisms including damage to nucleic acids, oxidation of proteins and lipid peroxidation. Two types of protective mechanisms are present in cells to combat these changes: cellular antioxidants e.g. tocopherol (vitamin E) and ascorbate (vitamin C), which react with the free radical and stop the chain reaction. Also enzymes such as superoxide dismutase (SOD), glutathione peroxidase and catalase, which catalyse the removal of reactive species. The presence of oxidative stress is indicated by: 1) the loss of reducing substances e.g. tocopherol, ascorbate and glutathione, 2) the decreased activity of protective enzymes e.g. SOD, 3) an altered redox status of cells e.g. an increased ratio of the oxidised compared with the reduced form of glutathione and 4) the appearance of molecular damage e.g. peroxidized lipids, oxidized proteins and damaged DNA.

The idea that PD may involve either an endogenous or an environmental toxin or toxic process has propagated the concept that excessive formation of reactive oxygen species and the onset of oxidative stress are key components of the pathogenesis of PD. The

hypothesis that reactive oxygen species and oxidative stress contribute to the pathogenesis of PD originates from two main sources. The discovery that MPTP is selectively toxic to nigrostriatal dopaminergic neurones provided an important model of parkinsonism and clues to the possible pathogenic mechanism in PD. Oxidation of MPTP to MPP^+ and its subsequent ability to impair mitochondrial function and generate oxidant stress are the key components of the toxic process initiated by this agent (Singer *et.al.*, 1987). Impairment of mitochondrial function can itself give rise to excessive formation of reactive oxygen species, but in addition, MPTP and its metabolites (MPP^+ and 1-methyl-4-phenyl-2,3-dihydropyridinium ion [$MPDP^+$]) can interact directly with biomolecules to form free radical species (Adams and Odunze, 1991). MPTP toxicity could also be due to inhibition of ATP formation through an impairment of mitochondrial function coupled with the generation of reactive oxygen species capable of exerting neurotoxicity. The discovery of MPTP toxicity led to the discovery of many analogues of MPTP, some of which also exert toxicity of the substantia nigra. Furthermore, several naturally occurring molecules e.g. isoquinolines and β-carbolines can exert MPTP-like toxicity and can be found in food and others may be generated by the brain itself. These, however, are relatively weak neurotoxins, and their relevance to PD is unknown, although it is possible that long-term exposure may lead to progressive neurodegeneration.

Oxidative stress in PD may also arise from the metabolism of dopamine itself by both chemical and enzymatic mechanisms. The autoxidation of dopamine leads to the production of semiquinones, which are themselves toxic and which may also lead to the generation of reactive oxygen species (Olanow, 1990). The semiquinone cascade leads to polymerisation and the formation of neuromelanin, although there is no evidence that increased dopamine oxidation or melanin formation occurs in individuals who develop PD. The enzymatic metabolism of dopamine leads not only to the deaminated metabolites homovanillic acid (HVA) and 3,4-dihydroxyphenlyacetic acid (DOPAC) but also to the generation of H_2O_2. Based on this concept, a theoretical scheme for the excess formation of the oxidant species H_2O_2 and $OH^\bullet$ formation has been devised. Increased dopamine turnover in the early stages of PD might generate excessive H_2O_2, which would normally be inactivated by glutathione (GSH) in a reaction catalysed by glutathione peroxidase. However, if the GSH system is impaired or deficient, H_2O_2 might be converted by the iron-mediated Fenton reaction to form highly reactive $OH^\bullet$, so initiating lipid peroxidation and cell death. Indeed the experimental elevation of dopamine turnover can lead to increased oxidative stress as determined by a rise in the formation of oxidised glutathione (GSSG) (Spina and Cohen, 1989).

Evidence for oxidative stress in Parkinson's disease.

Oxidative stress could be produced by several processes that take place in dopaminergic cells as well as in other monoaminergic cells (Feldman *et.al.*, 1996). First, hydrogen peroxide is one of the products of MAO deamination. Thus, every molecule of dopamine catabolised within the cell gives rise to a molecule of hydrogen peroxide (which can be converted to dangerous hydroxyl radicals). Second, catecholamines can undergo nonenzymatic auto-oxidation in the presence of molecular oxygen. This process gives rise to toxic quinones as well as hydrogen peroxide and oxyradicals as by-products. Moreover, DA auto-oxidation is considered to be the mechanism of neuromelanin formation. Hence, auto-oxidation may play a role in the particularly severe loss of melanised neurons in PD.

Finally, there is much interest in the possible role of iron in generating hydroxyl radicals. The formation of hydroxyl radicals from hydrogen peroxide can be catalysed nonenzymatically by ferrous ions in a so-called Fenton-type reaction. A by-product of this reaction is the oxidation of ferrous (Fe^{2+}) to ferric (Fe^{3+}) ions. Rats administered Fe^{2+} intracerebrally show increased lipid peroxidation (Triggs and Willmore, 1984). The substantia nigra contains a high concentration of iron, and neuromelanin appears to be capable of reducing Fe^{3+} to Fe^{2+}, thereby driving the Fenton reaction. There is general agreement that iron levels within the substantia nigra are elevated in PD (Dexter *et.al.*, 1989; Sofic *et.al.*, 1991; Gorell *et.al.*, 1995 and Gerlach *et.al.*, 1994) and this may mediate the formation of reactive oxygen species if the excess iron is in a reactive form. It has also been demonstrated that infusion of iron into the substantia nigra leads to a dose-related and progressive reduction in nigral neurons and striatal dopamine (Sengstock *et.al.*, 1993 and Ben-Schachar *et.al.*, 1991). However, there is dispute over whether the increased iron load in PD is in a reactive form. Much of this centres on whether iron is or is not bound to ferritin, since in a ferritin-bound form, iron is much less reactive. One study of the brain-specific ferritin isoforms indicates that neuronal ferritin levels are low in PD, but have failed to undergo the expected upregulation that would normally occur in the presence of increased levels of iron (Connor *et.al.*, 1995). Thus, it has not been ascertained whether the increased iron levels in PD exceeds the binding capacity of ferritin, and whether free iron is present in the substantia nigra. Therefore, the capacity of iron to generate reactive oxygen species in PD remains unknown. Even if the iron in the substantia nigra of patients with PD is in the reactive form, this may occur as a late and/or secondary change. A recent study demonstrated that iron secondarily accumulates within the substantia nigra following remote lesions of the nigrostriatal tract (Oestreicher *et.al.*, 1994). In addition increased iron levels may not be specific to PD and may occur in other basal ganglia degenerative disorders e.g. Alzheimer's disease (AD).

A further key to the pathogenesis of PD relates to alterations in mitochondrial function. The critical observation is the finding of impaired complex I function in the substantia nigra of PD patients in the absence of changes in any of the other mitochondrial complexes (Schapira *et.al.*, 1989; Mizuno *et.al.*, 1989). The deficit in complex I activity is specific to the substantia nigra in PD and is not found in other neurodegenerative disorders. Interestingly, it is exactly the same mitochondrial defect as occurs with MPP^+ toxicity. At the present time, however, the cause of this impairment is unknown. Studies on human PD fibroblasts indicate that complex II of the mitochondria is unaffected and it is thought that forcing metabolism through complex II increases free radical formation and the likelihood of developing oxidative stress. Thus complex I inhibition could lead to the generation of reactive oxygen species, but there is as yet no evidence that this mechanism is directly responsible for cell death in PD.

Nigral cell loss based on the concept of oxidative stress implies that antioxidant defence mechanisms in the PD brains may be impaired or inadequate. Many of the major antioxidant defences appear unimpaired e.g. catalase, vitamin C. However, there are changes in superoxide dismutase (SOD) and reduced glutathione. The activity of SOD in the substantia nigra pars compacta (SNc) in PD is increased (Marttila *et.al.*, 1988). This does not occur in other areas of the PD brain, but alterations in SOD have been described in other neurodegenerative disorders, including AD and amyotrophic lateral sclerosis (ALS). Whether the increase in SOD activity is associated with the inducible Mn-dependent mitochondrial form of the enzyme or the constitutive Cu/Zn-dependent cytosolic form is debated. Studies of the cerebrospinal fluid support an elevation of the Mn-dependent form in PD. Since the Mn-dependent form is found in mitochondrial membranes, this would be compatible with an impairment of mitochondrial function leading to over-production of superoxide radical with consequent induction of Mn-SOD activity. Increased SOD levels may be neuroprotective since transfection of the gene for SOD production protects nigral cells from MPTP toxicity, and leads to increased survival of transplanted foetal ventral mesencephalic cells.

Hydrogen peroxide is removed from the cell by its metabolism to water by either catalase or glutathione peroxidase. In the latter reaction, reduced glutathione (GSH) is converted to its oxidised form (GSSG) by glutathione peroxidase, a by-product of which is water, and GSSG can be returned to its reduced state by glutathione reductase. There is general agreement that levels of the total and the reduced species of GSH in the PD brain are decreased (Perry *et.al.*, 1982 and Sofic *et.al.*, 1992) and that there is no corresponding increase in the level of oxidised glutathione (GSSG). The loss of GSH is specific to the SNc and has not been demonstrated in other areas or in other degenerative diseases affecting the basal ganglia. Impairment of the GSH system may reduce the clearance of H_2O_2 and promote the formation of $OH^\bullet$ in a reaction catalysed by excess iron in the

substantia nigra. The decrease of GSH also appears to be an early component of the disease. In patients with incidental Lewy body disease (ILB, possible presymptomatic PD), levels of GSH are reduced to approximately the same degree as in patients with PD (Hirsch *et.al.*, 1991). In contrast, in ILB patients there is no change in iron concentration or in levels of mitochondrial complex I. Thus, a fall in GSH may be the earliest biochemical marker associated with nigral degeneration. Why GSH levels are decreased in PD remains unknown. Oxidative stress or mitochondrial abnormalities might deplete glutathione irreversibly, but this has not yet been established.

While measurements of iron levels, mitochondrial function and GSH content in the substantia nigra suggest increased formation of reactive oxygen species and that the SNc is in a state of oxidative stress in PD, they provide only an indirect measurement of free radical involvement.

The free radical hypothesis of the cause of PD is based on the concept that constant oxidation of dopamine may be deleterious to the nigrostriatal system, since the products of this oxidation may lead to oxidative stress and eventually neuronal damage. Yet all humans are exposed to this process throughout their lifetimes but only a small percentage develop PD. If dopamine oxidation is the key, then why does the pathologic process in PD spread well beyond the dopaminergic system to areas such as the locus coeruleus and the nucleus basalis of Meynert? And why doesn't everyone get the disease? A hypothesis which would answer the second question is that there is a genetic predisposition in certain individuals to PD. Environmental agents may also have a part to play in the aetiology and may contribute to oxidative stress.

Genetic factors influencing PD.

Although viral encephalitis or an environmental toxin such as MPTP are clearly capable of damaging the substantia nigra, the 1990s have seen a re-emergence of interest in the genetic causes of idiopathic PD. Familial clustering of PD was observed a century ago when 10-15% of PD patients were reported to have a positive family history (Nussbaum and Polymeropoulos, 1997). Accurate measurement of the frequency of PD among relatives of affected patients is made very difficult by the inaccuracy of diagnosis of PD from history, the variability in age of onset, and the rarity of autopsy data required for making the diagnosis of diffuse Lewy body disease in relatives reported to have PD. During the 1980's, a genetic contribution to PD was thought unlikely when a series of twin studies failed to demonstrate an increased concordance for PD in monozygotic versus dizygotic twins (Duvoisin *et.al.*, 1981; Ward *et.al.*, 1983; Marttila *et.al.*, 1988). As has been pointed out (Zimmerman *et.al.*, 1991), however, these studies are not easily interpretable because the number of twins studied and the duration of the observation to

either support or reject a genetic contribution to PD were inadequate. As nearly 80% of the function of dopaminergic neurones of the substantia nigra must be lost before symptoms occur, reliance on clinical diagnosis alone and a lack of follow-up makes a determination of concordance extremely insensitive. The use of positron emission topography can be used to measure ^{18}fluorodopa uptake into basal ganglia and to diagnose preclinical dysfunction of the substantia nigra. When this was carried out an increased concordance rate was observed among monozygotic twins when compared to dizygotic twins (Burn *et.al.*, 1992). As a result, the lack of increased concordance in twin studies cannot be taken as evidence that no genetic factors are involved in PD.

More recently, a number of epidemiological studies with differing methodological approaches and study populations have been published and found to support a familial contribution to PD (Duvoisin, 1992; Golbe, 1993; Johnson, 1991; Marder *et.al.*, 1996). In case control studies, positive family history was found to be the single greatest risk for PD. In family studies a family history for PD was found in 10-24% of patients. In the largest of these studies, the frequency of PD was 2% in 1458 first degree relatives of 233 PD patients, a significantly higher frequency than the 1% seen in the 7834 first degree relatives of 1172 age-matched controls (Marder *et.al.*, 1996).

In an attempt to integrate our current knowledge of the familial nature of PD, the possible role of defects in energy metabolism in causing the disease, the toxicity of MPTP and the role of dopamine metabolism in PD, there have been three major lines of research : 1) investigation of the mitochondrial genome for mutations in PD patients 2) looking for linkage of polymorphism's in drug metabolising enzymes in affected individuals 3) attempts at identifying linkage between PD and polymorphism's in genes involved in dopamine synthesis and breakdown. There have been several reports of deficiencies arising in complex I of the electron transport chain (Mizuno *et.al.*, 1989; Schapira *et.al.*, 1989 and more recently Shoffner *et.al.*, 1993; Brown *et.al.*, 1996) in patients with PD but whether these abnormalities are primary or secondary to the disease process is unknown. It is interesting, however, that the action of MPTP also involves inhibition of complex I activity. A few small studies have suggested a significant association of certain mitochondrial DNA polymorphism's with PD but the sample sizes were small and replication is ongoing (Shoffner *et.al.*, 1993; Brown *et.al.*, 1996). Thus, there appears to be some consistent abnormalities in oxidative phosphorylation, particularly of complex I, in PD but a direct causative role for inherited or acquired mutation of the mitochondrial genome remains unproved.

In view of the possible involvement of neurotoxins in PD (e.g. MPTP), research has also been directed towards identifying variation in certain drug metabolising enzymes that might predispose certain individuals to greater toxicity from environmental agents. Association

studies in PD have focused on polymorphism's in drug metabolising enzymes such as cytochrome P450IA1 (encoded by the *CYPIA1* gene) and the debrisoquine 4-hydroxylase cytochrome P450 (encoded by the *CYP2D6* gene), as well as the monoamine oxidase A and B enzymes (encoded by *MAOA* and *MAOB*). A number of studies have suggested significant association between PD and loci encoding cytochrome P450 enzymes and monoamine oxidase. Association studies with the *CYP2D6* gene revealed a highly significant 4-fold increased risk among patients with disease onset before age 50 in a Spanish population although no such association was seen in the United States and British samples (Sandy *et.al.*, 1996). Many studies have indicated association between the *CYP2D6* allele and early-onset PD (Agúndez *et.al.*, 1995) but no association with late-onset PD (Diederich *et.al.*, 1995). A particular haplotype at the *MAOA* locus was found to be 3-fold more common among PD patients as compared to controls while another haplotype was 3-fold less common among affected patients (Hotamisligil *et.al.*, 1994). No such associations were found at the *MAOB* locus (Ho *et.al.*, 1995). Thus, there is some evidence for a modest association for certain alleles at these loci with PD but, as with many association studies, replication of these findings is difficult and requires larger, carefully controlled studies before they can be accepted as definite.

Allelic association between genes involved in dopaminergic transmission and PD has also been investigated. No association was seen with a polymorphism in the gene encoding the dopamine transporter (Taussig *et.al.*, 1995 and Tanaka *et.al.*, 1993), but evidence of allelic association for the dopamine D2 receptor was detected among sporadic PD patients (Taussig *et.al.*, 1995) indicating a possible role in PD. However, these were preliminary data with a small number of individuals, and this allele association will have to be investigated further. Interestingly mice lacking dopamine D2 receptors show symptoms similar to PD: lack of spontaneous movement, akinesia and abnormal gait (Balk *et.al.*, 1995).

A genetic contribution to PD has received substantial support from the identification of a number of families in which PD with diffuse Lewy body disease was inherited as an autosomal dominant trait (Lazzarini *et.al.*, 1994; Dwork *et.al.*, 1993; Payami *et.al.*, 1995; Golbe *et.al.*, 1996 and Denson *et.al.*, 1997). Penetrance appeared to be age-dependent, rising from 43% early in adulthood to 85% after age 70. In one such family, from the town of Contursi near Salerno in Italy (Golbe *et.al.*, 1996), linkage analysis was carried out and the gene for PD mapped to chromosome 4 at 4q21-q23 (Polymeropoulos *et.al.*, 1996). Linkage mapping of a PD gene to 4q21-q23 in the Contursi pedigree suggested a number of candidate genes for PD which mapped to this region. One of them, α-synuclein, was a particularly good candidate. The protein is a neuron-specific presynaptic membrane protein (Iwai *et.al.*, 1995) that was originally identified as the peptide named NACP, (non-Aβ protein component of AD amyloid), isolated from plaques in AD.

Sequencing of the α-synuclein gene in affected individuals from the Contursi kindred revealed that affected members were heterozygous for a missense mutation, changing alanine->threonine at amino acid 53 of the protein, that segregated with PD in this family (Polymeropoulos *et.al.*, 1997). The same missense mutation was found in three additional unrelated PD families of Greek origin but was absent in 314 chromosomes from control European populations, including 200 chromosomes obtained from random controls from the area near Contursi itself. The evidence that this mutation causes PD is based entirely on finding the mutation in four unrelated families and finding it absent in a large set of controls. Definitive proof requires elucidation of the mechanism by which this mutation causes the disease e.g creation of a knock-out mouse for this gene.

Over the last few years, a major shift in thinking and focus for PD research has resulted in renewed interest in the genetic basis of this fascinating disease. This change in attitudes has already proved beneficial with the identification of one gene in which a particular missense mutation predisposes to PD.

1.2.5 Animal Models of Parkinson's Disease.

Animal models of human diseases are useful in two respects, they allow the development and testing of new therapeutic strategies and they can also provide insight into the specific cause of the disorder. Clearly an animal model of Parkinson's disease would be a valuable tool in both of these aspects of this disorder.

1.2.5.1 Chemically-induced animal models of PD.

MPTP

Within a year after the discovery that MPTP could cause parkinsonism-like symptoms in humans (Langston *et.al.*, 1983) and monkeys (Burns *et.al.*, 1983), repeated injections of MPTP in mice (Heikkila *et.al.*, 1984) were shown to cause prolonged depletion of striatal dopamine apparently via a neurotoxic mechanism. Clinically, the animals became akinetic and bradykinetic, flexed and rigid, and some had tremor. Histopathological examination of the brain revealed extensive degeneration of the substantia nigra zona compacta, and biochemically dopamine and its metabolites were profoundly depleted in the striatum of these animals. Also squirrel monkeys treated with MPTP, particularly in older animals, eosinophilic inclusions have been seen that are reminiscent of human Lewy bodies (Langston, 1996). In monkey and mice, MPTP causes degeneration of a similar population of nucleus A8, A9 and A10 neurons of the midbrain (the retrorubal field, the substantia nigra and the ventral tegmental area, respectively) as in human PD. There appears to be a large scale of MPTP sensitivity among the species tested. Primates appear

to be the most vulnerable of the species so far tested, to MPTP toxicity. Rats appear to be the least affected, exhibiting transient behavioural deficits after acute MPTP administration but are relatively resistant to the toxic effects of repeated drug treatment. Mice appear to fall some where in the middle. There are thought to be three main reasons for the difference in species sensitivity: MPP^+ is cleared from primate brains slower than any other, activity of MAO-B the capillary endothelium, in rats is high and converts most of the MPTP to MPP^+ at this site. Due to ionisation MPP^+ is unable to cross the endothelial cell membrane and gain access to nerve cells. Finally, the substantia nigra in primates appears to have a high concentration of neuromelanin which concentrates MPP^+ in these cells. However, recent evidence indicates that the relative insensitivity of rats to MPTP neurotoxicity is not accounted for by these mechanisms (Sundstrom and Samuelsson, 1997). Pretreatment of rats with deprenyl to prevent MAO-B-mediated oxidation in the capillary did not increase toxicity in the striatum. Synaptosomal uptake was also studied and was found to be no different in mouse and rat (Sundstrom and Samuelsson, 1997). Therefore, the lack of effect of MPTP in rats is not due to mechanisms specific for MPTP but probably to the ability of rat catecholamine neurons to cope with, and survive, impaired energy metabolism (Sundstrom and Samuelsson, 1997).

However, MPTP-induced parkinsonism differs from human PD in many respects. For example, noradrenergic and sertonergic systems may be less severely damaged (if not damage at all) than in idiopathic PD. Neurochemical differences were also found between MPTP-induced parkinsonism and PD e.g. equal losses of DA in the caudate and putamen of MPTP-treated animals (Burns, 1983), which differs from PD, in which the putamen is more severely affected. More recent work has demonstrated that appropriate drug treatment regimes can bring about neurochemical effects closely resembling those in PD and even the slow evolution of clinical symptoms (Bezard *et.al.*, 1997).

The 6-OHDA model.

The catecholamine neurotoxin 6-hydroxydopamine (6-OHDA) is transported into the cell bodies and fibres of dopaminergic and noradrenergic neurons. This leads to massive degeneration of the nerve terminals and can also affect the cell bodies, particularly when administered to cell body regions. Reasonable selectivity for the substantia nigra can be obtained by pre-treatment with despiramine, a noradrenergic transporter blocker that inhibits 6-OHDA uptake into the adrenergic neurons. Better selectivity can also be obtained when the toxin is injected directly into the striatum, substantia nigra or the medial forebrain bundle, which contains the axons.

The most widely used model is that of animals with unilateral lesions. The phenotype of these animals is normal but when challenged with amphetamine rotational behaviour is

elicited, ipsilateral to the side of the lesion. When L-Dopa is administered contralateral rotation is obtained. Animals which have received bilateral lesions more closely resemble PD, they display severe bradykinesia and L-Dopa is seen to enhance their motor function (Sakai and Gash, 1994). However, not many studies are carried out on animals treated in this way, as after lesioning the animals have difficulty in eating, drinking and are difficult to maintain.

Intrastriatal application of 6-OHDA initiates a delayed and progressive loss of nigral dopaminergic neurons and may resemble the slow developing neuropathology of PD. Studies carried out by Zigmond (Zigmond *et.al.*, 1990) investigated the characteristics of the 6-OHDA model when compared to human PD. Extracellular levels of dopamine in the striatum as measured by microdialysis do not decrease until tissue dopamine depletion exceeds 80% and behavioural impairment is observed only after severe (bilateral) damage. Therefore, some compensatory mechanisms may under lie the disparity between total tissue dopamine and extracellular dopamine levels including increased firing by the remaining neurons and increase in the amount of dopamine released per action potential. This mirrors human PD where symptoms do not appear until striatal dopamine loss reaches 80% and the remaining nigral cells show increased firing and dopamine turnover.

The mechanism by which 6-OHDA acts as a neurotoxin in still unknown but several hypotheses have been put forward. 6-OHDA can generate highly cytotoxic free radicals (i.e. hydrogen peroxide and the hydroxyl radical). Peroxidative membrane damage probably due to free radical generation has been observed after intrastriatal injection of 6-OHDA (Kumar, 1995). It has also been shown that 6-OHDA, similar to MPTP is a potent inhibitor of respiratory chain enzymes, suggesting a neurotoxic pathway for 6-OHDA not primarily involving oxidation products (Glinka and Youdim, 1995). In addition, disturbance of intracellular calcium homeostasis by excessive entry of calcium and/or release from intracellular storage sites either may be a causal factor for neurotoxin-mediated cell death or may represent a common final pathway involving other mechanisms (Gerlach, 1996). Specifically, it is not clear whether intrastriatal 6-OHDA acts directly on the nigral cell bodies (following specific uptake and retrograde transport) or whether the toxin mediates a rapid destruction of striatal DA terminals and the progressive nigral cell degeneration is caused by another mechanism (e.g. lack of a target-derived neurotrophic factor).

These chemically-induced models of PD do, to some degree resemble the human condition but as yet no spontaneous occurring models of PD have been observed in animals.

1.2.5.2 A genetic model of PD.

The Weaver mouse

The principal phenotype of the weaver mouse is a weaving gait that is due, in part, to a severe hypoplasia of the cerebellum marked by a near total loss of midline granule cells (the most numerous cell type in the CNS). However, it is not only the cerebellum which is affected in the weaver phenotype, a progressive loss of dopaminergic cells from the substantia nigra pars compacta is also observed. This was particularly interesting as these are the type of cells lost in PD . In Parkinson's disease and weaver mice, the involvement of dopaminergic mesencephalic neurons is heterogeneous: it is prominent in the substantia nigra (SN) (A9), especially in the lateral areas, but less marked in the retrorubral area (A8) and the ventral tegmental area (A10) (Triarhou *et.al.*, 1988). It has also been shown that calbindin-$_{D28k}$ positive neurons are relatively spared in the SN in both PD patients and weaver mice (Gaspar *et.al.*, 1994). Calbindin-D_{28k} is thought to reduce free intracellular calcium levels and neurons expressing this protein are better protected against excitotoxicity.

The weaver mouse mutation was shown to be a single-base substitution in *GIRK2* which encodes a inward rectifying potassium channel (Patil *et.al.*, 1995). The base change leads to a substitution of amino acids in the pore region of the protein, which is thought to block the channel, leading to increased excitotoxic stress and resulting in nigral cell death (Bandmann *et.al.*, 1996). Excitotoxic stress may cause increased radical production and impaired mitochondrial metabolism both of which have been described in PD (Jenner, 1992). It was therefore thought that abnormalities of the channel may contribute to the aetiology of PD (Goldowitz and Smeyne, 1995). A study of the GIRK2 gene was carried out by Bandmann and colleagues (1996) in idiopathic and sporadic cases of PD to evaluate the possibility of a shared genetic defect in weaver mice and PD, but the sequence was normal in all cases. This suggested a different aetiology of nigral cell loss in PD and weaver mice. There are many other differences between PD and the weaver mouse which suggested a different aetiology: behaviourally, weaver mice differ from the akinetic-rigid features seen in PD in that they display ataxia and fine tremor, this is due to severe involvement of the cerebellum with profound cell loss of granule cells. In PD, the cerebellum is spared (Gibb, 1992). Other frequently affected areas in PD such as the nucleus raphe dorsalis or the locus coeruleus (Gibb, 1992) are normal in weaver mice (Lane *et.al.*, 1977). Thus, the limited damage of the nigrostriatal system in weaver mice does not match the distribution and extent of the widespread morphological and biochemical changes seen in PD.

1.3 The AS/AGU rat.

Rats homozygous for a mutation in the *agu* gene display movement abnormalities similar to those seen in human patients with Parkinson's disease (PD). Phenotypically these rats are characterised by a reduced ability to initiate movement, an abnormally wide gait of the hind paws, rigidity of the hindlimbs resulting in a staggering gait and a tendency to fall over every few steps (Clarke and Payne, 1994, Campbell *et.al.*, 1996). A series of locomotor tests have been carried out to investigate the exact phenotype of these animals including mid-air righting, rate of movement within a defined area and balancing; animals homozygous for the *agu* mutation show reduced abilities in all of these tests. The phenotype can be detected as early as postnatal day 10 through a combination of clumsy gait, high stepping, tail elevation and slight whole body tremor. In older rats the fully developed condition includes difficulty in initiating movement. Injection of L-Dopa and fetal midbrain grafts are observed to increase performance in the described motor tests (Payne *et.al.*, in press). The *agu* mutation arose spontaneously within a closed breeding population of Albino-Swiss rats at the Department of Anatomy, at the University of Glasgow (Clarke and Payne, 1994).

1.3.1 Anatomy of the AS/AGU rat.

Anatomical investigations of the AS/AGU rat brain were carried out in an attempt to determine the basis of this disorder. No gross abnormalities were observed in any CNS structures and the cerebellum and cerebral hemispheres appeared normal and were the appropriate size and orientation. The substantia nigra appeared smaller, with a distorted shape and the pars compacta was thinner than normal (Clarke and Payne, 1994). Tyrosine hydroxylase (TH) immunostaining revealed that there were major deficits in the number of TH-immunoreactive cells in mesencephalic regions, particularly the substantia nigra (Figure 1.5). Counts of TH immunoreactive neurons were carried out on the substantia nigra in nine mutant strain rats and in three controls of the parent strain (Albino Swiss), mean deficits of 20% were seen in the numbers on TH-immunoreactive neurons in this region (Clarke and Payne, 1994).

1.3.2 Pharmacology of the AS/AGU rat.

The reduction in size of the substantia nigra and the general phenotype of AS/AGU rats suggested an involvement of the neurotransmitter, dopamine in the production of the phenotype. Investigations were therefore carried out to determine the effect the *agu* mutation has on dopamine levels in the neostriatum, the target of nigrostriatal dopaminergic neurons (Albin *et.al.*, 1989 and Beckstead *et.al.*, 1979). At 12 months dopamine levels in the caudate-putamen (CPU) of the corpus striatum were determined.

AS/AGU rats had lower levels of neostriatal dopamine than control AS rats, with the greatest discrepancy in the dorsal CPU which showed a reduction of 30-35%, moderate loss in the lateral CPU and small losses in the ventral CPU. Differential patterns of dopamine loss within the striatum are also observed in PD brains, where dopamine loss is reported to be most pronounced in the dorsal and intermediate regions (Kish *et.al.*, 1988).

The deficits in striatal dopamine levels were detectable from about 6 months (Campbell *et.al.*, 1997), suggesting that locomotor disorders which develop in the mutant AS/AGU animals before six months are due not to a gross reduction in levels of dopamine, but does not rule out some other deficiency in dopaminergic function. However, micropunch-derived data cannot distinguish between intra- and extra-cellular levels of transmitters, therefore a study was carried out to measure the extracellular levels of dopamine and its metabolite 3,4-dihydroxy-phenylacetic acid (DOPAC) in the dorsal caudate putamen of conscious AS (control) and AS/AGU rats. At all ages, microdialysis levels of dopamine were 8-10 fold lower in AS/AGU rats than in the AS strain. However, levels of DOPAC were 2.5-5 fold higher in AS/AGU than in AS (Campbell *et.al.*, 1998). These results can even be detected at 3 months, in the absence of a detectable loss of whole tissue dopamine (Campbell *et.al.*, 1997). Extracellular dopamine in the dorsal-caudate putamen of conscious animals was reduced to 10-20% of control levels.

Age	Dopamine (pg/sample)	DOPAC (pg/sample)
3 months		
AS(n=6)	105.7 ± 26.5	20.2 ± 1.3
AS/AGU (n=6)	16.2 ± 1.4	48.6 ± 3.2
p	< 0.01	< 0.01
6 months		
AS (n=6)	37.3 ± 1.3	7.2 ± 0.9
AS/AGU	4.1 ± 0.5	25.2 ± 6.3
p	< 0.01	< 0.01
9 months		
AS (n=6)	27.4 ± 1.8	3.6 ± 0.9
AS/AGU (n=6)	2.3 ± 0.5	16.7 ± 2.7
p	< 0.01	< 0.01

Table 1.3 Concentrations of extracellular dopamine and DOPAC in striatal dialysis of AS and AS/AGU rats. The data are taken from Campbell *et.al.*, 1998.

Other aminergic systems are also depleted in PD, including the number of serotonergic cell bodies in the dorsal raphe and the locus coerulus, a study was undertaken to see if similar deficits occur in AS/AGU rats. There are modest decreases in dopamine in the ventral tegmental area (-40%) and the locus coerulus, while the locus subcoeruleus was unaffected (Scott *et.al.*, 1994). There was wide variation in the number of serotonergic cell bodies in both the median and dorsal raphe and the locus coerulus of AS/AGU rats. HPLC-ECD measurements of biogenic amines reveal overall depletion's of serotonin in AS/AGU rats in a ventral tegmental area containing the median raphe nuclei (-70%) and in a dorsal tegmental area containing the dorsal raphe nuclei (-50). The data suggests that, as in human PD aminergic deficits are not confined to dopaminergic systems.

Significant depletion of glucose utilisation is also observed in the substantia nigra pars compacta, subthalamic nucleus and ventrolateral thalamus (Lam *et.al.*, in press) of AS/AGU rats.

The *agu* mutation produced a very interesting phenotype in the rat which could prove a useful tool in the investigation of basal ganglia disorders e.g. Parkinson's disease. The obvious similarities between the human phenotype and pathology of Parkinson's disease and the phenotype and pathology observed in the AS/AGU rat made the investigation of the mutation an interesting possibility.

1.3.3 Genetic investigation of the agu mutation.

AS/AGU rats were originally crossed to AS animals and all of the F1 progeny had normal locomotion. The F1 progeny were then backcrossed to AS/AGU and the progeny of the backcross fell into two phenotypic classes; those with normal locomotion (50%) and those with abnormal locomotion (50%). The ratio of 1:1 for affected and non-affected progeny indicated the involvement of a single locus and the mutation was seen to be recessive and fully penetrant in backcross progeny. There did not appear to be maternal or X-linked patterns of inheritance, indicating that this gene was contained on an autosomal chromosome, rather than a sex or mitochondrial chromosome. The karyotype of AS/AGU rats appeared normal and there were no gross chromosomal abnormalities.

Using a large rat backcross to map agu.

The mutation within the *agu* gene which gives rise to this phenotype will be identified by what is termed positional cloning (Collins, 1992). There are two stages to this process: the first stage is the use of formal linkage analysis to find flanking DNA markers that must lie very close to the gene of interest. Using these markers, the second stage of the process

involves cloning across the region that contains the gene responsible for the phenotype, and then identifying the gene itself.

The first stage of this process requires fine genetic mapping of the *agu* gene. Genetic linkage is a direct consequence of the physical linkage of two or more loci within the same pair of DNA molecules that define a particular set of chromosome homologs within the diploid genome (Silver, 1995). To map a mutationally defined locus, one will have to generate progeny in which segregation of the mutant and wild-type alleles can be followed phenotypically in animals prior to DNA preparation for marker locus typing. This could be performed to map the *agu* mutation, as the phenotype could be followed easily in off-spring.

A decision was made to use a backcross to produce offspring which would allow mapping of the *agu* gene. The first mating in this scheme is always an outcross between the mutant strain and a inbred strain. Once F_1 hybrid animals are obtained, they are subsequently bred to the mutant strain. In the backcross, therefore the F_1 hybrid animal will be heterozygous at both two linked loci, which results in two complimentary sets of coupled alleles-A B and a b. The genotype of this animal is therefore, AB/ab. In the absence of crossing over between homologues during meiosis, one or the other coupled set-either A B or a b will be transmitted to each gamete, producing offspring either AB/ab or ab/ab after mating with the homozygous (ab) mutant strain. However, if a cross-over event does occur between the A and B loci, a non-parental combination of alleles will be transmitted to each gamete. The frequency of recombination between loci A and B can be calculated directly by determining the percentage of offspring formed from gametes that contain one of the two non-parental, or recombinant, combination of alleles (Silver, 1995).

To a degree, crossing over occurs at random sites along all of the chromosomes in the genome. A direct consequence of this randomness is that the farther apart two linked loci are from each other, the more likely it is that a crossover event will occur somewhere within the length of chromosome which lies between them. Thus, the frequency of recombination provides a relative estimate of the genetic distance. Genetic distances are measured in centimorgans (cM) with 1 cM defined as the distance between two loci that recombine with a frequency of 1%. 1 cM is taken to be approximately 2 Megabase (Mb) in physical distance in the mouse genome but unfortunately not known in rat. However, it is important to be aware that the rate of equivalence can vary due to genetic interference, gender-specific differences in rates of recombination, recombination hotspots and the region of chromosome under investigation. Although the frequency of recombination between two loci is roughly proportional to the length of DNA that separates them, when this length becomes too large, the frequency will approach 50%, which is indistinguishable from that expected from unlinked loci.

The analysis of backcross data is very straightforward, and when all loci are known to map on the same chromosome, it is possible to derive linkage relationships. By looking at an ordered set of markers, one can visualise the actual meiotic products contributed by the F_1 parent in the form of individual haplotypes. Every recombination event between the mutation locus and a marker can be detected and the frequency of recombination can be easily determined. The major disadvantage with the backcross is that it is not universally applicable to all genetic problems. In particular, it cannot be used to map loci defined only by recessive phenotypes that interfere with viability or absolute fecundity in both males and females (Silver, 1995).

1.3.4 Choosing the inbred strain and number of animals for a backcross.

Upon commencing a new linkage study, a decision will have to be made concerning the two parental rat strains that will be used to establish the backcross. Obviously in the backcross situation one of these strains is already determined i.e. the mutation carrying strain. The most important consideration for the choice of the other strain will be the degree of polymorphism that exists between the two parental strains, and the ease with which they, and their offspring, can be bred to produce a large panel of second-generation animals for DNA typing. Backcross construction is significantly more difficult in the rat than in the mouse in one important respect. Genetic mapping in the mouse can exploit crosses with different subspecies or species (e.g. *M.castaneus* and *M.spretus*) that have SSR polymorphism rates with laboratory strains of about 90%, rather than intraspecific crosses in which the polymorphism rate is only about 50% (Jacob *et.al.*, 1995). Because similarly distant rat strains are not available, at best only about half of the SSR markers isolated are informative in any given mapping cross. An informative marker is defined as a marker which displays a polymorphism between the individuals or species being tested.

To determine the inbred strain to be used in the backcross a set of 73 microsatellite loci were typed in the AS, PVG, F344 and BN rat strains to determine the strain with the highest level of polymorphism with AS (the *agu* mutation arose within the AS strain, and would presumably only differ from the AS strain at the *agu* locus). These strains were chosen as they were among the most common used in mapping studies. The microsatellite loci typed were optimised and covered the entire rat genome, and would prove useful at a later date. AS differed from BN, F344 and PVG at 62%, 47% and 43% of loci, respectively (Shiels *et.al.*, 1995) (work carried out by Miss M.B. Durán Alonso and Dr.P.Shiels). As BN and F344 displayed the largest rates of polymorphism with AS they were both selected to be used to establish a backcross with AS/AGU.

The number of animals produced in a backcross determines the level of resolution obtained from that backcross. The greater number of animals produced, the greater number of recombination events which can be identified. Assuming random sites of recombination, the average distance in centimorgans, between crossover events observed among the offspring of a backcross can be calculated using the simple formula (100/N), where N is the number of meiotic events that are typed (Silver, 1995). With 1,000 meiotic events, the average distance will be only 0.1 cM. Therefore, it was decided that a resolution of 0.05 cM would be useful, meaning 2000 progeny from each backcross would have to be produced. This would produce a physical distance resolution of approximately 50 kb. However, as mentioned previously crossover events do not always occur randomly and this figure is an approximation.

1.4 Genetic mapping in rat.

The laboratory rat, *Rattus norvegicus*, was the original mammalian species used in scientific research but has fallen behind the mouse as the choice of animal for genetic studies for many reasons: the smaller size of the mouse simplified housing requirements and many behavioural mutants were available. As a result, the range of genetic markers identified within the rat genome has been sparse when compared with that of mouse. In the last five years this situation has improved slowly. The recent convergence of molecular genetics with physiology and the availability of a wide array of rat strains has made the rat the species of choice in the study of many complex genetic disorders. Identifying genomic loci which influence traits that exhibit continuous or quantitative variation in organisms amenable to breeding experiments has become the focal point of a great deal of research. The rat has become the organism of choice in the investigation of quantitative trait loci (QTL) which influence many complex phenotypes e.g.. hypertension (Gu *et.al.*, 1996), diabetes (Gaugier *et.al.*, 1996), arthritis blood pressure and stroke. As the rat is utilised more frequently as a model for such disorders complete genetic linkage maps are required.

The first construction of a rat genetic map was reported by Serikawa and colleagues in 1992 who isolated one hundred and seventy-four rat loci which contained short tandem repeat sequences. This was followed by Jacobs *et.al.*(1995) who reported the first complete genetic linkage map of the laboratory rat consisting of 432 SSLPs with an average spacing of 3.7 cM. From then onwards an increasing number of rat genetic mapping studies have been published concerning nearly every chromosome of the rat. The most recent rat genetic map (September, 1997) from the Whitehead Institute/MIT Centre for Genome Research contains 2,275 markers, bringing the total on all of their maps to 3,139 SSLP markers (WIBR/MIT CGR version 2.0).

Another area of improvement where genetic mapping of the rat genome is concerned is the availability of genomic libraries. Rat genomic libraries rat are important when a novel gene is to be isolated which corresponds to an observable phenotype, in the process known as positional cloning. The absence of libraries also limited mapping of the rat genome, in particular physical mapping of small areas. The only genomic library available before 1997 was a P1 library constructed by Southard-Smith (1994), when compared to the many different libraries available for mouse and man it is evident why the rat has lagged behind these two species in mapping projects. In 1997, however, three rat genomic libraries became available, the first a Yeast Artificial Chromosome library constructed by Cai *et.al.*, (1997) followed by another YAC library (Haldi *et.al.*, 1997) and finally a P1 Artificial (PAC) library constructed by The Roswell Park Cancer Institute. This is a moderate start for rat genomic mapping resources, but as more and more genetic mapping studies are carried out within the rat for such diseases as hypertension etc., the demand for resources will increase, as will the available resources.

1.5 DNA Markers

There are three criteria that define the perfect DNA marker. First, they should be extremely variable to provide a good possibility that any two chromosome homologues in a species will carry different alleles. Second, they should be easily identified so that one can develop a set of markers for the analysis of any species. Finally, they should be easy to genotype rapidly in large numbers of individuals. A large number of types of markers have been identified that fulfil all of these criteria. However, experience within our laboratory has shown that detection of variation by PCR at microsatellites and by identifying an SSCP (single-strand conformational polymorphism), are the most efficient ways of genotyping large numbers of backcross progeny.

1.5.1 Microsatellites

Microsatellites fulfil all of the criteria above for DNA markers and have been utilised extensively in recent years for mapping projects in nearly all species. Microsatellites can be defined as relatively short (<100 bp) runs of tandemly repeated DNA with repeat unit lengths of 6 bp or less. Microsatellites are used extensively as markers for establishment of linkage maps of all eukaryote genomes as they occur at high frequency throughout genomes (approximately 50,000-10,000 copies/haploid genome, Sun *et al.*, (1996), tend to be highly polymorphic and are easily assayed by the polymerase chain reaction (PCR). A microsatellite (also known as a simple sequence repeat - SSR) is a genomic element that consists of a mono-, di-, tri- or tetrameric sequence repeated multiple times in a tandem array. Allelic variation is based entirely on differences in the number of repeats present in the tandem array rather than specific basepair changes. Thus, the only way in which

alleles can be distinguished is by measuring the total length of the PCR product containing the microsatellite.

Novel microsatellites can be identified within genomic clones by hybridisation with repeat sequence oligonucleotides. The most common repeat sequence observed in the rat genome in a database survey carried out by Beckman and Weber (1992), was the $(CA)_n$ repeat element, accounting for 36% of all microsatellites surveyed. It was estimated during an investigation of the Genbank database that a $(CA)_n$ repeat element where $n>6$ occurred approximately every 21 kb within the rat genome (Stallings *et.al.*, 1991). Therefore, this oligonucleotide should always be utilised first in the search for new microsatellites in the rat. Serikawa observed that dinucleotides in the rat tend to be variable in length once a threshold size of 20 bp has been reached (Serikawa *et.al.*, 1992). PCR primers can then be generated flanking the novel microsatellite and used to identify repeat length differences within this sequence between our different rat strains, and subsequently used for mapping relative to the *agu* mutation.
The properties of microsatellites make them useful tools in all mapping projects and they will be extremely useful in mapping the *agu* gene.

1.5.2 SSCP

Single strand conformation polymorphism (SSCP) takes advantage of the fact that even single nucleotide changes can alter the three-dimensional equilibrium conformation that single strands will assume at low temperatures (Orita *et.al.*, 1989). If a sample of DNA is denatured at high temperature and then quickly placed on ice, reformation of DNA hybrids will be inhibited. Instead, each single strand will collapse onto itself in what is often called a random coil. In fact, it is now clear that each single strand will assume a most-favoured conformation based on the lowest free energy state. Even a single base change could conceivably disrupt the previous most favoured state and promote a different one, which, if different enough, would run with an altered mobility on a gel, allowing the detection of a strain difference which can be used for mapping.

1.6 Positional Cloning

Positional cloning is a powerful strategy for identifying disease genes with unknown biological function (Collins, 1994). Application of this approach relies upon initially determining the chromosomal localisation of the responsible gene followed by additional fine mapping carried out to narrow down the responsible region (Figure 1.5), however this is generally limited by the number of informative meioses available. In general in human mapping studies, about 100 events are available, so fine mapping is often limited to genetic intervals of about 1 cM. Mapping studies in mouse and rat have an advantage as

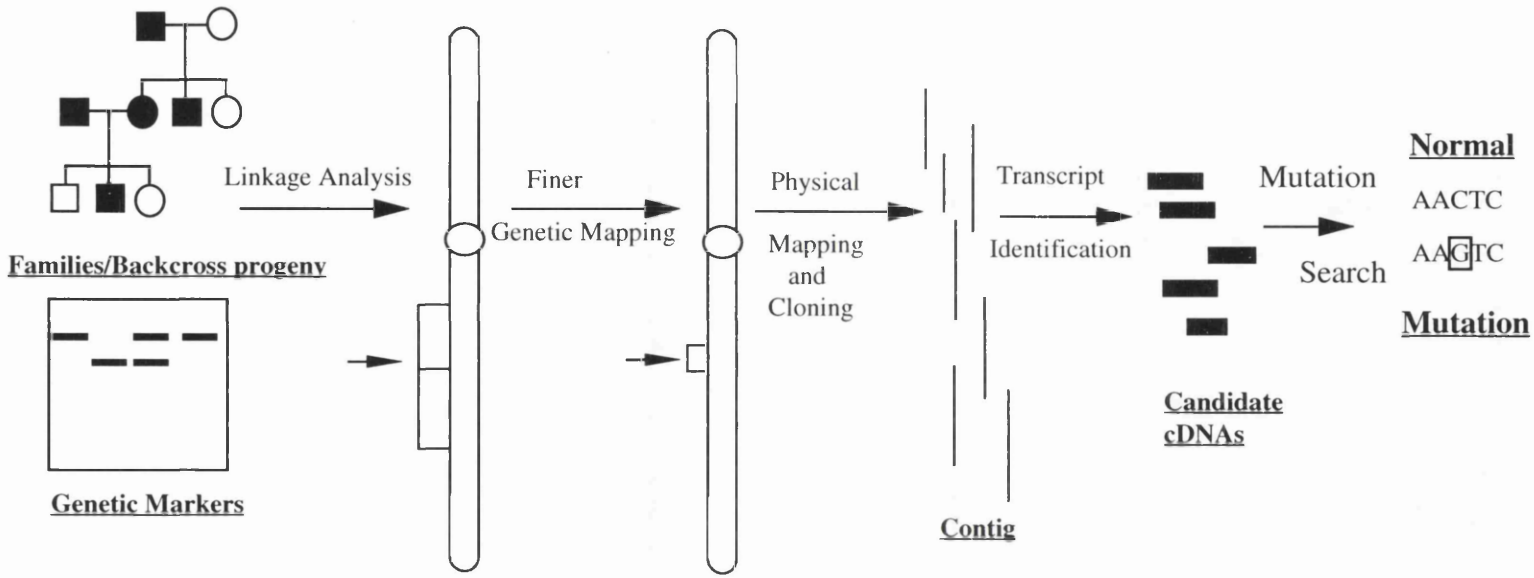

Figure 1.5 Schematic representation of the processes involved in positional cloning.
The figure was adapted from Collins, 1992.

the number of meioses generated is determined only by limitations on animal numbers. Fine mapping of the region is followed by an examination of the transcripts in the area, with the aim of identifying a gene that contains a mutation. After the correct disease gene has been cloned, a biochemical analysis then ensues to understand the encoded protein and its function.

The development of a clone-based contig map encompassing the critical region bridges the gap between genetic studies and transcript (cDNA) identification. Previously, YAC clones were isolated for this purpose, since they contained large inserts, simplifying and accelerating the coverage of extensive stretches of the genome. However, it has become preferable to use P1, PAC or BAC clones to establish a contig, as problems such as chimaerism and instability can arise in YAC cloning. Chromosome Walking is the name given to a systematic process which allows the isolation of large (greater than 100, 000 bp) regions of complex genomes in an ordered array of overlapping recombinant DNA clones (Cross *et.al.*, 1986). Chromosome walking is typically performed using YAC, BAC, PAC or cosmid clones. Typically, fragments from both ends of the insert of the "founder" clone are isolated and used as hybridisation probes to screen a library for over-lapping clones. This approach assumes that the new clones will extend bilaterally, significantly beyond the founder clone. The walk then proceeds in a linear fashion in steps by isolation of new end probes from the new clones and repeating the process. However, chromosome walking is a laborious and time consuming procedure, no walk can proceed faster than the speed and length it takes to make each individual step, and this has limited its general application and also restricted the length of walk that can be contemplated. This is the disadvantage of using clones with relatively small inserts e.g. P1 clones and BACs, as short distances will only be taken at each step, when compared to large insert YAC clones.

The clones identified by chromosome walking then provide an important resource of easily manipulable DNA, suitable for generating markers to refine genetic maps. These clones can also easily be used for fingerprinting to allow overlaps between clones to be established.

Following this, strategies for rapidly identifying transcripts directly from cosmid, YAC, PAC, BAC and P1 clones are utilised, such as exon-trapping and cDNA selection techniques (Lovett *et.al.*, 1991; Korn *et.al.*, 1992).

1.7 Progress in mapping the *agu* mutation.

Genetic and physical mapping of a gene locus, identification of the gene and eventually identification of a mutation in the gene which gives rise to a specific phenotype is termed

reverse genetics (Collins, 1992) or positional cloning. This process involves a set of defined steps as detailed previously. The first step involved decisions made on a breeding scheme, rat strains involved etc., this work was detailed previously. Two backcrosses were initiated between F344 and AS/AGU and BN and AS/AGU with both to eventually comprise 2000 offspring each.

The next step involved a chromosomal localisation of the *agu* locus. To accomplish this the set of 73 microsatellite markers, used in determining the rat strains to be used for the backcross, were used in a genome wide scan for linkage. This involved typing at least one informative marker per rat chromosome, with the exception of chromosomes 9 and X which did not have any informative markers, being assayed for linkage with the *agu* mutation. Linkage was observed with the marker R33 (Serikawa *et.al.*, 1992) which was localised to chromosome 1 (work carried out by Dr.P.Shiels and Miss M.B.Durán Alonso). This marker mapped approximately 30 cM from *agu* and therefore defined a region of genome of approximately 50 cM from R33 which contained *agu.*

1.8 Aims of current study.

The aim of the work detailed in this thesis is to establish a physical (DNA) map of a defined, small region of the rat genome that contains the *agu* gene. The situation at the beginning of my work has been outlined in Section 1.7. Therefore, the experimental work presented here has two major components:

- Identification of new genetic markers to allow fine mapping of the *agu* gene in a genetic interval of < 1 cM.

- Establishment of a genomic clone based contig of this region by chromosome walking.

Chapter 2

Materials and Methods

2.1 Basic Molecular Techniques

2.1.1 Gel Electrophoresis of DNA

DNA was visualised and resolved in multi-purpose agarose from Boehringer Mannheim in 1X TBE. Conditions such as voltage and length of time of DNA resolution were adjusted to suit the purpose of the gel and the samples to be resolved. All agarose gels are loaded with 200 μg of 1kb ladder from GibcoBRL and DNA was visualised by adding ethidium bromide (10 mg/ml) to the molten agarose.

2.1.2 Bacterial strains utilised

Bacterial Strain	Genotype of strain	Reference
TG-1	SupE hsdΔ5 thiΔ (lac$^-$ proAB) F' [tra D36 pro AB$^+$ lac I^q Lac ZΔM15]	Gibson *et. al.*, 1984
DH10B	F$^-$ mcrA Δ(mrr$^-$ hsdRMS$^-$ mcrBC) ϕ80d lac Z ΔM15 ΔlacX74 deoR recA1 endA1 araΔ139 D(ara, leu) 7697 gal U gal K λ$^-$ rpsL nupG	Grant *et. al.*, 1990
NS3529	recA$^-$ mcrA$^-$ Δ(hsdR hsdM mcrB mrr) (λ imml LPI) (λ imm434-P1; Cre+)	Pierce *et. al.*, 1992
F3	DH10B [F::Tn10d-Cam]	Kimmerly *et. al.*, 1994
INV α F'	F' endA1 recA1 hsdR17(r_k^-,m_k^+) supE44 thi-1 gyrA96 relA1 ϕ80lacZΔM15 Δ(lacZYA-argF) U169 λ$^-$	Invitrogen® Version B 150626 25-0024

Table 2.1 Bacterial strains utilised in this study

2.1.3 Production of Competent E.coli Cells

An overnight culture of the bacterial strain TG-1 was grown from a single colony in 2XYT. The following day 100 mls of 2XYT was inoculated with 1 ml from the overnight culture. The cells were grown for approximately 2 hours until the OD_{595nm} was approximately 0.6. The cells were then pelleted at 3, 000 rpm for 5 minutes. The pellet was resuspended in 25 mls of ice cold 50 mM calcium chloride and incubated on ice for 20 minutes. The cells were centrifuged again and resuspended in 5 mls of ice cold 50 mM calcium chloride. The cells were then kept on ice until required.

2.1.4 Transformation of competent E.coli cells

100 µl of cells, prepared as above, were utilised in all transformations. DNA or ligation reactions at the appropriate concentration were incubated along with the *E.coli* cells for 30 minutes on ice. The DNA was then transformed into the cells by performing a heat shock at 42°C for 2 minutes. The cells were then placed back on ice for 2 minutes. 250 µl of 2XYT is then added and the cells allowed to recover at 37°C for 1 hour. 100 µl of cells were then plated onto an agar plate containing antibiotic.

2.1.5 Small scale preparation of plasmid DNA

Small scale preparation of plasmid DNA (mini-prep) was carried out using the Promega™ SV Wizard mini-prep® kit as described by the manufacturer.

2.1.6 Large scale preparation of plasmid DNA

Large scale preparation of plasmid DNA was carried out using the Qiagen™ tip 100 kit (Qiagen) as described by the manufacturer.

2.1.7 Transfer of DNA to Nitrocellulose (Southern blotting)

DNA was transferred from agarose gels onto nitrocellulose (MSI) as the method described in Sambrook *et. al.*, (1989). The agarose gel was soaked in denaturing solution for 20 minutes, followed by 20 minutes in neutralising solution. The gel was then briefly rinsed in 2X SSC. Nitrocellulose and 3 sheets of 3MM Whatmann paper were cut to size and soaked in 2X SSC before use. The blotting apparatus was then assembled as Sambrook *et.al.*, (1989). The gel was kept in contact with the nitrocellulose for 16 hours to allow DNA transfer by cappillary action. The nitrocellulose was then washed with 2X SSC to remove traces of agarose and baked at 80°C for 2 hours to fix the DNA to nitrocellulose.

2.1.8 Automated Sequencing

2.1.8.1 Preparation of plasmid templates for sequencing

Plasmid DNA was prepared using the standard Birnboim and Doly alkaline lysis technique (1979), followed by chloroform extraction and PEG precipitation as follows : bacterial cells from a 3 ml culture were pelleted and resuspended in 200µl GTE buffer (50 mM glucose, 25 mM Tris pH 8.0, 10 mM EDTA pH 8.0). The cells were lysed by the addition of 300 µl of 0.2 M NaOH, 1% SDS and inverted gently. 300 µl of neutralising solution was then added (3 M potassium acetate pH 5.5). The solution was centrifuged at

14, 000 rpm for 10 minutes and the supernatant removed to a new tube. The supernatant was treated with RNaseA at a final concentration of 1 mg/ml. The supernatant was then chloroform extracted using an equal volume of chloroform/isoamyl alcohol 24:1. To the aqueous phase was added an equal volume of isopropanol and centrifuged at 14, 000 rpm for 10 minutes. The pellet was then washed with 70% ethanol and allowed to air dry. The pellet was then resuspended in 32 µls of dH_20 and 48 µls of a PEG salt mixture (8 µl 4M NaCl + 40 µl 13% PEG 8000). This mixture was vortexed briefly and incubated on ice for 20 minutes. The mixture was then centrifuged at 14, 000 rpm for 20 minutes at 4°C. The pellet was washed in 70% ethanol, allowed to dry and resuspended in 20 µl. The DNA was visualised on a agarose gel to estimate concentration.

2.1.8.2 Preparation of PCR products for sequencing

PCR products were sequenced directly without prior cloning. The PCR reaction was carried out as in Section 2.2, in a total reaction volume of 50 µl. The PCR reaction was then passed through a MicroSpin™ S-400 HR Sephadex column (Pharmacia) to remove excess primers. The sequencing reaction was then carried out as described 2.1.8.c.

2.1.8.3 Sequencing Reactions

Sequencing reactions were carried out in a 20 µl reaction volume containing 3.2 pmoles of primer, approximately 0.5 µg of template DNA and 8 µl of the Amersham dye- terminator cycle sequencing Thermosequenase mix (Amersham). The reactions were carried out in a Perkin Elmer GeneAmp PCR System 9600 (Perkin Elmer) as follows : 96°C 2 mins, 25 cycles of 94°C 10 secs, 50°C 5 seconds and 60°C 4 mins. Any excess primer, or dNTP mix were then removed by precipitating the reaction using 2.5 volumes of 95% ethanol and 1/10th volume 3 M sodium acetate, washed with 70% ethanol and allowed to dry completely. The pellet was then resuspended in 4 µl of formamide stop buffer.

Primer	Sequence of primer 5'->3'
T7 P1	CCGCTAATACGACTCACTATAGGG
SP6 P1	GGCCGTCGACATTTAGGTGACAC
T7	TAATACGACTCACTATAGGG
T3	ATTAACCCTCACTAAAGGG
M13 Forward	CATTTTGCTGCCGGTCA
M13 Reverse	GGAAACAGCTATGACCATG

Table 2.2 Sequencing primers used in this study.

2.1.8.4 Electrophoresis of sequencing reactions

All sequencing reactions were resolved on the ABI 373 stretch automatic sequencing machine and analysed with software provided by ABI.

2.1.9 Transfer of DNA from bacterial colonies to nitrocellulose

Bacterial colonies can be transferred from agar plates onto nitrocellulose to allow colony hybridisation with radioactive probes. Nitrocellulose filters (MSI) were laid on top of the bacterial colonies for thirty seconds and marked with asymmetric dots to allow orientation after hybridisation. The nitrocellulose was then removed and placed DNA/colony side up on a denaturing solution for 5 minutes. The nitrocellulose was then transferred onto a neutralising solution for 5 minutes. The nitrocellulose filters were then washed for 20 minutes in 2X SSC to remove bacterial cell debris. Bacterial colonies were always colony lifted in duplicate. Nitrocellulose filters were then baked at 80°C for 2 hours to bind DNA to the filter.

2.1.10 Hybridising Southern Blots with Oligonucleotides

Oligonucleotides (synthesised by GibcoBRL) were radiolabelled with γ-^{32}P dATP (NEN DuPont, 3000 Ci/mmol) using T4 polynucleotide kinase (Promega). The total reaction volume of 30 µl contained 50 pmoles of oligonucleotide, 1X kinase buffer, 50 µCi of γ-^{32}P, 20U of T4 polynucleotide kinase and dH_20. The reaction was incubated at 37°C for 1 hour and the enzyme heat killed at 65°C for 20 mins. After labelling the probe was purified in Sephadex™ columns. Filters for probing were incubated at 42°C for 1 hour in a solution of 1X Dernhardts, 5X SSC, 50 mM sodium phosphate, 1 mM sodium pyrophosphate, 0.1 mg/ml salmon sperm DNA and 20% formamide previous to addition of the probe. The probe was then added to the pre-hybridisation solution and incubated overnight at 42°C. Filters were washed at room temperature in 2X SSC, 0.1% SDS for 15 mins, followed by two washes in 1X SSC, 0.1% SDS for 15 mins at room temperature. The filters were then exposed to X-ray film (Fuji) at -70°C for approximately 15 hours.

2.2 Polymerase Chain Reaction (PCR)

All PCR reactions were performed in a reaction containing 1X magnesium free Thermo buffer (Promega), 1 mM magnesium chloride (Promega) and each dNTP at 125 µM (Promega). All primers for PCR were synthesised by GibcoBRL™ and each primer was added at a final concentration of 5 ng/µl. Table 2.3. contains the sequence of all PCR primers utilised and the conditions at which they were optimal. Template was usually added to final concentration of 10 ng/µl. Samples were heated to 99°C for 5 mins before

the addition of 1U Taq (Promega) at 80°C. This was followed by 25 or 30 cycles of denaturation at 94°C for 15 secs, annealing for 30 secs and an extension step at 72°C for 30 secs. These were followed by a final extension step of 72°C for 2 mins. The reactions were carried out in a Perkin Elmer GeneAmp PCR System 9600 (Perkin Elmer). PCR reactions were generally visualised on a 2% TBE/agarose gel stained with ethidium bromide (10 mg/ml) (Sigma) and visualised by Ultra Violet. The primer pairs are designed with the forward primer (F) designed 5' to 3' and the reverse (R) primer designed 3' to 5'.

Positive control for the PCR reaction were generally carried out on Brown Norway genomic DNA at a final concentration at 10 ng/µl. Negative controls were carried out which did not contain any DNA. PCR contamination problems were eliminated by dispensing PCR solutions and aliquoting these within a laminar flow hood. A clean set of pipettes was also used and oil over laid onto the PCR reaction to prevent air borne contamination.

PCR Assay	Gene	Primers Sequences 5' to 3'	PCR parameters
GU100	Bgp2	F - GCATTCCAGATTCTCTGTCACGG	55°C/25 cylces
		R - GGCTCCAGGATACACCTTTTCTTC	
GU101	Atp4a	F- CATAGTCCCACACCCAGGAAAGTAC	55°C/25 cycles
		R- AACCCTCTTGTCCAGATGGAGTC	
GU102	SCNIB	F- GCATGATGGGTGAAGCAATATGG	55°C/30 cycles
		R - TAGGAGGTGTCACAGGAAGGGAAC	
GU103	GRIK5	F - CAGTTTCTGGTGAAGTCCAAGCC	60°C/30 cycles
		R - AAGTGTGGAGAGCCGTGTCAAG	
GU104	GRIK5	F- CAGTTTCTGGTGAAGTCCAAGCC	55°C/27 cycle s
		R - AAGTGTGGAGAGCCGTGTCAAG	
GU106	SSR	F - CACCGTCTTTGTCTCTGTCTT	60°C/25 cycles
		R - GCTTGTCCAGTCTGTCAGTG	
GU10	SSR	F - CAAAGATCCTGAGGAAACTGGC	55°C/32 cycles
		R - CCTGCGGAGATGAAAGAGGAAAGG	
KSP6	End P1	F - ATACAAAGTGAGTTCCAGGG	58°C/30 cylces
	cloneK	R - CCTTCTCCTTGTGTGGCTGC	
F20	SSR	F - GTTGGACTAGAAGCACCCAGC	65°C/30 cycles
		R - TTGTTCAGGCCTGCTGGGTCC	
F34	SSR	F - GGCAGAGGTAGACAGAGTTCG	62°C/30 cycles +
		R - TCCTCATTCGCTATTCTTGG	5% formamide
F61	SSR	F - GTGTGAATTCTCACTGCAGC	55°C/30 cycles
		R - CCTGTTCTGTCTTGTTCTACC	
F101	SSR	F - GCCCACATGTCCATCAATTGATGG	60°C/33 cycles
		R - TTAGCACAGCATGCTGACCTCC	
F110	SSR	F - TAGGAAGTGGCCCACATGTCC	65°C/30 cycles
		R - GCATGCTGACCTCCAGTCCCTCC	
H31T	SSR	F - CCTGTCTTCTGCATAGATCACTG	68°C/30 cycles
		R - GTAAAGATCAGGTGTGCATGCG	
H31C	SSR	F - CGCATGCACACCTGATCTTTAC	69°C/30 cycles
		R - GCAAGGTGAGGAAATACCTGTGG	
KSP62	End P1	F - CCATCACTGTTACACACAGAAACCC	54°C/32 cycles
	cloneK	R - TCCATAAATCCACGGCACTCC	
R158	marker	F- AGAACCCTTCACTGCTGCTCACC	60°C/30 cycles
		R - AGAAAGTCCCAGAAAGTGGC	
NCA	Atpl	F - CTGCCAGTGACGATTTCAGCC	57°C/30 cycles

		R - GCTGCTCCACAGACACATGAATAG	
KT7	End P1	F - GTTTCTGAGGGGCAGTAATGGCGG	67°C/27 cycles
	cloneK	R - GCTGCACAACTGGGGTACTGTGGC	
K66	SSR	F - GATTCCCAACACCCATACCAGG	65°C/30 cycles
		R - GAGCAACGCCAAATGCTTCTTCC	
K100	SSR	F - GACTCCCACACTTGACTTCAGACC	65°C/30 cycles
		R - CTCTGACCACAACACATGTGTGCC	
K106	SSR	F - TTGGGCTCCCACCTTGCTTTTCC	65°C/30 cycles
		R - CTGGAAGTCAGATTTCTGGTCTCC	
K3	3' UTR	F - ATGTAATCTCATCTGCTGCCGC	55°C/30 cycles
	of PKC	R - TTCTACAACTGAAGTGGAGG	
GU 9	Ferittin	F - TGACTTCTTGGAAAGCCACTTCC	65°C/30 cycles
	light chain	R - AAGAGATACTCGCCCAGAGATGCC	
K5	5' UTR	F - CAGTAGTTCTCCGTTGCGTTCC	54°C/30 cycles
	of PKC	R- AGGTTTCCTCTCTTGAGTTCCTCC	
SRY		F - CAAGTTGGCTCAACAGAATCCCAG	55°C/27 cycles
		R - GGCACTTTAACCCTTCGATGAGG	
D1 Mgh7	SSR	F - CCACACTATGTCCATGTGTACAA	50°C/25 cycles
		R - GGAAACTCAAAGGTAGACAAAACA	
D7 Mit178	SSR	F - ACCTCTGATTTCAGAACCCTTG	50°C/32 cycles
		R -TAGAGAGCCACTAGCATATCATAAC	
D7 Mit243	SSR	F - TTCCCTTCACTCATGATGTAAGA	48°C/30 cycles
		R - GGCTGCCATACTGTTGAACA	
D7 Mit75	SSR	F - AAAGATGTGGTGACCATGATTG	-
		R - CCTTTACACATGCATACACATACA	
D7 Mit 168	SSR	F - CCCAAAACATTTAAAAAGCCA	-
		R - GCTATGGCACATGCACAAGT	
D7 Mit152	SSR	F - GCCTAGCACACGCCAAAG	50°C/32 cycles
		R - CCTTGTGCATGGTTGCTATG	
D7 Mit153	SSR	F - TGGTTTGAATTTCTATTTGATTTCC	-
		R - ATAGAAAGGCATGGGTGTGTG	
D7 Mit76	SSR	F - CATGAGCACGTGGAGAAAGA	50°C/32 cycles
		R - CGTGGAAACCTGATAAACTGA	
D7 Mit190	SSR	F - TGTGATTACACACTCATAATCACACA	50°C/32 cycles
		R - GGCCAGGGTCAGTAACAAAA	
D7 Mit56	SSR	F - AATGAAGATACCCACAGAAGCTG	50°C/32 cycles
		R - GATGGGAACTGGGAACTTAGC	
D7 Mit65	SSR	F - TAATTGAATAGTGTGCTGTGACCA	50°C/32 cycles
		R - CATGGCTTTGAAGAATTGTGTT	
D7 Mit191	SSR	F - TTGGGTTTGTACTACCTAGATACCTC	50°C/32 cycles
		R - CCTCTAGGGCTCTTGCACAC	
D7 Mit244	SSR	F - CATGCATACACATGTGCCCT	50°C/32 cycles
		R - ATGCCTATCAAAAAGAATGAGTG	

Table 2.3 PCR primers utilised, the sequence and annealing temperature and cycle number used in routine PCR from rat genomic DNA.

2.3 Analysis of backcross progeny

2.3.1 Isolation of DNA from backcross progeny

DNA was isolated from the spleens of animals produced from both backcrosses. DNA was isolated as the technique described by Davis *et.al.*, (1980). This protocol has been

adapted to produce a genomic DNA isolation kit by Puregene (Gentra). After isolation of the DNA a spectrophotomic reading was taken at OD_{260} to ascertain the concentration of the DNA. The DNA was then diluted to 100 ng/µl for PCR and 1 µl used in the PCR reaction.

2.3.2 Genotyping backcross progeny

2.3.2.1 Genotyping PCR products on Metaphor gels

PCR reactions were carried out as described for the standard reaction, any modifications made are cited within Table 2.3. Metaphor™ (Flowgen) gels were prepared as the manufacturer's specifications in 1X TBE buffer. The total PCR reaction volume was loaded onto a 4% TBE/Metaphor gel in 1X TBE and 125V were applied to the gel for approximately 4 hours. The gel was then stained with ethidium bromide (10 mg/ml) and visualised by Ultra Violet.

2.3.2.2 Genotyping of Radioactively-labelled PCR products

The PCR primer radioactive-labelling reaction was carried out as performed for hybridisation with oligonucleotides, containing 50 ng of forward primer to be used in the PCR reaction. A PCR reaction was performed as standard with the addition of the radioactively-labelled primer in a ratio of 1:300 to the forward primer which was not labelled. The PCR reaction was then carried out under mineral oil (Sigma) in a Perkin Elmer Cetus DNA Thermal Cycler. Again Taq (Promega) was added after an initial denaturing step at 99°C for 10 mins. The PCR reactions were then carried out as above. After the PCR has been performed 2 µl of formamide stop buffer was added to the reaction and 4 µl of this was loaded on to a 6% acrylamide denaturing gel. The PCR products were resolved on the gel at 60W for approximately 2 hours depending on size. The gel was then dried and exposed to X-ray film (Fuji) overnight at room temperature.

2.4 Utilisation of the P1 library

The P1 library was provided in groups of P1 clones, containing between 300-1500 clones, named superpools. These superpools were provided as glycerol stocks. The library was kindly provided by Dr.R. Mac Donald (University of Texas) and described in Southard-Smith *et.al*, (1994).

2.4.1 Making lysates of P1 Superpools

A small scraping was taken with a toothpick from the superpool glycerol stock into 100 µls of dH_20 and boiled for 20 mins at 99°C. These lysates were stored at -20°C and 1 µl used in a PCR reaction.

2.4.2 Screening superpool lysates

The P1 library was screened by PCR. Firstly the 209 superpools were screened always performing 30 cycles in the PCR reaction. The PCR reactions were carried out as before, with a positive and neagtive control as described (Section 2.2). The products were then resolved on a 2% TBE/agarose gel. Once a positive superpool had been identified, a scraping was taken from the top of the glycerol stock of that pool and was placed into 3 mls of L-Broth. The superpool was then plated onto L-agar plates containing kanamycin at a final concentration of 25 µg/ml. The plates were incubated overnight at 37°C. Single colonies from these plates were then picked into 100 µls of dH_20 and screened by PCR as batches of 10 colonies. These batches of 10 were boiled for 20 mins before PCR carried out. While these colonies were being picked they were also streaked again as single colonies onto a gridded L-agar plate containing kanamycin (25 µg/ml). The PCR reactions were then carried out as before containing 1 µl of the lysate. The reactions were resolved as before. Once a positive batch of 10 had been identified the 10 colonies contained within this were picked on toothpicks into a PCR reaction as before.

2.4.3 Isolation of P1 DNA

Three methods of isolating DNA from P1 clones were tested within in our laboratory.

2.4.3.1 Qiagen™

A P1 clone single colony was grown in 50 mls of LB culture containing 25 µg/ml kanamycin and 5% sucrose. The following day 500 mls of 2X YT containing kanamycin was inoculated with 500 µl of the overnight culture. The culture was then incubated for 4 hours at 37°C. After this time 5 mls of 0.1 M IPTG was added and the culture grown for a further 3 hours or until the OD_{550} was 0.8. The cells were then harvested at 5K for 10 minutes. The supernatant was removed and the cell pellet resuspended in 8 mls of the Qiagen P1 buffer (GTE). 8 mls of buffer P2 (0.2 M NaOH, 1% SDS) was then added, mixed gently and incubated at room temperature for 5 mins. Chilled buffer P3 (3 M Potassium acetate, pH 5.5) was then added, mixed gently and incubated on ice for 15 minutes. This was then centrifuged at 4°C for 30 minutes at 15,000 rpm and the supernatant removed promptly. The Qiagen-tip 100 was equilibrated with 4 mls of buffer

QBT and the column allowed to empty by gravity flow. The supernatant was then applied to the column and allowed to enter the resin. The Qiagen column was then washed with 40 mls of buffer QC. The DNA was eluted with warmed (47°C) QF buffer. The DNA was precipitated with 0.7 volumes of isopropanol and centrifuged at 4°C at 12, 000 rpm for 30 minutes. The DNA was washed with 5 mls of 70% ethanol and allowed to air dry for 5 minutes. It was then re dissolved in 250 µl of TE.

2.4.3.2 Nucleon kit

The Nucleon I kit (Scotlab bioscience) was used to isolate genomic DNA from cultured cells, tissue and blood. To isolate P1 clone DNA 3 mls of culture was pelleted and resuspended in 340 µl 400 mM Tris-HCl (pH 8.0), 60 mM EDTA, 150 mM NaCl and 1% SDS. The resulting solution was treated with RNaseA. To remove proteins the solution was shaken for 20 minutes at 37°C after the addition of 100 µl of 5M sodium perchlorate. Then incubated at 65°C for 20 minutes. The DNA was extracted using chloroform, shaking at room temperature for 20 minutes. The DNA was then precipitated.

2.4.3.3 Caesium chloride

This method is described in detail in the paper by Kimmerly *et.al.*, 1994. A single colony of a P1 clone was inoculated into 15 mls L-Broth containing kanamycin (25 µg/ml) and grown overnight at 37°C. The cells were collected and lysed as standard Birnbiom and Doly lysis (Birnboim and Doly, 1979). After lysis the DNA was precipitated using an equal volume of isopropanol. The pellet was then resuspended in 3.5 ml of TE buffer (10 mM Tris, pH 8.0 and 1 mM EDTA) and then 4g CsCl and 100 µl 10 mg/ml ethidium bromide were added. The CsCl-DNA solution was transferred to Beckman Quick Seal tubes, heat sealed and then centrifuged in the VTi65.2 rotor (45 krpm, 20 hours, 18°C). P1 DNA was removed from the gradient using a 1ml syringe. Ethidium bromide was removed from the sample by multiple extractions with isopropanol saturated with 20X SSPE buffer (3.6 M sodium chloride, 0.2 M sodium phosphate and 10 mM EDTA, pH 7.0). Finally the sample was precipitated with ethanol and suspended in sterile water.

2.4.3.4 Phenol/chloroform

50 ml culture of a P1 clone was grown overnight at 37°C containing 25 µg/ml kanamycin. The cells were pelleted, suspended in 2 mls of GTE and incubated at room temperature for 5 minutes. 3 mls of 0.2 M sodium hydroxide, 1% SDS was added, inverted gently and incubated on ice for 10 minutes. 3mls of 3 M potassium acetate, pH 5.5 were added inverted gently and incubated on ice for 10 minutes. This was followed by centrifugation at 15, 000 rpm for 15 minutes. The liquid was removed with a pipette and an equal

volume of phenol/chloroform 1:1 was added and inverted gently. This was centrifuged again at 15, 000 rpm for 15 minutes. The aqueous phase was removed and precipitated with 2 volumes of absolute ethanol. The pellet was washed with 2 mls of 70% ethanol and allowed to dry. Then resuspended in 500 µls of dH_20. This was then treated with RNAse at a final concentration of 1 mg/ml.

2.4.4 Transfer of P1 clones into DH10B

This method was carried out by the method conceived by Kimmerly *et.al.*, 1994. A single colony of the P1 clone was picked from a kanamycin plate, as this clone was isolated from the library it was contained within the bacterial strain NS3529. A single colony was also picked from a plate containing the bacterial strain F3 (provided by Dr. W. Kimmerly). Both of these were grown overnight at 37°C. The 1 ml culture containing the P1 clone contained 50 µg/ml of kanamycin and the 5ml culture containing the F3 strain contained chloramphenicol at 10 µg/ml. The next day 100 µls of the F3 overnight was added to 100 µls of the P1 clone overnight and added to 1.8 mls of L-Broth in a glass 50 ml test tube. This was incubated at 37°C in a shaking water bath at 30 rpm to allow bacterial conjugation to occur. This mixture was then diluted approximately 1/1000 and 30 µls plated onto L-agar plates containing 50 µg/ml kanamycin and 10 µg/ml chloramphenicol. As a control 5 ml of F3 and of each P1 clone were spotted onto a agar plate containing 50 µg/ml kanamycin and 10 µg/ml chloramphenicol. The plates were then incubated overnight at 37°C.

For the second round mating a single colony was picked into 1 ml L-Broth + 50 µg/ml kanamycin and 10 µg/ml chloramphenicol and grown overnight at 37°C. A single colony was also picked from a plate containing the bacterial strain DH10B into 5 mls of L-Broth and grown overnight. The second round matings were carried out as before with 100 µl of DH10B and 100 µl from the culture obtained from mating round 1. The mixture was then diluted as before and plated onto L-agar plates containing kanamycin, chloramphenicol and streptomycin at 100 µg/ml. As a control 5 µls of DH10B and of each F/P1 donor were spotted onto a L-agar plate containing kanamycin, chloramphenicol and streptomycin.

2.4.5 Isolation of P1 DNA from Superpools

A scraping was taken from the top of the glycerol stock as for making lysates into 3 mls of L-Broth and 100 µls plated out onto L-agar plates containing kanamycin at 25 µg/ml and 5% sucrose. The number of colonies plated was calculated to give at least a 95% coverage of the original superpool. After incubation overnight at 37°C the colonies were washed from the plates with 3 mls of L-Broth. 1 ml was taken from this to make two DNA

preparations and 800 µls used to make a new glycerol stock. DNA was isolated by the standard Burnboim and Doly followed by two phenol/chloroform extractions. DNA was resuspended in 200 µls of dH_20. These DNA preps were used to make megapools for screening. Again PCR reactions carried out as before.

2.4.6 Southern Blotting of P1 DNA

500 ng of DNA was digested at 37°C for 1.5 hours in the standard buffers for each enzyme (Promega). The digestion products were generally resolved overnight on a 0.5% TBE/agarose gel. Prior to blotting the gel was treated with 0.25 M hydrochloric acid to depurinate the DNA, which was then transferred onto nitro-cellulose membranes (MSI) by standard Southern blotting. (Sambrook *et.al.*, 1989)

2.4.7 Sub-cloning of P1 clones

P1 DNA (500 ng) was digested for 1.5 hours at 37°C with *Sau* 3AI in 1X React 4 Buffer (GibcoBRL), 1U/µl of enzyme and dH_20. 200 ng of pUC18 DNA was also digested with *Bam* HI using the conditions as above containing 1X React 3 buffer (GibcoBRL). The digested vector fragment was then band isolated from a 1% TBE/agarose gel using the QiaexII gel extraction system(Qiagen) or the Qiaquick gel extraction kit (Qiagen). Ligation reactions were performed in 1X ligase buffer (Promega), 1 mM ATP, 3U/µl of ligase (Promega) 10 ng of vector and insert at concentrations ranging between 10 ng and 20 ng. Ligations were generally performed overnight at 16°C. Half of the ligation was then transformed into the *E.coli* strain TG-1, previously made competent using CaCl. The cells were plated out onto L-agar plates containing 100 µg/ml ampicillin, 2% X-gal and 20 mg/ml IPTG. The plates were then incubated overnight at 37°C. White colonies were picked onto a gridded plate, in duplicate, and were again incubated overnight. Bacterial colonies were then transferred onto nitro-cellulose (Sambrook *et.al.*, 1989) for hybridisation. Hybridisation with oligonucleotides was carried out as the conditions for Southern Blots.

2.4.8 Identification of novel SSRs

The P1 clone from which the simple sequence repeats (SSRs) were to be isolated was shot-gun cloned into pUC18, as described for the sub-cloning of P1 clones (see previous methods) using *Sau3AI.* pUC18 was digested with *BamHI* and treated with 1U of shrimp alkaline phosphatase (Amersham Life Science) for 10 minutes at the end of the digestion. The digest was then resolved on a 1.0% agarose gel and the vector band was isolated from the gel prior to ligation. Ligations were carried out in the presence of 3U of ligase (Promega), 1X ligase buffer and 1 mM ATP at 16°C overnight. Half of the ligation is then transformed into the *E.coli* strain TG-1 competent cells. The transformed cells

were then plated onto L-agar plates containing ampicillin, 5-bromo-4-chloro-3-indolyl-β-D-galactoside (X-gal) and isopropyl-β-D-thiogalactosidase (IPTG) for blue/white selection. The plates were incubated overnight at 37°C. The bacterial colonies were then transferred onto nitro-cellulose, in duplicate, for hybridisation as previously described. Colonies were screened using a $(CA)_{10}$ repeat oligonucleotide (synthesised by GibcoBRL). The oligonucleotide was radioactively-labelled with γ-^{32}P dATP (NEN DuPont, 3000 Ci/mmol) using T4 polynucleotide kinase (Promega). To a total reaction volume of 30 µl is added 50 pmoles of oligonucleotide, 10X kinase buffer, 50 µCi of γ-^{32}P, 20U of T4 polynucleotide kinase and dH_20. The reaction was incubated at 37°C for 1 hour and then the enzyme heat killed at 65°C for 20 mins. After labelling the probe was purified in Sephadex™ G25. Filters for probing were incubated at 42°C for 1 hour in a solution of 1X Dernhardts, 5X SSC, 50 mM sodium phosphate, 1mM sodium pyrophosphate, 0.1 mg/ml salmon sperm DNA and 20% formamide previous to addition of the probe. The probe was then added to the pre-hybridisation solution and incubated overnight at 42°C. Filters were then washed at room temperature in 2X SSC, 0.1% SDS for 15 mins, followed by one wash in 1X SSC, 0.1% SDS for 15 mins at room temperature. The filters were then exposed to X-ray film at -70°C for approximately 15 hours. Colonies containing repeat sequences were identified and picked into L-Broth containing ampicillin and incubated overnight at 37°C. DNA was isolated using the mini-prep method previously described. Sequencing was then carried out on the positive clones using M13 forward and reverse primers. Once the repeat sequence had been identified PCR primers were designed to the region of sequence flanking the repeat and prior to ordering these primers were submitted to the BLAST programme (NCBI) to verify that they do not match any repetitive element within the genome e.g. LINE elements. The primers were then synthesised by GibcoBRL. The repeats were investigated for alleleic variation by the techniques previously described.

2.4.9 Identification of end sequences in a P1 clone

There are two ways of sequencing the end sequences of P1 clones to allow "walking" : a) direct sequencing from the P1 clone b) sub-cloning the end fragment and sequencing.

2.4.9.1 Direct sequencing from the P1 clone

DNA template for sequencing was isolated as the phenol/chloroform extraction method for the isolation of P1 clone DNA. Once the template had been made it was best if the sequencing reaction was carried out as soon as possible. Sequencing reactions were carried out as described with 2 µg of P1 DNA.

2.4.9.2 Sub-cloning P1 ends

Shot gun sub-cloning of the P1 clone was carried out as described and the white colonies transferred to nitrocellulose as described. The membranes were then probed with the T7P1 and SP6P1 oligonucleotides which flank the cloning site in the P1 vector. After preparation of DNA from sub-clones sequencing of the insert can then be performed with the original oligonucleotide used for probing or the M13 forward and reverse primers.

2.5 Identification of YAC clones

2.5.1 Screening of the YAC library

The Harvard/EC/HGF rat yeast artificial chromosome (YAC) library was obtained from Research Genetics. The library was supplied in twenty-four 96-well microtiter plates as DNA ready for PCR screening. The library is arrayed in 67 superpools of DNA which allows the location of a positive superpool in 67 PCR reactions. An additional 28 PCR reactions are then carried out resulting in the plate, row and column address of a single YAC clone. The library was screened by PCR as before, a 10 µl reaction was performed and 2 µl of template used from the library. However, in some cases the reaction volume of the PCR has to be increased to 25 µl and 5 µl of template, this is generally dependent on the primers. A positive control containing rat genomic DNA was included (Section 2.2) and a negative containing yeast genomic DNA and a negative containing no DNA. After the identification of the address of a particular clone the YAC clone was obtained from Research Genetics.

2.5.2 Growth of YAC clones

Individual YAC clones were streaked onto SD plates (2% glucose, 0.072% CSM -trp, -ura, 0.67% yeast nitrogen base) minus uracil and tryptophan. The colonies were grown on plates at 30°C for 2 days. YAC clones were originally grown in culture in SD medium, as above. YAC clones can also be grown in a culture of AHC medium containing 0.17% yeast nitrogen base without amino acids and $(NH_4)SO_4$, 0.5% $(NH4)_2SO4$ and 0.1% acid-hydrolyzed caesin (Unitied States Bio) and 1mg/ml adenine hemisulfate (Sigma), supplemented with 1% glucose. The cultures are grown at 30°C for approximately 2 days or until a slight pink colour is observed in the culture.

2.5.3 Identification of the correct YAC clones

Four single colonies were picked from each of the original streaked clone plates and were streaked onto SD plates minus uracil and tryptophan, to allow further purification. After a

further 2 days grown on plates "whole cell PCR" was carried on a single colony from each of the streaks to identify the correct YAC clone. A single colony from each of the 4 streaks for each clone was picked into 500 µl of dH_20 and 10 µl of this was used in a 25 µl volume PCR. The PCR was then carried out as standard. Once the correct colony had been identified the yeast clone was grown in liquid culture, SD -ura, - tryp, for 2 days in a shaking incubator at 30°C. A glycerol stock was made from the liquid culture in a final concentration of 20% glycerol and stored at -70°C.

2.5.4 Isolation of DNA from YAC clones

Crude DNA for PCR can be isolated from the YAC clones. Cells were pelleted from 100 µl of yeast culture by centrifugation for 10 minutes at 2, 000 rpm. The cells were resuspended in 50 µl of SCE (1 M sorbitol, 0.1 M sodium citrate and 0.06 M EDTA pH 7.0) and then pelleted again. After removal of the supernatant 25 µl of Lyticase solution (4 mg Lyticase - 5,000-20,000 U/mg protein (Sigma), 100 µl of 100 mM dithiothreitol and 900 µl of SCE)were added and incubated for 1 hour at 37°C. 60 µl of 0.14 N NaOH was then added and incubated for 10 minutes at room temperature. 60 µl of 1M Tris-HCl pH 8.0 was then added and the sample can then be frozen at -20°C. 1µl from this is then used in a PCR reaction.

2.5.5 Production of YAC DNA in agarose plugs for CHEF gel analysis.

Agarose plugs containing YAC clones were made in the following way : a 10 ml culture of yeast was pelleted at 3, 000 rpm for 10 minutes. The cell pellet was then washed in 10 mM Tris-HCl and 50 mM EDTA pH7.5. The pellet was then washed in SCE (see above). The cell pellet was then resuspended in 40 µl of SCE for each block to be made. To this Novozyme (Novo Biolals) at a final concentration of 8 mg/ml was added and incubated at room temperature for 10 minutes. The yeast cells were then briefly incubated at 50°C before the addition of an equal volume of 1.5% Low Melting Point agarose (Seaplaque® GTG® agarose, Flowgen) in SCE. The mixture was quickly mixed and then pipetted into previously chilled block formers. These were then incubated on ice for 15-30 minutes. The plugs were pushed out of the formers and into a solution of 0.4 M EDTA, 1% Sarkosyl (BDH) and 2 mg/ml proteinase K (Sigma). The plugs were then incubated for 24-48 hours at 50°C. Following this the plugs were washed in 10 mM Tris-HCl and 50 mM EDTA (2X 30 minutes) and can be stored at 4°C. Prior to loading onto a gel the plugs were equilibrated in 0.5X TBE for 2 hours.

2.5.6 CHEF Gel Analysis of YAC clones.

All CHEF analysis was carried out on the CHEF-DR® II system from Bio-rad. The analysis was carried out in Low Melting Point agarose (Seaplaque® GTG® agarose,

Flowgen). For conditions used for CHEF gel electrophoresis see chapter X. Markers utilised in CHEF electrophoresis were Promega-Markers® Yeast Chromosomal DNA and Promega-Markers ® Lambda ladder.

2.6 Mouse Primers

Mouse MapPairs™ were supplied by Research Genetics. The PCR reactions were carried out as for a standard reaction, with some modifications. The PCR primers were used at a final concentration of 0.1139μM as per the protocol supplied by Research Genetics. The reactions were carried out as follows: 4 minutes at 94°C, 1U of Taq added at 80°C, at least 30 cycles of 94°C for 15 secs, 50°C for 2 minutes, 72°C for 2 minutes followed by a final extension time of 7 minutes. The primer sequence and conditions for PCR from rat genomic DNA are given in Table 2.3.

2.7 SSCP Analysis

SSCP analysis was performed using PCR reactions as stated in Section 2.2. The PCR reaction was carried out using a final concentration of 5 ng/μl of primers, 20 mM dNTPs and 20 ng of template. The Thermo buffer and magnesium were at the concentrations as standard PCR. Again a hot start was performed and 1U of Taq added at 80°C. PCR reactions were carried out for 25 cycles on the Perkin Elmer Cetus DNA Thermal Cycler. After PCR 2 μl of the reaction was diluted into 30 μl 20 mM EDTA, 0.1% SDS. 2 μl from this is then diluted into 2 μl formamide stop buffer and loaded onto the SSCP gel. SSCP gels used were 6% non-denaturing acrylamide gels containing 10% glycerol, 0.5X TBE. Acrylamide (Anachem) was used in two forms 19:1 or 34.5:1 acrylamide to bis-acrylamide ratio depending on SSCP to be resolved. The SSCP was resolved at 30 watts for 4.5 hours at 4°C in 1X TBE.

2.8 Utilisation of a PAC Library

The PAC library is avaliable from Dr. P. De Jong at BAC/PAC resources, The Roswell Centre (Buffalo, N.J.). The library construction and ordering details can be found on the World Wide Web homepage : http://bacpac.med.buffalo.edu.

2.8.1 Screening the PAC library

Screening of the PAC library was carried out by hybridisation. The colony filters were firstly incubated at 65°C in approximately 20 mls of 5X Dernhardts, 5% dextran sulphate, 5X SSC, 0.5% SDS with 100 μg/ml Herring Sperm DNA. The PCR product used in screening was band isolated from a 2% agarose gel using the QiaexII gel extraction kit

(Qiagen). After band extraction 4 µl was resolved on a 2% agarose gel to determine concentration. 20 ng of DNA was then denatured in 47 µl of dH_20, chilled and finally added to the Ready-to-Go DNA labelling kit (Pharmacia). 30 µCi of $\alpha^{32}P$ dCTP (NEN DuPont, 3000 Ci/mmol) was then added and the reaction incubated at 37°C for 30 minutes. The probe was then purified using a G50 Sephadex™ column (Pharmacia). *Escherichia coli* DNA was also isolated from the bacterial strain DH10B and labelled using the Ready-to-Go DNA labelling kit as before. After purification the probes were both added to the pre-hybridisation solution at cpm/ml and incubated overnight at 65°C. The filters were then washed at 50°C for 30 minutes in 2X SSC, 0.1% SDS, followed by a final wash in 1X SSC, 0.1% SDS at 50°C. The filters were then exposed to X-ray film at room temperature overnight.

2.8.2 Utilisation of PAC clones

Protocols involving the growth of PAC clones and the isolation of DNA are citied on the World Wide Web homepage : http://bacpac.med.buffalo.edu.

2.9 Cloning in T-vector

PCR product cloning was carried out using the TA cloning kit (Invitrogen). 10 ng of PCR product to be cloned was incubated overnight at 16°C with 1X ligation buffer, 50 ng of the pCR™ II vector, sterile dH_20 and 4 units of T4 DNA ligase. 2 µl of the ligation was then transformed into INV αF' cells in the presence of 0.5 M β–mercaptoethanol, as for normal bacterial transformations and then incubated in SOC medium before plating. The transformants were plated onto ampicillin plates containing 20 mg/ml IPTG and 2% X-gal.

2.10 Computer Programs

PCR primers were designed using the MacVector software. Sequence alignments were performed using the Gene Jockey II Software from Biosoft.

2.11 Internet Resources

Sequence verification and identification are carried out by submitting any sequence to the National Centre of Biotechnology Information (NCBI) Basic Local Alignment Sequence Tool (BLAST-BLASTN) programme (Altschul *et.al.,* 1990) on the World Wide Web (http://www.ncbi.nlm.nih.gov.). The RepeatMasker programme can be found at the WWW site http://www.genome.washington.edu. Loci from mouse and rat chromomes 1 and 7 were found at the Mouse Genome Database (http://www.informatics.jax.org/) and the RATMAP (http://ratmap.gen.gu.se/) WWW homepages.

2.12 Somatic Cell Hybrid Panel

The somatic cell hybrid panel was supplied by Dr. C. Spirzer. The mouse and rat species used in the construction of the panel are BWTg3 and HRSRD, respectively. The Somatic cell hybrid panel was analysed by PCR. All PCR reactions were as standard. Reactions were firstly tested on the mouse and rat templates to ascertain that a difference can be observed between the two strains, if a difference was seen i.e. a length difference observed in the PCR product or no signal seen in the mouse. PCR was then carried out on the panel using approximately 100 ng of template DNA. The reactions were resolved on a 2% agarose gel and scored for the presence of the rat specific band.

2.13 Production of Rat Genomic Southern Blots

10 μg of Brown Norway genomic DNA was isolated as described previously and digested using 5U of *Bam*HI, *Bgl*II and *Eco*RI. The DNA was then loaded onto a 0.7 % agarose gel and resolved overnight at 10V. The gel was treated with 0.25 M HCl for 20 minutes. Before treatment with denaturing and neutralising solutions for 20 minutes. Then transferred to nitrocellulose by Southern blotting overnight.

Solutions

SOC medium

2% tryptone
0.5% yeast extract
10 mM NaCl
2.5 mM KCl
10 mM $MgCl_2$
10 mM $MgSO_4$
20 mM glucose (dextrose)

10XTBE(1 litre)

108g Tris
55g Boric acid
7.4g EDTA
Make to 1 litre
with dH_2O

20XSSC (1 litre)

175g NaCl
88.2g Na citrate
Make to 1 litre
with dH_2O.

2XYT (1 litre)

16 g bacto-tryptone
10g bacto-yeast extract
5g NaCl
pH 7.0

LB(Luria-Bertani) medium and plates

1.0% tryptone
0.5% yeast extract
1.0% NaCl
pH 7.0

Denhardt's reagent(50X)

5g Ficoll
5g polyvinylpyrroliodone
5g bovine serum albumin
Add dH_2O to 500 ml and filter.

TE

10 mM Tris-HCl (pH 7.4)
1 mM EDTA (pH 8.0)
pH 7.4

AHC medium

1.7 gm yeast nitrogen base without amino acids and $(NH_4)_2SO_4$ (Difco#0335-15)
5.0 gm $(NH_4)_2SO_4$
10 gm acid-hydrolysed caesin (U.S. Biochem. Corp., Cat#12852, low salt)
20 mg adenine hemisulphate (Sigma #A-9126)
Bring to 1 litre with dH20 and adjust pH to 5.8

Chapter 3

Identification of new genetic markers to allow more precise mapping of the *agu* locus, by isolation of microsatellite markers from P1 clones of rat genomic DNA.

Section 1 - Identification of new genetic markers from P1 clones of rat genomic DNA, isolated to contain the genes encoding GRIK5 and ATP4A.

3.1 Introduction

3.1.1 Identifying new genetic marker loci for mapping

The initial localisation of the *agu* gene to a genetic region of approximately 10 cM had involved the use of all the informative markers published to date for rat (Figure 3.1). As discussed previously (Chapter 1, Section 1.3), coverage of the rat genome with genetic markers was inadequate when compared to mouse and man. Localisation of *agu* to chromosome 1 was based on very few mapping marker loci. Therefore, further markers from within this interval of chromosome 1 in the rat were required to establish a map position and allow finer mapping of *agu.* Therefore much of the work carried out at this time was focused on the identification of new genetic markers from this region of rat chromosome 1.

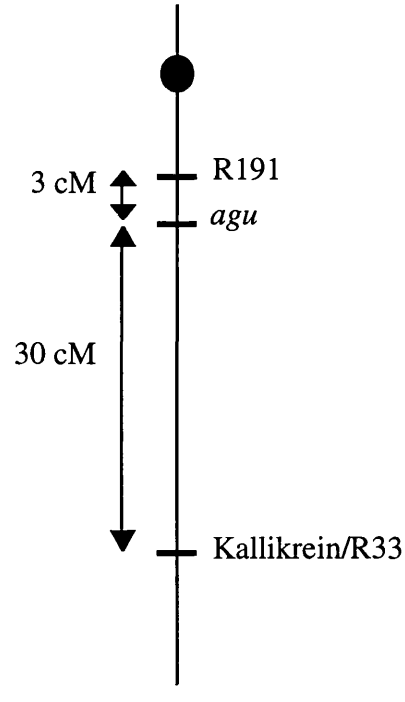

Figure 3.1 Markers and genes mapped flanking the *agu* locus on rat chromosome 1 (data as October, 1995). The Figure shows markers and genes shown by mapping to be the closest flanking marker loci to the *agu* locus in October, 1995. The markers were identified by Serikawa *et.al.,* 1992 and Jacob *et.al.,* 1995 and mapped on the F344/AS/AGU and BN/AS/AGU backcrosses. The black circle represents the centromere.

Three approaches for the identification of new genetic markers were followed: 1) identification of microsatellite sequences in P1 clones isolated from the interval containing *agu* in rat, 2) investigation of rat genes which had previously been shown to map within the interval, for strain differences using SSCP and 3) investigation of genetic marker loci previously mapped in the syntenic chromosome in mouse, for strain differences in rat.

The work described in this chapter concerns the identification of novel microsatellite sequences from P1 clones containing genes considered likely to map within the relevant interval. The bacteriophage P1 system permits cloning of DNA fragments of 75-100 kb as plasmids (Pierce *et.al.,* 1992; Sternberg, 1994). This system has three main advantages over other cloning systems ; the DNA can be faithfully replicated as a low copy number plasmid in *E.coli* (thus minimising rearrangements) but can be amplified to high-copy number using IPTG, cloning efficiency in the P1 system is better than in YAC clones (Sternberg, 1994) and DNA can be readily isolated as supercoiled circles by standard techniques. P1 clones were isolated using PCR primers designed by the Mac Vector programme (Chapter 2, Section 2.10) to these genes and microsatellite sequences identified from within the clone. Microsatellite sequences are identified by hybridisation to oligonucleotides synthesised as dinucleotide repeat units e.g. repeat $(CA)_{10}$. PCR primers are then designed to sequence flanking the microsatellite.

3.1.2 Genes identified for investigation.

Four genes were chosen for investigation in view of their positions within conserved regions of syteny between mouse, man and rat chromosome 1. The interval of rat chromosome 1 thought to contain the *agu* locus was syntenic to a region of mouse chromosome 7 and human 19q13.2 -13.4 (Yamada *et.al.*, 1994; The Mouse Genome Database (October 1995); and Stubbs *et.al.*, 1996; Figure 3.2 and 3.3). The genes encoding GRIK5, ATP4A, ferritin light chain (FTL) and ATPL were chosen for investigation. The investigation of the genes encoding ATP4A, FTL AND ATPL is described in Section 2, work on GRIK5 follows.

3.1.2.1 GRIK5

The rat gene GRIK5 encodes the kainate-preferring glutamate receptor subunit KA2. It was previously located to chromosome 1 in rat using a rat x mouse somatic cell hybrid panel (Szpirer *et.al.,* 1994) but had not been mapped to a specific region within this rat chromosome. The authors also reported the mapping of the mouse gene in interspecific backcrosses to the proximal region of mouse chromosome 7 and to human chromosome 19q13.2 by fluorescence in situ hybridisation (FISH). These regions had previously been

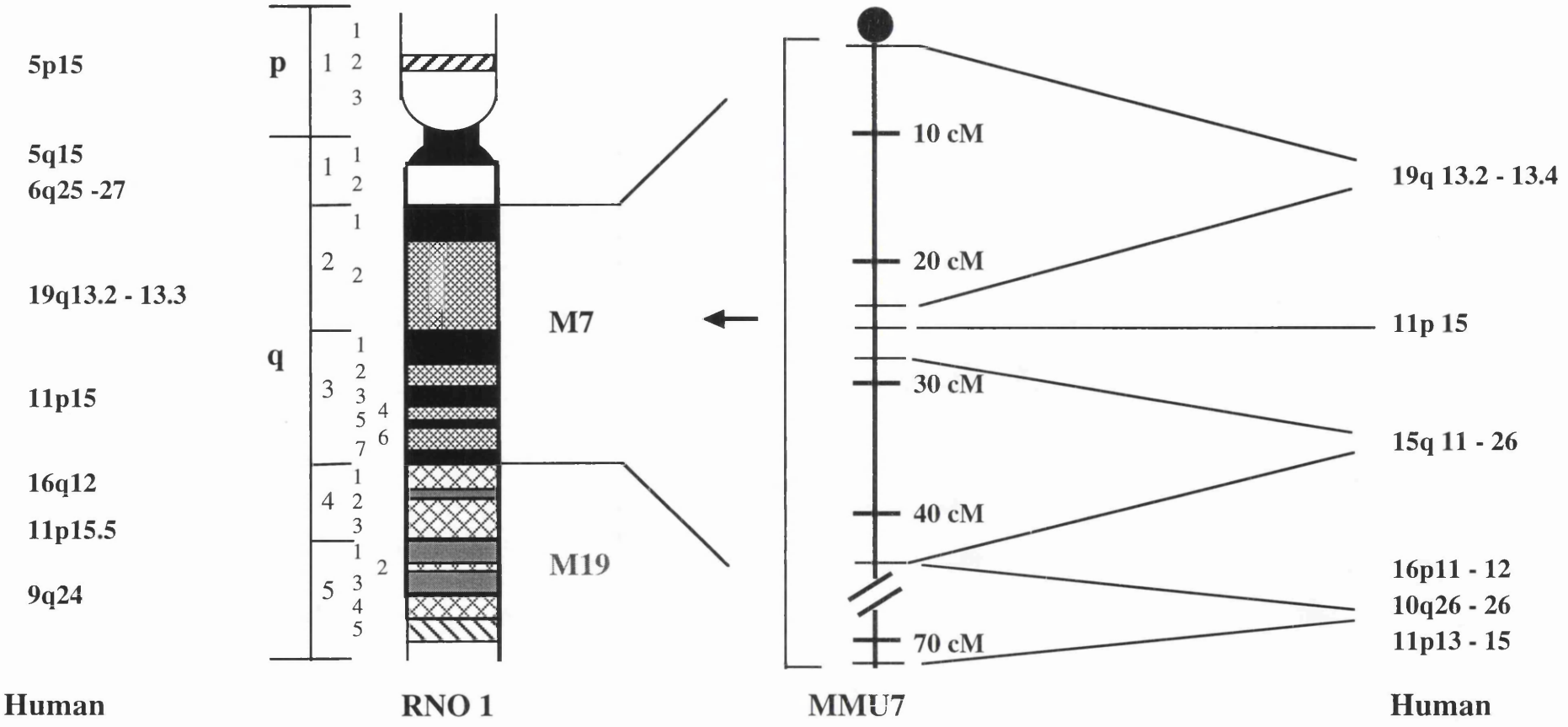

Figure 3.2 Conserved regions of synteny between rat chromosome 1 and mouse chromosome 7. Also conserved regions of syteny on human chromosomes to mouse chromosome 7. The rat/mouse data was taken from Scalzi and Hozier, 1998; the rat/human data from Szpirer, *et.al.*, 1997 and the human/mouse from The Mouse Genome database (28/3/1998).

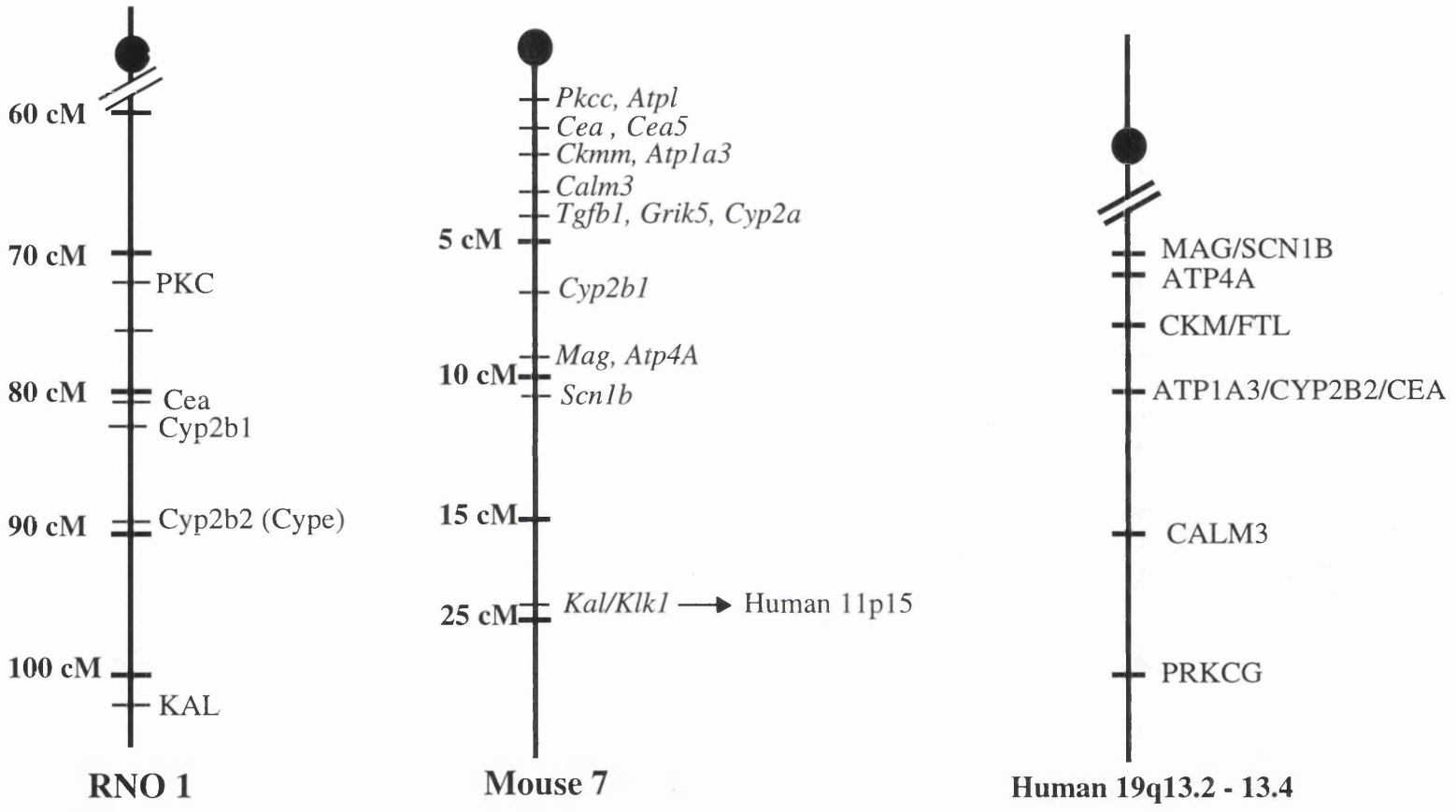

Figure 3.3 Detailed conserved regions of synteny in mouse and man with the interval of rat chromosome 1 containing *agu* (as October 1995). PRKCG/Pkcc and PKC are the genes encoding protein kinase C γ in all three species. Atpl = see text; Cea = family of pregnancy specific gylcoproteins encoded by genes 1 - 5; Ckmm/CKM = muscle creatine kinase; FTL = see text; ATP1A3/Atp1a3 = the gene encoding Na, K - ATPase alpha 3 subunit; GRIK5 = see text; Tgfb1 = transforming growth factor beta 1; Mag/MAG = myelin associated glycoprotein; Cyp2b1/2b2 = genes encoding cytochrome enzymes 2b1 and 2b2; KAL/Kal = gene encoding kallikrein 1; Calm 3 = gene encoding calmodulin 3; Atp4a/ATP4A = see text; Scn1b/SCN1B = sodium channel, voltage - gated, type I, beta polypeptide. Data taken from Serikawa *et.al.*, 1992; Stubbs *et.al.*, 1996 and The Mouse Genome Database (28/3/1998).

reported to be syntenic to the region of chromosome 1 in the rat within which the *agu* gene was contained (Fig.3.3) (Yamada *et.al.*, 1994; Cavanna *et.al.*, 1990).

3.1.2.2 Atp4A

The rat gene Atp4A encodes the rat stomach (H^+ and K^+)-ATPase (Shull *et.al.*, 1986) and was mapped at 9 cM on mouse chromosome 7 and to human chromosome 19q13.1 (Malo *et.al*, 1993), placing it within the a conserved region of sytenys for rat chromosome 1. The gene encoding the 16 kDa subunit of V-ATPases (*Atpl*) was mapped in the mouse to < 1 cM from the gene encoding protein kinase C gamma (*Pkcc*) and mapped to approximately 5 cM from the gene encoding GRIK5 on mouse chromosome 7 (Figure 3.3).

The justification for choosing the genes encoding ATPL and ferritin light chain (FTL) and the work carried out on them, are detailed in Chapter 3, Section 2.

Three other members of the research group (Dr.P.Shiels, Miss M. B.Duran Alonso and Mr M. Canhan) were also involved in the isolation of P1 clones and new microsatellites from this interval. Most of these genes e.g. Cype1 encoding cytochrome P450e, Cea 1- 5 encoding the CEA gene family of proteins and Atp1a3 encoding Na^+K^+ transporting, alpha 3 polypepetide, had previously been mapped to the correct interval in the rat genetic map (Serikawa *et al.*, 1992, Jacob *et al.*, 1995 and Gu *et.al.*, 1996). However, all the published markers proved to show not detectable allelic differences between the rat strains BN, AS/AGU and F344.

3.2. Results

3.2.1. Screening the P1 library for the pools of clones containing the GRIK5 gene

The cDNA sequence of the GRIK5 gene was retrieved from the National Centre for Biotechnology (NCBI) nucleotide database (Accession number : U08258) and the MacVector programme was used to design PCR primers to the cDNA. The primer pair GU103 forward and reverse were designed to amplify a PCR product of 224 bp from the GRIK5 gene. These primers were synthesised and optimised using rat genomic DNA (strain BN). The PCR product obtained was sequenced to verify that the correct product was obtained. Once this had been ascertained the PCR primer pair GU103 forward and reverse were used to screen the rat P1 library superpool lysates for the presence of the GRIK5 gene. Initially only the first 50 pools were tested as this had been shown to be sufficient to locate a clone (P. Shiels, personal communication). A PCR product of the correct size was observed in the pool of clones number 47 (Figure 3.4).

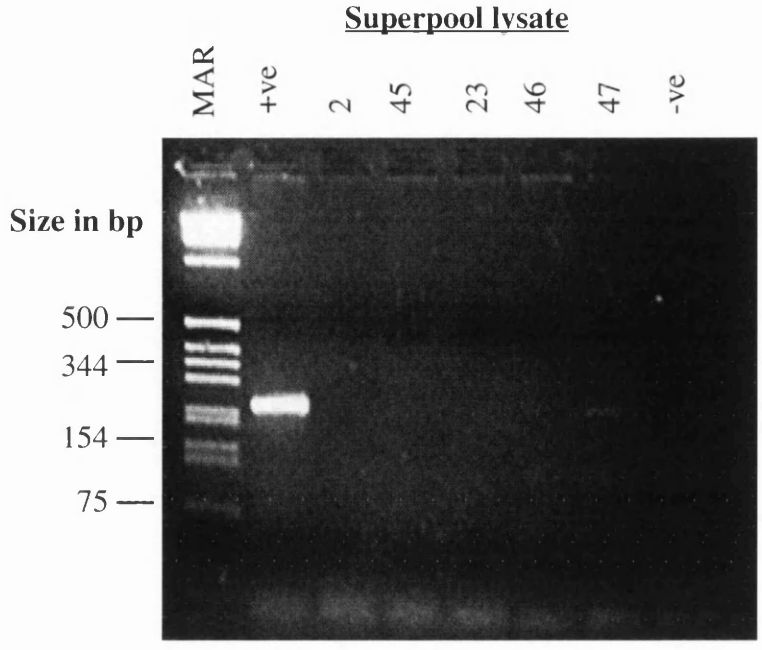

Figure 3.4 Identification of a positive P1 superpool with GU103
The +ve control was BN DNA and the -ve lacked DNA. Superpool 47 was the only strong positive signal.The marker (MAR) is 1 kb ladder.

3.2.2 Identification of a P1 clone containing the rat GRIK5 gene.

As a preliminary experiment pool number 47 was grown in liquid culture from the glycerol stock and plated onto agar plates containing kanamycin and 5% sucrose to select against vector without an insert. Superpool 47 contains 950 clones and approximately 2500 colonies were replica-plated and grown overnight to provide two identical sets of 15 plates. The bacterial colonies were washed from one set of plates and a PCR assay for GRIK5 carried out on dilutions of the wash containing the colonies. This procedure twice failed to detect a positive signal for GRIK5.

In this experiment, clones contained within the superpool were passed through three rounds of growth, the first in liquid culture. If the P1 clone for GRIK5 is at a growth disadvantage compared to other clones in the superpool then it may be have been competed out. Alternatively, the P1 clone insert may be unstable. Southard-Smith *et.al.*, 1994 reported one clone which was unstable and had to be purified in a single round of growth. However, this was only a preliminary experiment and the numbers of colonies screened were too small to be positive of these conclusions. A new system for isolating P1 clones was therefore devised.

A scraping was taken from the frozen glycerol stock of superpool 47 and was diluted in L-Broth medium, before plating onto agar plates with kanamycin and sucrose. Single colonies were picked, streaked onto another plate in grid formation and grown overnight. Samples of ten colonies at a time from the grid were picked into dH_20 to make lysates. These lysates of ten colonies were then screened for GRIK5. This new procedure reduced the number of times the colonies were grown before they were screened for a gene and only allowed clones to grow as isolated colonies on an agar plate, thus reducing competition between clones. In this way 560 colonies from pool number 47 were tested for the presence of the GRIK5 gene using the primers GU103 forward and reverse. A positive signal was obtained from lysate 54 (colonies 531-540) (Figure 3.5 a). These colonies were picked from the gridded plate and tested individually for GRIK5. A positive signal in the PCR was obtained from colony 534 (Figure 3.5 b). This P1 clone was named GRIK5/P1/1.

3.2.3 Isolation of plasmid DNA from P1 clones

Various methods of isolating DNA from P1 clones were evaluated within the laboratory: Qiagen kit, tip 100 purification of DNA, phenol/chloroform extraction after alkaline lysis, Wizard mini-prep and caesium chloride gradient purification. The Qiagen kit was initially used to isolate P1 DNA. This involves a standard bacterial cell lysis technique followed by purification of the DNA on a resin column. The plasmid copy number was increased by growing the bacterial culture in the presence of IPTG. The Qiagen protocol was modified by adding double the volume of solutions P1, P2, P3 and QC from the kit. However, the DNA yield was low (2.5 μg of DNA from 500 ml of culture) and of poor quality; some shearing of the DNA was observed (Figure 3.6 a) and some preparations were resistant to restriction enzymes. The problems encountered could be a result of purifying large plasmid DNA using resin columns; a large volume of bacterial cell culture is required for high DNA yield, and the resulting bacterial debris in the column could be reducing the efficiency of the purification.

Caesium chloride gradient purification gave high quantities of good quality DNA. However, the method is lengthy and expensive, and the yield and quality of DNA was comparable with standard alkaline lysis followed by phenol/chloroform extraction of the DNA. This procedure produced relatively large quantities of DNA (20 μg of DNA from 50 ml of culture) which was readily digestible. Shearing was reduced by using pipette tips with cut ends (Figure 3.6 b). This method was adopted as the standard procedure for extracting DNA of P1 clones.

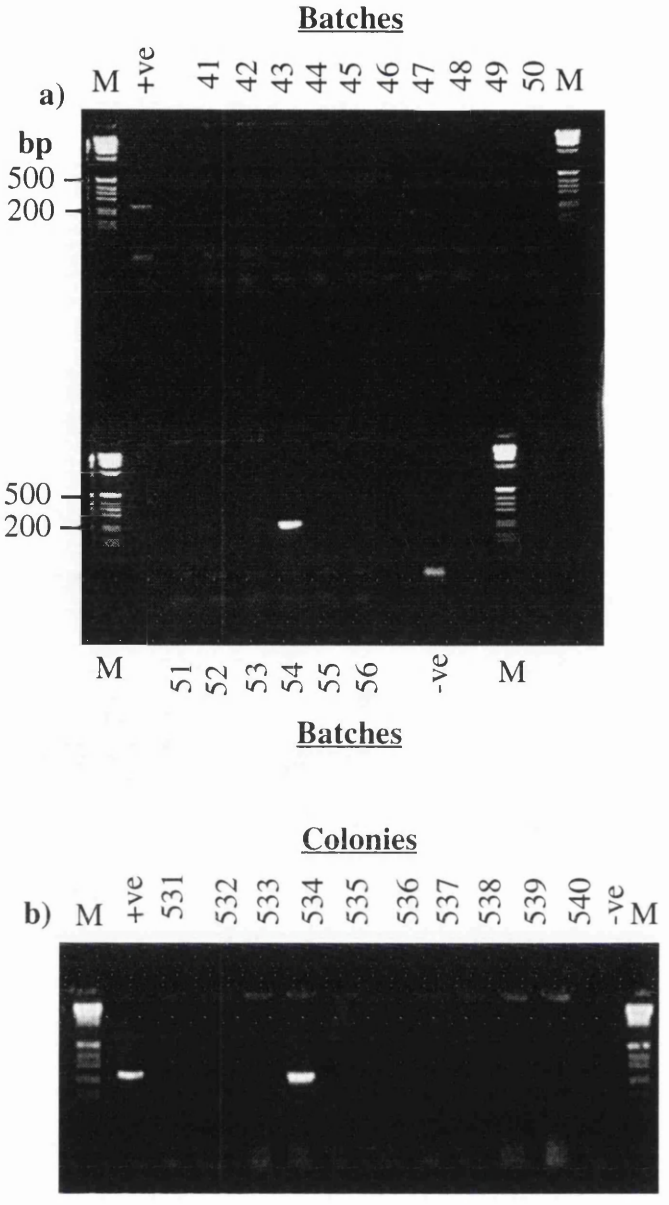

Fig. 3.5 PCR assay for GRIK5 in a screen of P1 library superpool 47.
Colonies were in batches of ten and the mixed template was screened by PCR.
a) PCR tests of batches 41-56. A positive signal was seen for batch 54.
b) PCR tests colonies 531-540, from batch 54. The +ve control was a PCR reaction carried out in the presence of BN genomic DNA as template. The negative control (-ve) is a PCR reaction without DNA. The marker (M) was a 1 kb ladder (Materials and Methods, Section 2.1.1).

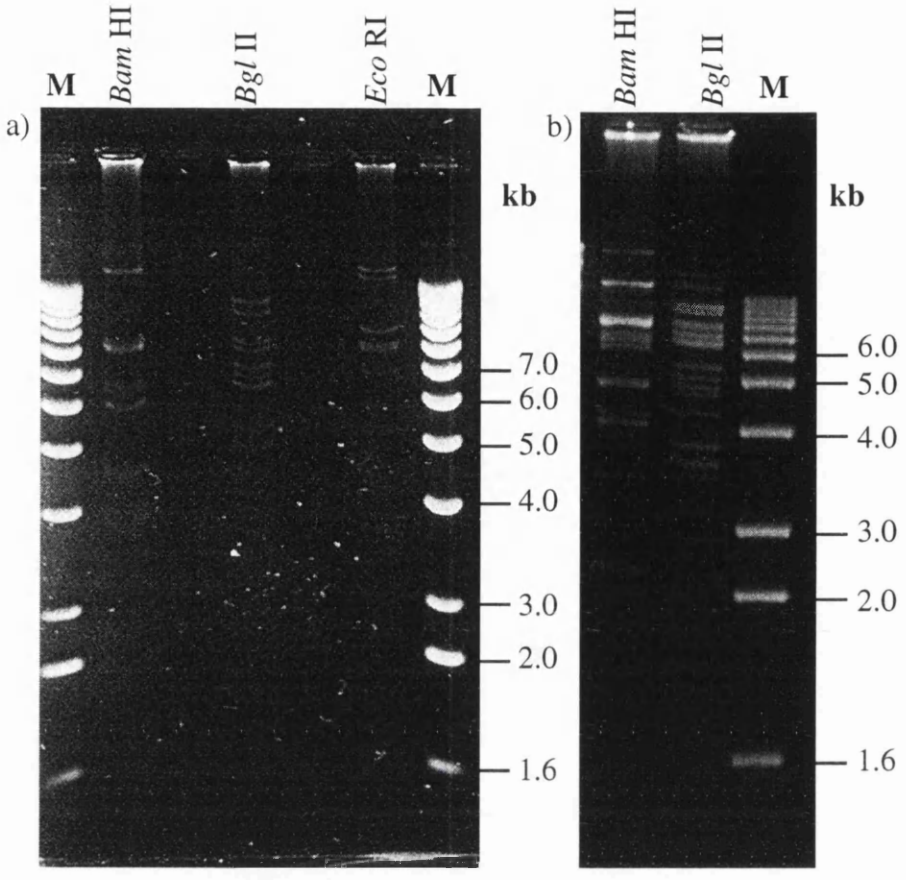

Figure 3.6 Digestion patterns of DNA from GRIK5/P1/1 isolated by two different methods.

a) The Qiagen kit using the tip 100. 1/10 of the final yield of DNA was digested.

b) NC1 DNA isolated by the phenol/chloroform extraction method. 1/50 of the final yield was digested. DNA fragments were resolved on a 0.5% agarose gel. The marker (M) was a 1 kb ladder.

3.2.4 Identification of novel SSRs in the P1 clone GRIK5/P1/1.

DNA isolated for GRIK5/P1/1 using the phenol/chloroform purification method was digested with *Bam* HI, *Bgl* II and *Eco* RI and the digestion products resolved on a 0.5% agarose gel. (Figure 3.7 a) The gel was Southern blotted and the blot probed with a ^{32}P labelled $(CA)_{10}$ oligonucleotide the most frequent repeat in the rat genome (Beckmann and Weber, 1992). At least five different $(CA)_n$ repeats were identified in clone GRIK5/P1/1 (Figure 3.7 b), which corresponded to the number expected if repeats occur on average every 21 kb of genomic DNA (Stallings *et.al.*, 1991), and the average P1 clone contains an insert of 75-100 kb.

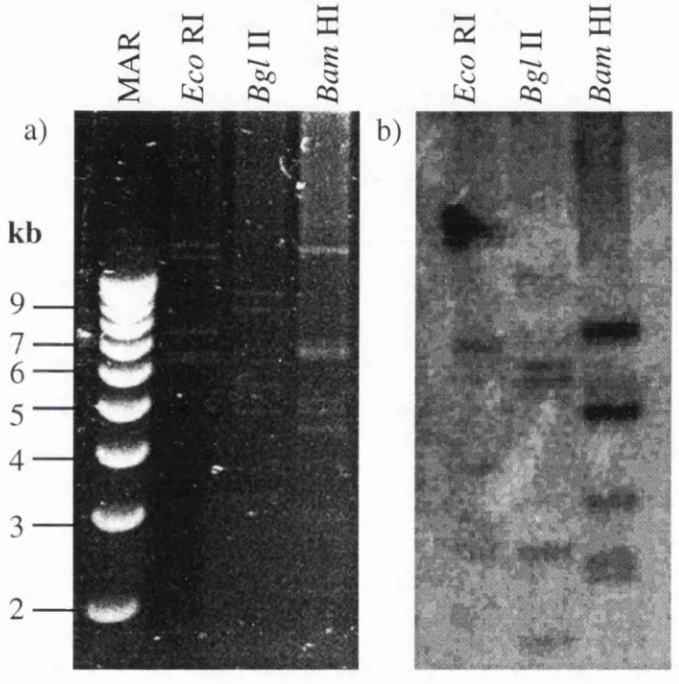

Figure 3.7 a) P1 clone GRIK5/P1/1 cut with *Bam* HI, *Bgl* II and *Eco* RI and the digests resolved on a 0.5% agarose gel. The marker was 1 kb ladder.
b)This gel was Southern blotted and the blot probed with a radioactively-labelled (CA)10 oligonucleotide. At least 5 bands were identified in the *Bam* HI digestion products.

The *Bam* HI digestion products from GRIK5/P1/1 were shot-gun cloned into pUC18, because on Southern blots the size range of fragments with $(CA)_n$ repeats were smallest when digested with Bam HI. DNA from the resulting colonies was screened by hybridisation for $(CA)_n$ repeats. Five positive clones were identified, with insert sizes between 1.8 and 7 kb (T1.1, T1.3, T1.11, T1.13, T1.16) (Figure 3.8).

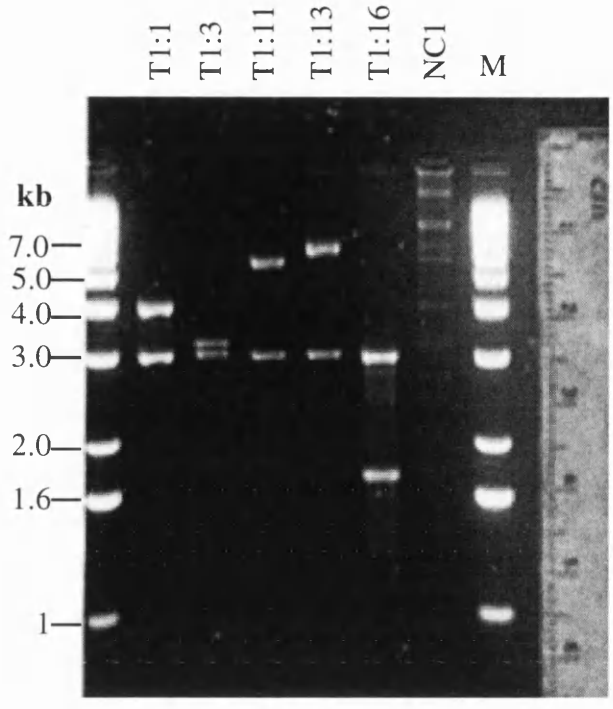

Figure 3.8 Comparison of digested sub-clones from GRIK5/P1/1 containing (CA) repeats compared to the digest of the P1 clone. The cloned inserts were digested from sub-clones with *Pst* I and *Xba* I and compared to digested bands from GRIK5/P1/1 digested with *Bam* HI. The marker was a 1kb ladder.

Clone T1.16 (Figure 3.8) had the smallest insert (1.8 kb), and a $(CA)_{21}$ repeat was found when it was sequenced (Figure 3.10). This sequence enabled me to specify the primer GU106 forward on one flank of the repeat but it was necessary to sub-clone the repeat to obtain quality data from the other flank. A 900 bp *Sst* I fragment was shown to contain this repeat (Figure 3.9) and was sub-cloned into pBluescript. Sequencing from GU106 and from the M13 reverse primer yielded acceptable sequence from which a pair of PCR primers (GU106 forward and reverse) were designed (Figure 3.10). PCR products amplified with GU106 forward and reverse showed no length variation between F344, AS/AGU and BN.

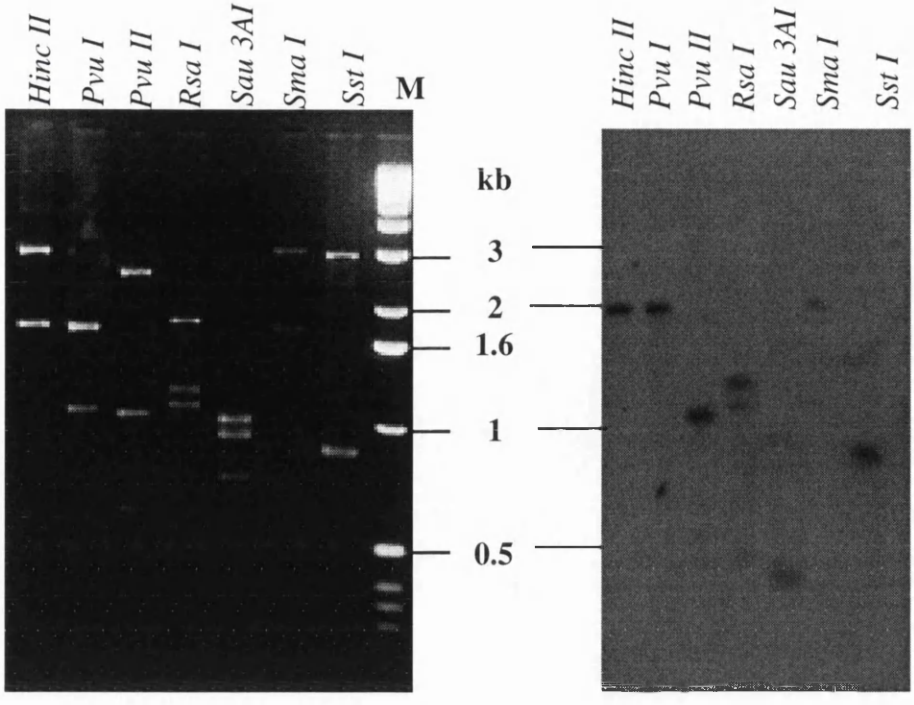

Figure 3.9 Subcloning of a microsatellite. a) Double digest of T1:16 with *Bam* HI and a second enzyme, as indicated, to identify a smaller fragment containing the (CA) repeat in order to allow sequencing. The marker was a 1 kb ladder. b) A Southern blot of the gel (a) was probed with a $(CA)_{10}$ oligonucleotide. A 900 bp fragment containing the (CA) repeat was detected in the *Bam* HI/*Sst* I digest.

GU106 F →

151 CCTTGCTCCC AGCACTCAGC GTCGCCTGCC TT**CACCGTCT TTCTCTCTGT**

201 **CTT**TCTTTCC CATTTTCTTC TCCCTTCCCC CTGCCCCTGG CCTTCTGGTC

251 ACTCTTCTCT GGTCCCAGTG AGTGCCTCGT CAGCCACTGA CAGAACCAGA

301 *CACACACACA CACACACACA CACACACACA CACACACACA* CAGGAGACAT

← GU106 R

351 AAGGATGGAC AAACAGGCCC AGATACAGAA ATGGTTAAA**C ACTGACAGAC**

401 **TGGACAAGC**A GAGAGAGGGA CACACTGACA AATGCAGACT GATAGACACA

451 GCTCCTCTGA GA

Figure 3.10 Identification of sequence flanking the repeat in T1.16. This allowed the primer pair GU106 forward (F) and reverse (R) to be specified to amplify the repeat. The $(CA)_{21}$ sequence is shown in italics and the primers shown in bold.

Considerable time was expended on clone T1.16, the first clone containing a repeat to be investigated, without finding a useful marker for mapping. It was therefore important to increase the rate of experimentation. I therefore adopted the strategy of digesting the entire NC1 P1 clone with *Sau* 3A. This yielded smaller fragments which required fewer rounds of sub-cloning in pUC 18. The resulting colonies were screened by colony hybridisation with the oligonucleotide $(CA)_{10}$ (Figure 3.11). Four positive clones were identified (T3:39, T3:40 T3:42, T3:60), all having inserts around 600 bp, which can be completely sequenced using the vector primers. Sequence analysis showed that sub-clones T3:40 and T1:16 contained the same repeat. T3:39 contained a $(CA)_{15}$ repeat, which the primer pair GU111 forward and reverse was designed to amplify. T3:40 was observed to contain a $(CA)_{16}$ repeat.

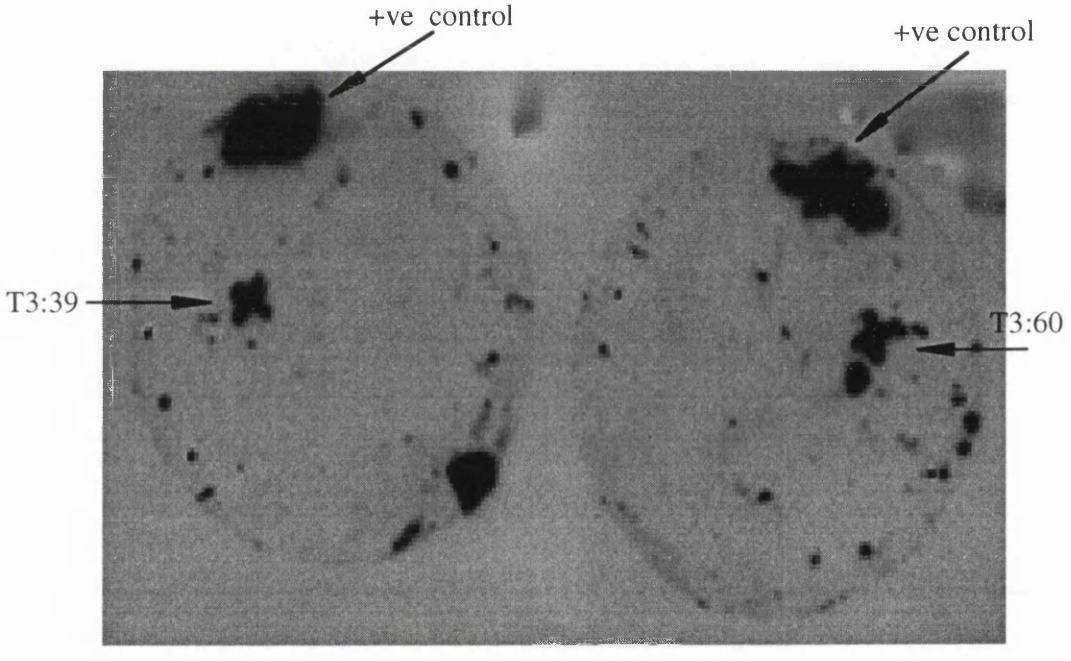

Figure 3.11. Hybridisation blots of colonies resulting from a sub-cloning of GRIK5/P1/1, with a radioactive $(CA)_{10}$ oligonucleotide. Colonies were gridded, each streaked in the shape of a cross, onto agar plates. Duplicate plates were also streaked in this way. The positive control was a T1.16 colony streaked onto the plate. The positive colonies T3.39 and T3.60 are indicated by arrows.

3.2.5 Mapping of a new marker from clone GRIK5/P1/1

A $(CA)_{20}$ repeat followed by an interrupted $(CA)_n$ repeat of 144 bp was identified in the sub-clone T1.13 when it was sequenced with the M13 forward primer (Figure 3.12). PCR primers (GU10 forward and reverse) were used to amplify the repeat and the

products were assessed for length variations between the rat strains BN, AS/AGU and F344.

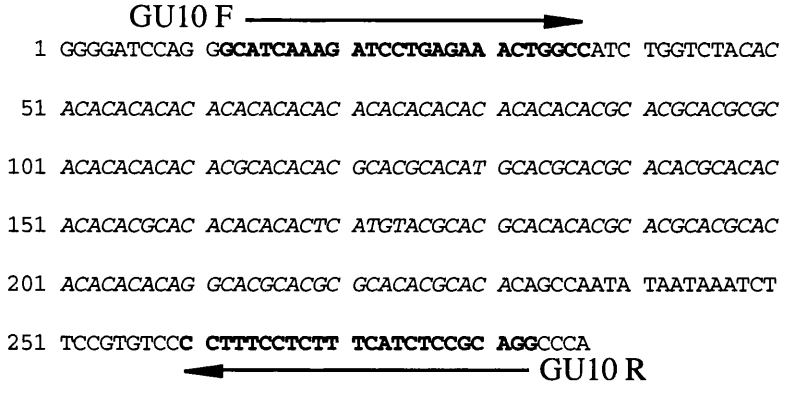

Figure 3.12 Identification of a (CA) repeat within sub-clone T1.13. T1.13 DNA was sequenced using the M13 forward primer. The PCR primers (GU10) were designed to amplify the repeat and are indicated by arrows and shown in bold. The repeat is shown in italics.

PCR reactions were resolved on 4% Metaphor gels, an agarose which can resolve a difference of 2% in the length of a product in the size range of 200 to 800 bp. A length difference was observed with the primer pair GU10 forward and reverse, with AS/AGU > F344 (Figure 3.13). The primer pair GU10 forward and reverse was then used to genotype 205 progeny from the F344/AS/AGU backcross (Appendix 2). An example of the mapping data is given in Table 3.1. The resulting recombination fraction between GRIK5 (GU10) and *agu* was 0.06 (12 recombinant animals from 205 backcross progeny typed). This placed GRIK5 and the marker GU10 approximately 6 ± 1.6cM from the *agu* mutation using the Kosambi estimate of map distance (Kosambi, 1944). PCR products from the rat strains were cloned into the PCR II cloning vector and sequenced to identify the length variation between the three strains: the F344 PCR product was 12 bp smaller than the AS/AGU PCR product and the BN PCR product (BN = AS/AGU > F344) (Fig.3.14).

However, other markers isolated from the P1 clone NC1 were non-informative in these rat strains on 4% metaphor ; they were not resolved on 6% acrylamide which is capable of resolving differences of a single repeat unit (i.e. 2 base pairs).

Animal number	Phenotype of animal	Genotype at the locus GU10	Genotype
F671-95	Ataxic	Heterozygote	**Recombinant**
F672-95	Ataxic	Homozygote	Parental
F673-95	Ataxic	Homozygote	Parental
F674-95	Ataxic	Heterozygote	**Recombinant**
F675-95	Normal	Heterozygote	Parental
F676-95	Ataxic	Homozygote	Parental
F677-95	Normal	Heterozygote	Parental
F678-95	Ataxic	Homozygote	Parental
F679-95	Normal	Heterozygote	Parental
F680-95	Ataxic	Homozygote	Parental

Table 3.1 Sample mapping data of the *agu* gene relative to marker GU10.

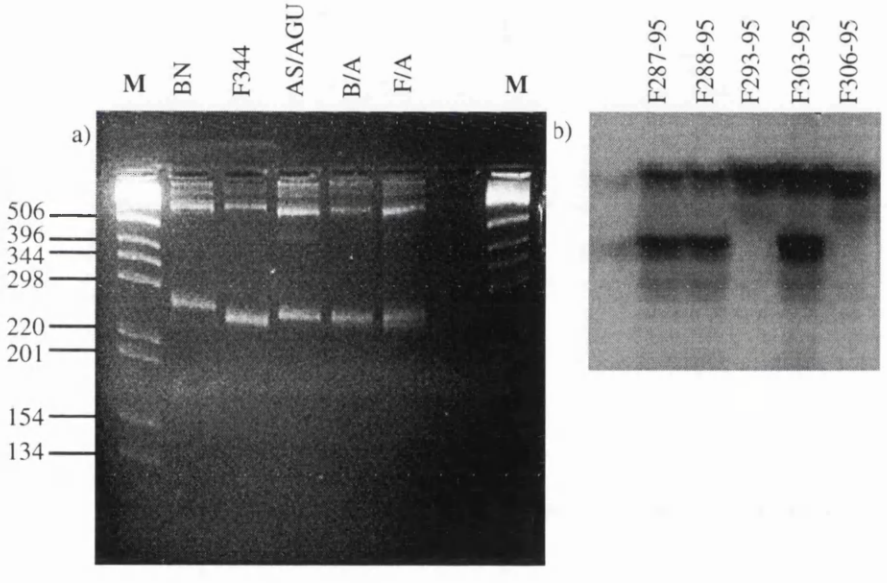

Figure 3.13 Typing of F344 backcross progeny with the marker GU10.

a) Resolution of the PCR products from the primer pair GU10 forward and reverse, on 4% Metaphor agarose. The PCR products display a difference of AS/AGU > F344, as shown on the gel. The B/A and F/A animals are heterozygote animals from each backcross. The marker (M) was 1 kb ladder.

b) Resolution of the PCR products from the primer pair GU10 forward and reverse, on a 6% acrylamide gel. One of the primers was labelled and the PCR product resolved on an acrylamide gel. The samples shown are backcross progeny from the F344 backcross; the animal numbers are indicated at the top of the gel.

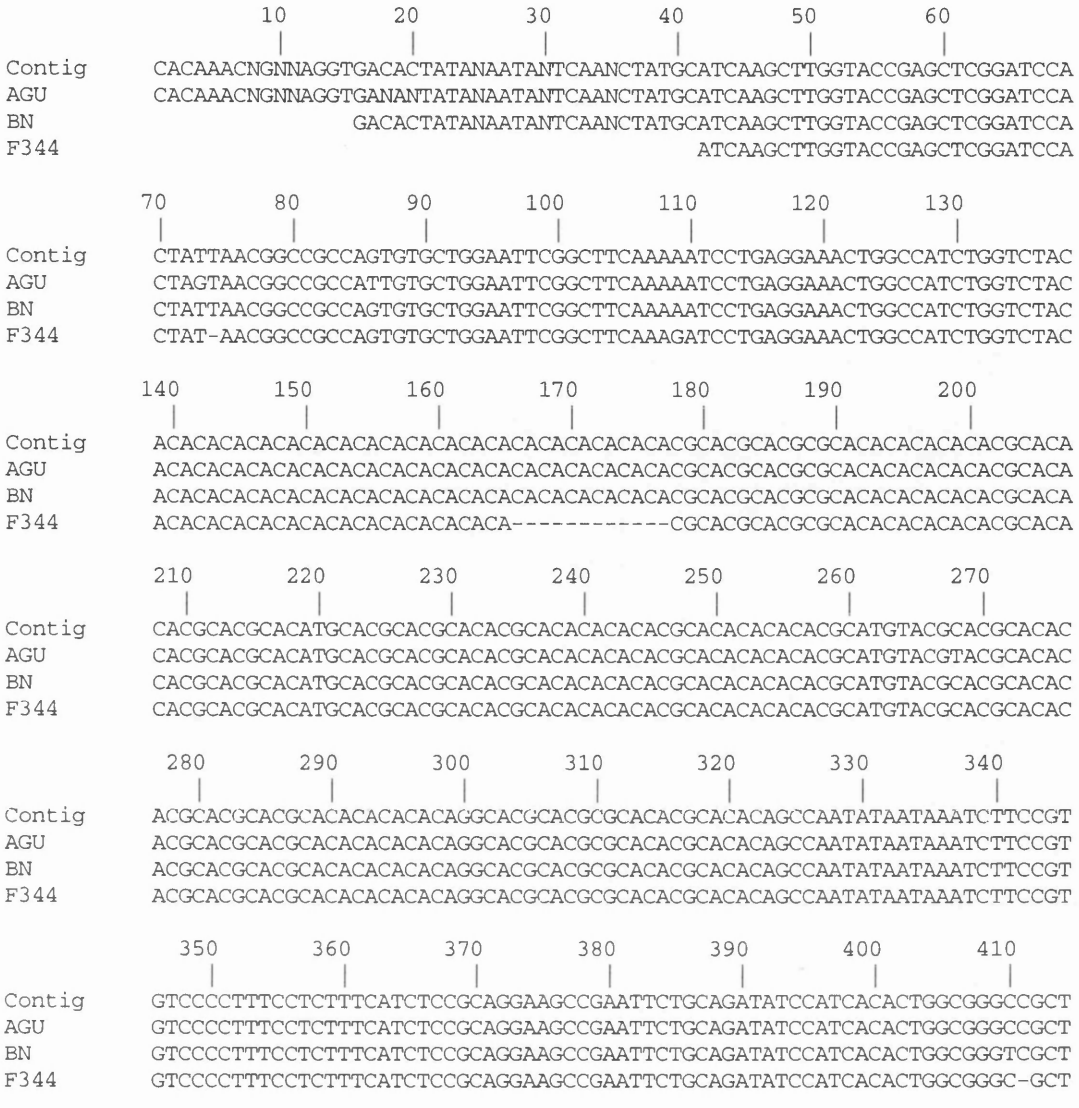

Figure 3.14. Sequence alignment of PCR products obtained from the strains BN, F344 and AS/AGU using the primers GU10 forward and reverse. Strain F344 has a deletion of 12 bp between bases 165 and 178 as indicated by a dashed line.

3.2.6 Screening the P1 library for a clone containing the gene encoding Atp4A.

PCR primers (GU101 F and R) were designed to the cDNA for the rat Atp4A gene (Accession number: J02649). Once optimised to give a PCR product of approximately 228 bp, the primers were used in a screen of the rat P1 library pool lysates. A PCR signal was obtained from library pool number 45 (Figure 3.15) which contained approximately 950 clones. 1400 colonies from this pool were plated out onto four agar plates. Colonies were picked into pools of ten and these screened by PCR, as described for the P1 clone screened for the GRIK5 gene (Section 3.2.2). However, after a total of 820 colonies had

been screened in this way, no positive signals were obtained. GU10, identified from a P1 clone containing the gene encoding GRIK5, had been mapped 6 cM from *agu* and as the gene *Atp4A* mapped centromere distal to *Grik5* on mouse chromosome 7 and was therefore expected to be located distal to *agu* than GU10 in the rat. No further work was carried out on this gene.

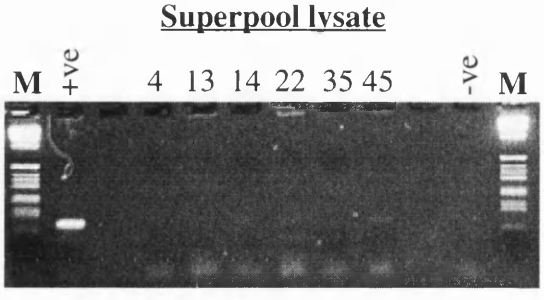

Figure 3.15 Screening of selected P1 library pool lysates with primer pair GU101 forward and reverse, for the gene encoding Atp4A. The pool lysates (numbered above the gel lanes) had previously been tested and had shown faint signals; this experiment showed the result to be reproducible. The positive control (+ve) contained BN DNA and the negative (-ve), no DNA. The marker (M) was 1 kb ladder.

Section 2 - Identification of new genetic markers from P1 clones of rat genomic DNA, isolated to contain the genes encoding ATPL and FTL.

3.3 Introduction

Chronologically the work carried presented in this chapter was carried out after the mapping of markers R158 (Section 5.2) and GU10 (Section 3.2.5), but as the work detailed also involves isolation of markers from P1 clones, I will describe the work within this chapter. Mapping of markers from within our original region of study e.g. GRIK5/GU10 and R158, produced a narrower field for investigation. Further genes, previously mapped within the mouse genome, were also identified, as the region of synteny between mouse and rat became clearer. Genes were identified for study from genetic mapping within the mouse which were observed to map close (< 1 cM) to the closest marker to *agu*, R158. Therefore, the genes encoding *Atpl* and ferritin light chain (*ftl*) were chosen because in mouse they map within 1 cM of *Pkcc* i.e. R158 (MGD). Also the gene encoding ferritin light chain was considered a putative candidate gene and had been mapped to the conserved region of syteny in man.

3.3.1 Atpl

The cDNA encoding the 16 kDa subunit of vacuolar H^+-ATPase was cloned from rat liver by Nezu *et.al.*, (1992). Vacuolar H^+-ATPases are distributed in membrane systems of eukaryotic cells e.g. vacuoles, Golgi apparatus and plasma membrane. V-ATPases function as a proton pump coupled with ATP hydrolysis and maintain the interior acidic pH of these organelles. The gene encoding the 16 kDa subunit of V-ATPases (*Atpl*) was mapped in the mouse to < 1 cM from the gene encoding protein kinase C gamma (*Pkcc*). Both of these genes were identified to be approximately 5 cM centromere proximal from GRIK5 on mouse chromosome 7 (Figure 3.3 and 3.16). Isolation of a P1 clone containing the rat *Atpl* gene and mapping of new microsatellites would allow mapping of the rat gene and facilitate further mapping of *agu*.

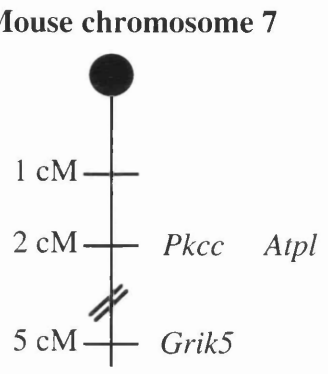

Figure 3.16 Mouse genetic map of chromosome 7. Taken from The Mouse Genome Database.

3.3.2 FTL

Ferritin is the major intracellular iron store in all organisms. Increasing evidence indicates that iron-induced oxidative stress may participate in the cascade of events leading to nerve cell death in Parkinson's disease (PD). Levels of iron in the substantia nigra are increased from 35% to 77% in PD cases compared to normal controls (Dexter *et.al.*, 1989, Hirsch *et.al.*, 1991 and Sofic *et.al.*, 1991). The expression of ferritin is regulated by the intracellular iron concentration, and when iron levels are high ferritin mRNA is translated leading to iron storage. It could be expected that the expression of the ferritin protein is affected in the substantia nigra of PD brains leading to excessive levels of iron within the brain. Mammalian liver and spleen ferritin consist of 24 subunits of two species, the heavy and light subunits. Brown *et.al.* (1983) presented evidence that in the rat, the two species of subunits are coded by separate mRNAs. By studying human/Chinese hamster hybrid cells and use of a radioimmunoassay specific for human ferritin, Caskey *et.al.* (1983) showed that human chromosome 19 encodes the structural gene for ferritin. By study of hamster-human and mouse-human hybrid cells, some with translocations involving chromosome 19, Worwood *et.al.* (1985) concluded that light subunits of ferritin are coded by a gene in the segment 19q13.3. The gene encoding ferritin light chain therefore mapped to the region of the human genome syntenic to the rat genomic region containing the *agu* mutation and was considered a likely candidate gene to contain the *agu* mutation.

3.4 Results

3.4.1. Identification of a new genetic marker from a P1 clone containing DNA sequence from the rat Atpl gene.

PCR primers were designed with the aid of the Mac-Vector software, to the rat cDNA encoding the 16 kDa subunit of the vacuolar H^+-ATPase (Accession numbers : D10874

and D01244). The primers (NCA forward and reverse) were designed to the 3' untranslated region of the cDNA and were optimised to produce a 149 bp product from rat genomic DNA (strain BN). These primers were used to screen the P1 library superpool lysates. Library pool number 65 produced a PCR product of the correct size (Figure 3.17) and contained 950 clones. A slightly different strategy was then used to identify the P1 clone containing the ATPL gene sequence: 5,000 colonies from the superpool were plated onto agar plates containing kanamycin and the plate divided into quarters and the colonies scraped into L-Broth. PCR was then carried out on lysates of these quarters to identify one containing the sequence encoding ATPL. One quarter was identified as positive from this PCR (Figure 3.18) and the clones from this were plated out. These colonies were picked into lysates containing ten colonies and were screened by PCR. 720 colonies were screened from this positive quarter and a positive lysate identified, the single colonies were tested and one positive obtained. This clone was called ATPL/P1/2.

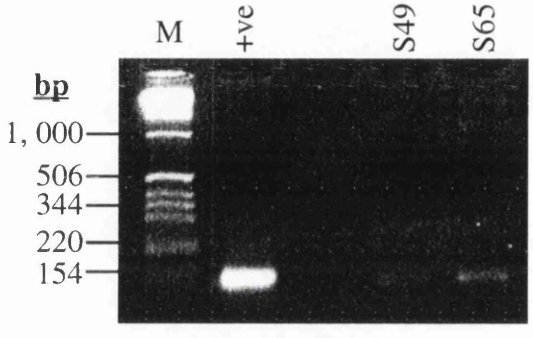

Figure 3.17 Identification of a superpool (S65) containing the gene encoding ATPL by PCR. The superpool 49 (S49) also gave a weak signal. The marker (M) was a 1 kb ladder.

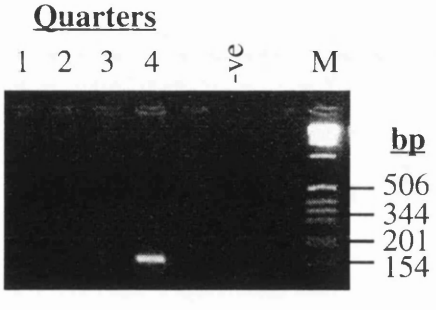

Figure 3.18 Identification of a positive quarter taken from a plate containing colonies from superpool 65. Quarter four was the only positive. The marker (M) was a 1 kb ladder.

ATPL/P1/2 DNA was cut, electrophoresed, Southern blotted and probed with a radioactively-labelled $(CA)_{10}$ oligonucleotide to identify the microsatellite repeats within this clone. Two positive fragments were identified from ATPL/P1/2. P1 clone ATPL/P1/2 was restricted with *Sau* 3A and shot-gun cloned into pUC 18. Colony

hybridisation was performed on the resulting blot from the colonies with the radioactively-labelled $(CA)_{10}$ repeat probe to identify sub-clones containing this microsatellite. One was identified. The positive sub-clone was sequenced using the M13 forward and reverse primers and a $(CA)_{22}$ repeat identified within the sub-clone (Figure 3.19). This sub-clone also contained a $(TA)_{24}$ repeat. The PCR primer pairs (H31C and H31T forward and reverse, respectively) were designed to amplify a PCR product containing both of these repeat structures (Figure 3.19).

Figure 3.19 Sequence identified from a sub-clone from ATPL/P1/2 containing $(CA)_{17}$ and $(TA)_{24}$ microsatellites (shown in italics). The PCR primers are shown in bold.

The PCR products produced from the primer pairs H31C and H31T forward and reverse were assessed for length differences between PCR products containing these repeats. Both sets of PCR products were resolved on 6% acrylamide gels and H31T displayed a length polymorphism (BN>AS/AGU). This marker was then used to genotype progeny from the BN/AS/AGU backcross. The marker produced from H31T forward and reverse was shown to be unlinked to *agu* (it displayed >50% recombination between the marker and *agu* $p = > 0.1$), however, only a small number of animals was tested ($n = 20$). Subsequent testing with the primers H31T forward and reverse on a somatic cell hybrid panel indicated that this marker mapped to rat chromosome 4 (Figure 3.20 and Table 3.2)

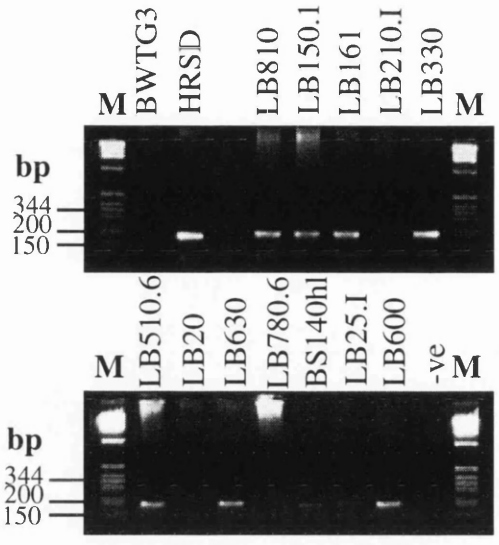

Figure 3.20 Analysis carried out on the somatic cell hybrid panel. (Section 2.12) with H31T forward and reverse (Atpl). BWTG3 is the mouse strain and HRSD the rat strain used in the construction of the panel. The other lanes contain hybrids from the panel. The marker (M) was a 1 kb ladder.

		Chromosome 4	
H31T		+	-
	+	9	0
	-	0	3

Table 3.2 Contingency table for H31T showing localisation on chromosome 4.

3.4.2. Mapping of a rat ferritin light chain gene.

PCR primers, GU9 forward and reverse, were designed to amplify a fragment from exon four of the rat ferritin light chain gene (Accession number : J02741). The primers were used to screen the P1 library and identified a positive clone, F16 from superpool 39. This P1 clone was digested with *Sau* 3A and shot-gun cloned into pUC 18; the resulting colonies were screened for (CA) microsatellites by hybridisation to colony blots with a radioactively-labelled $(CA)_{10}$ repeat oligonucleotide. Five colonies were identified that contained this microsatellite (Figure 3.21). The cloned DNA inserts were sequenced using the M13 forward and reverse primers and the microsatellites within these clones were identified (Figure 3.22). PCR primers were designed to the sequence flanking the microsatellite (Table 3.3).

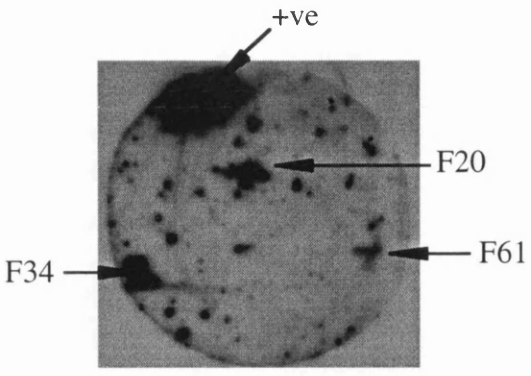

Figure 3.21 Shot-gun subclones from F16 probed with a radioactively-labelled $(CA)_{10}$ repeat oligonucleotide. The positive control (+ve) is a colony from a sub-clone from GRIK5 known to contain a $(CA)_n$ microsatellite by sequencing. The colonies F20, F34 and F61 are positive.

Marker	Microsatellite	Strain difference	Mapping
F20	$(GT)_{19}$	No	-
F34	$(CA)_{27}$	BN>AS/AGU	22/52 = 42.3 ± 6.8
F61	$(CA)_{17}$	No PCR product	-
F101	$(CA)_{12}$	BN>AS/AGU	-
F110	$(CA)_{13}$	No	-

Table 3.3 Summary of microsatellite markers identified from F16. F16 is a P1 clone containing the ferritin light chain.

The genetic marker amplified by the primers F34 forward and reverse displayed a strain difference between BN and AS/AGU (BN > AS/AGU) and was used to genotype 52 BN/AS/AGU backcross progeny to 42.3 ± 6.8 cM from *agu*.

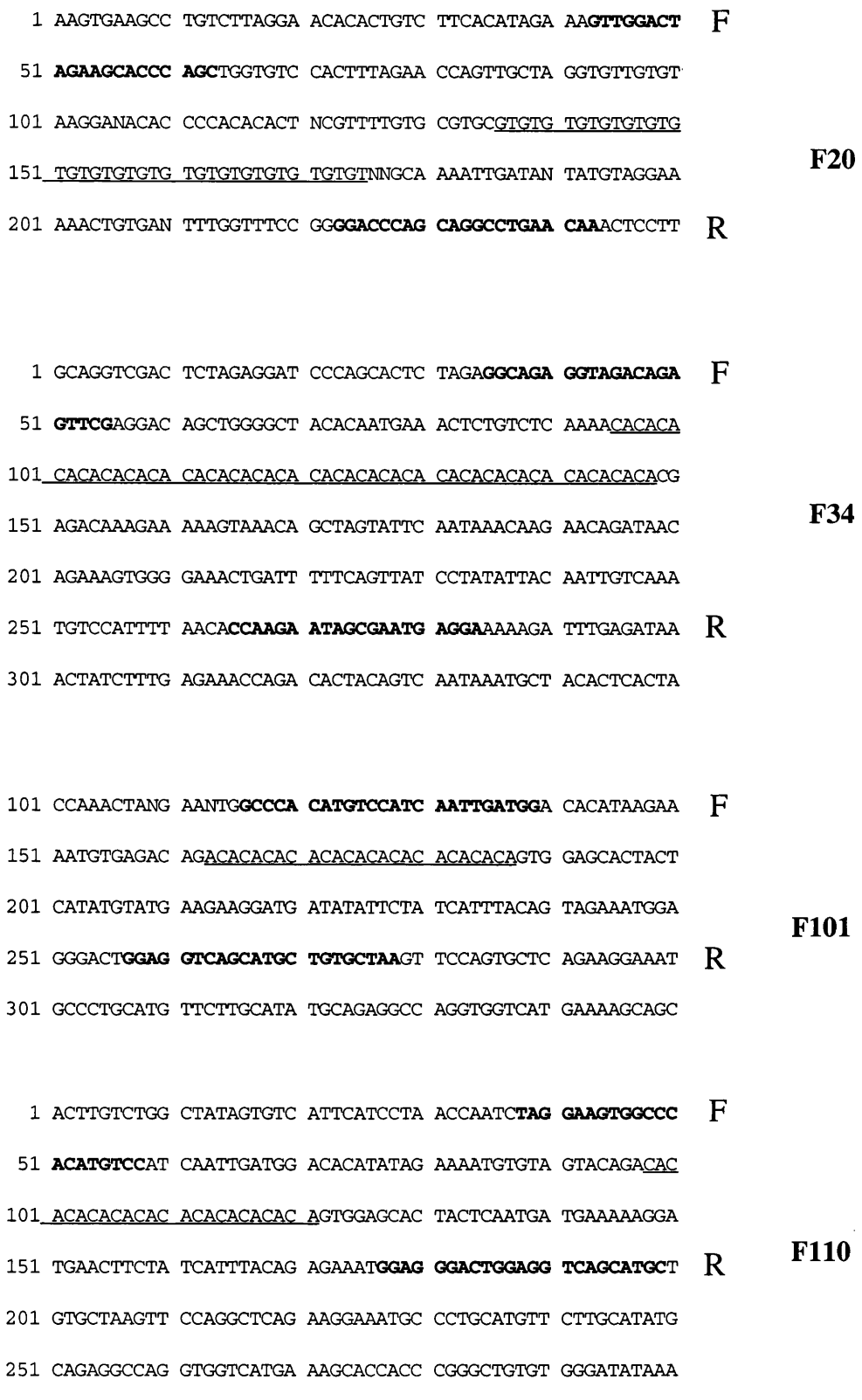

Figure 3.22 Microsatellite sequences generated from sub-clones of the P1 clone F16, containing the gene encoding ferritin light chain. The microsatellite sequences are underlined and the PCR primers designed to amplify them are shown in bold, the forward (F) and reverse primers (R) indicated.

3.5 Discussion

The object of this work was the identification of new rat genetic markers to map the *agu* gene. Isolation and mapping of novel microsatellites within 10 cM of *agu* will provide a finer genetic map for the positional cloning of *agu*.

Data obtained with the primer pair GU10 forward and reverse allowed the mapping of the GRIK5 gene relative to *agu* and relative to published markers on this chromosome e.g. D1Mgh7 and D1Mit1. A recent paper by Szpirer *et. al.*,(1997) positioned GRIK5 to 1q21 on the rat chromosome by fluorescence in situ hybridisation (FISH) allowing the integration of the linkage and cytogenetic maps. This confirmed the mapping of GRIK 5 to this region of rat chromosome 1 (Figure 3.23).

The methods used in the identification of new P1 clones, containing genes of interest, were laborious and time consuming. The problems encountered with the isolation of P1 clones may be due to the instability of certain P1 clones or the rarity of others. Therefore, the screening for a P1 clone containing the rat gene Atp4A was discontinued, as this gene mapped further centromere distal from the proposed site of *agu* on mouse maps, when compared to GRIK5.

Mapping of the marker defined by H31T forward and reverse, on the BN/AS/AGU backcross and from mapping on a somatic cell hybrid panel indicated that the gene encoding Atpl was actually contained on rat chromosome 4. This contradicted where this gene was expected to map in rat. However, Nezu *et.al.* (1992) who reported cloning of the cDNA for Atpl also reported that on genomic Southern blots there are three genes homologous to Atpl. It is not clear if these are functional genes or pseudogenes. Simkces *et.al.*, (1996) reported that in mouse there also appeared to be three independent genes present on chromosomes 6, 7 and 17. Preliminary human mapping data identified at least two gene loci on chromosomes 3 and 16 (Hasebe *et.al.*, 1992). It is possible therefore that we have cloned the Atpl gene not from chromosome 7 in the mouse (chromosome 1 in rat) but from another chromosome. In fact chromosome 4, to which a microsatellite from the Atpl P1 clone mapped in rat, has a conserved region of syteny with mouse six which is syntenic to human chromosome 3 all of which are reported to contain a member of the Atpl gene family.

The marker F34 positioned the P1 clone containing the ferritin light chain to 42.3 ±6.8 cM from *agu*, and indicated that either the gene was not contained within the conserved region of syteny on rat chromosome 1 or that an event had taken place during cloning which caused this P1 clone to be chimaeric. Also the possibility exists that we have actually isolated another member of the ferritin light chain gene family. A recent study in mouse

(Filie *et.al.,* 1998) identified twelve family members; one expressed gene and eleven pseudogenes. The expressed gene in mouse corresponds to the ferritin light chain mapped to 19q13.3-q13.4 in man and mapped to the syntenic chromosome in mouse, chromosome 7. Therefore, it is assumed that a number of rat ferritin light chain genes also exist and this is the one cloned in P1 clone F. This would explain some of the results obtained from the somatic cell hybrid panel screen.

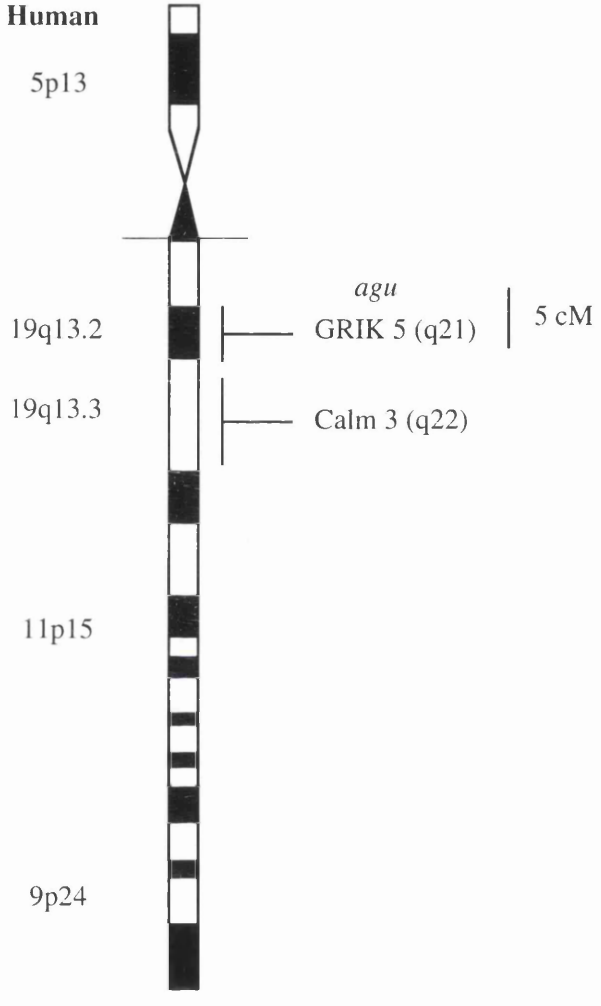

Figure 3.23 Cytogenetic map of rat chromosome 1 with the position of GRIK 5 shown. The *agu* gene is just 5cM centromere proximal to this marker.

It would appear that in the case of Atpl and the ferritin light chain, I have in fact isolated a member of the gene family which does not map to the correct chromosome in rat. At the beginning of this work, only one rat gene encoding ferritin light chain had been identified. However, since this time genetic mapping carried out in mouse has identified 11 pseudogenes contained on 11 different chromosomes in mouse (Filie *et.al.*, 1998). It is possible, therefore, that I have isolated a pseudogene from rat.

Southern hybridisation of rat genomic DNA with a cDNA probe for Atpl had identified three distinct bands (Nezu *et.al.*, 1992). However, the genes corresponding to these bands have not been isolated or sequenced. Therefore, when designing PCR primers to

screen the P1 library for Atpl, I specified them to an area of sequence which was not conserved between rat, mouse and man. This would hopefully be less well conserved and may not be present in other family members. However, this approach was not successful and another gene corresponding to one found on mouse chromosome six (rat chromosome 4) was isolated.

The approach taken in the identification of these P1 clones and microsatellites from them, is obviously flawed. More consideration should have been taken of gene families, which can lead to the problems detailed above. Therefore, if future work of this type is to be carried out either a probe specific for a particular family member must be used. Or once the genomic clones have been isolated, they should be used in a FISH analysis of a rat chromosome spread to confirm their presence on rat chromosome 1.

Chapter 4

Alternative approaches to identifying new genetic markers

4.1 Introduction

As very few markers or genes had been localised on genetic maps of the rat genome, new markers which would allow mapping of *agu* were a major requirement of this project. The mouse genome is extremely well characterised when compared to the rat genome, and has a greater number of markers and genes which have been accurately genetically mapped. Although microsatellites are widely regarded as anonymous sequences, it has been demonstrated that the location of (CA) repeats tends to be conserved between mammalian species (Hino *et.al.*, 1993). The sequences immediately flanking the microsatellite motif, which serve as priming sites, are likely to diverge at a significant rate. Therefore, some microsatellite markers from the extensive syntenic mouse maps maybe be used for mapping within the rat (Kondo *et.al.*, 1993; Hino *et.al.*, 1993 and Sun and Kirkpatrick, 1996). Hino and colleagues (Hino *et.al.*, 1993) identified 14 universal mapping probes derived from human chromosome three that hybridised to rat, thus allowing transfer of information from a "map rich" organism to a "map poor". Hindo and colleagues achieved the same objective from mouse to rat (Hindo *et.al.*, 1993).

Microsatellites have become the genomic region routinely used for mapping in mammals and the region most commonly investigated for polymorphisms. However, this is not the only region of the genome where polymorphisms can be identified. Single-strand conformation polymorphism (SSCP) is a sensitive method for detecting single base differences in polymerase chain reaction (PCR) products (Orita *et.al.*, 1989). The technique is based on the detection of a single-base substitution which alters the conformation of single-stranded DNA under non-denaturing conditions. SSCP has been utilised heavily in recent years for mapping in the mouse. A recent study carried out within our laboratory was able to detect a polymorphism in greater than 90% of PCR products tested from the 3' UTR in the mouse strains *Mus spretus* and C57/BL6 (A.S.McCallion, 1997). Therefore, SSCP was used to test various rat PCR products, in an attempt to identify strain differences between the three rat strains AS/AGU, BN and F344.

4.2 Results

4.2.1 SSCP analysis of PCR products from the 3' UTR of rat genes.

The 3' UTR region of genes has been preferentially used for SSCP analysis (Avramopoulos *et.al.*, 1993), as this is region is less conserved when compared to other gene regions e.g. exons and introns, and therefore has a greater chance of containing a nucleotide difference. Three pairs of PCR primers (GU 101 forward (F) and reverse (R), 102 F and R and 104 F and R) were designed to amplify a fragment of less than 300 bp

from the 3' UTR of the rat genes encoding Atp 4a, SCNIB and GRIK5 respectively, to allow SSCP analysis to be carried out between the rat strains. PCR products were resolved on 6% non-denaturing acrylamide gels at 4°C in the presence or absence of glycerol and with two different ratios of acrylamide to bis-acrylamide. The conditions for resolving SSCPs are discussed in A.S. McCallion (1997). No SSCP was observed between any of the PCR products from the rats strains AS/AGU, BN and F344 (an example is given in Figure 4.1). A summary of the PCR products tested for SSCPs is given in Table 4.1.

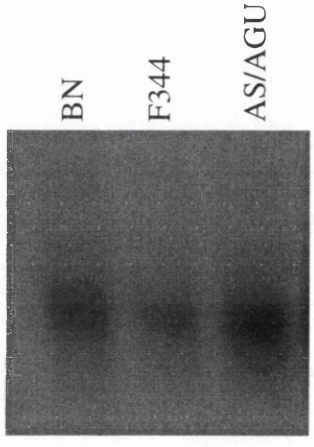

Figure 4.1 SSCP analysis carried out on the PCR product from GU104. The gel conditions are as follows :- electrophoresised at 4°C for 4 hours at 30W. The gel was a 6% acrylamide non-denaturing gel containing 10% glycerol.

SSCP test	Gene	Location in gene	Product size	Strain difference	Accession number
GU 101	Atp 4a	3' UTR	107 bp	No	J02649
GU 102	SCNIB	3' UTR	276 bp	No	M91808
GU 104	GRIK5	3' UTR	224 bp	No	U08258

Table 4.1 Summary of SSCP analysis carried out on PCR products from the 3' UTR of genes from rat.

4.2.2 SSCP analysis of PCR products from microsatellite markers.

SSCP analysis can also be carried out on PCR products from microsatellite markers which had proved to be non-informative after resolution on denaturing 6% acrylamide gels. A base change in the area surrounding the microsatellite or within the microsatellite motif itself would be sufficient to display an SSCP. Many microsatellite markers previously tested within our laboratory were non-informative on agarose or acrylamide gels. Eleven of these were tested by SSCP. Also three markers which had been isolated from the ends

of the P1 clone K (Chapter 6), presumably from unique sequence not derived from any gene were tested. All of these were tested for an SSCP under various conditions but again no strain difference was observed (Examples are given in Figure 4.2). A summary of the results obtained is given in Table 4.2.

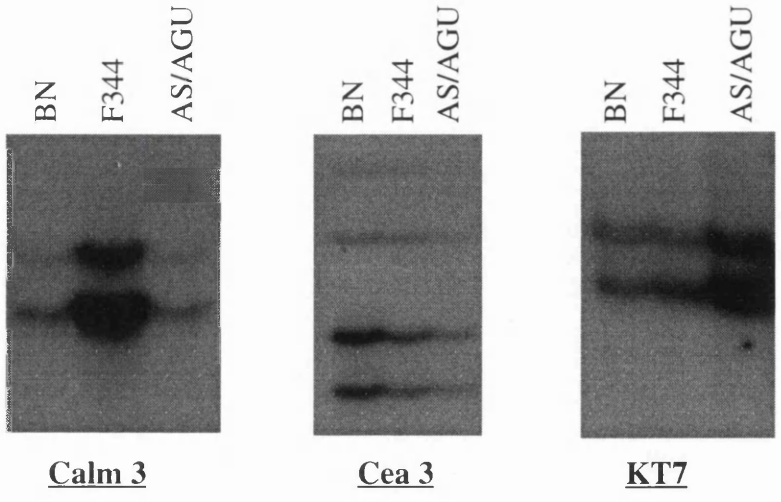

Figure 4.2 SSCP analysis carried out on microsatellite markers from rat. The markers shown are Calm 3, Cea 3 and KT7. All three were tested on the rat strains BN, F344 and AS/AGU.

Marker	Reference	Strain difference
D1Mco 1	Gu *et.al.*, (1996)	No
R 94	Serikawa *et.al.*, (1992)	No
D1Mgh 5	Jacob *et.al.*, (1995)	No
R 100	Serikawa *et.al.*, (1992)	No
Calm 3	Gu *et.al.*, (1996)	No
DØGU 14	M.B. Duran Alonso, (1997)	No
Atp 1a3	Gu *et.al.*, (1996)	No
D1Kyo1(M 105)	Kondo *et.al.*, (1993)	No
Cea 3	M. Canham, (1997)	No
CKM	M.B. Duran Alonso, (1997)	No
D8GU 18	M.B. Duran Alonso, (1997)	No
KSP6	Chapter 6	No
KSP62	Chapter 6	No
KT7	Chapter 6	No

Table 4.2 Summary of SSCP analysis carried out on PCR products from microsatellite markers from rat.

4.2.3 Utilising markers from the mouse genome.

The mouse genome has been extensively mapped in recent years and the mouse genome therefore has a greater number of mapped genetic markers when compared to the rat genetic map (Chapter 1). It was postulated that some of these markers could be used for genetic mapping in the rat. The *agu* locus had been located to a genetic interval within 0.1 cM of R158 (Chapter 5), therefore mouse genetic markers were selected within 2 cM (Figure 4.3) of the gene encoding PKC (Pkcc in mouse) which contains the microsatellite for the marker R158 in it's 3'UTR. The markers were obtained from Research Genetics and their map position taken from the Mouse Genome Database (MGD).

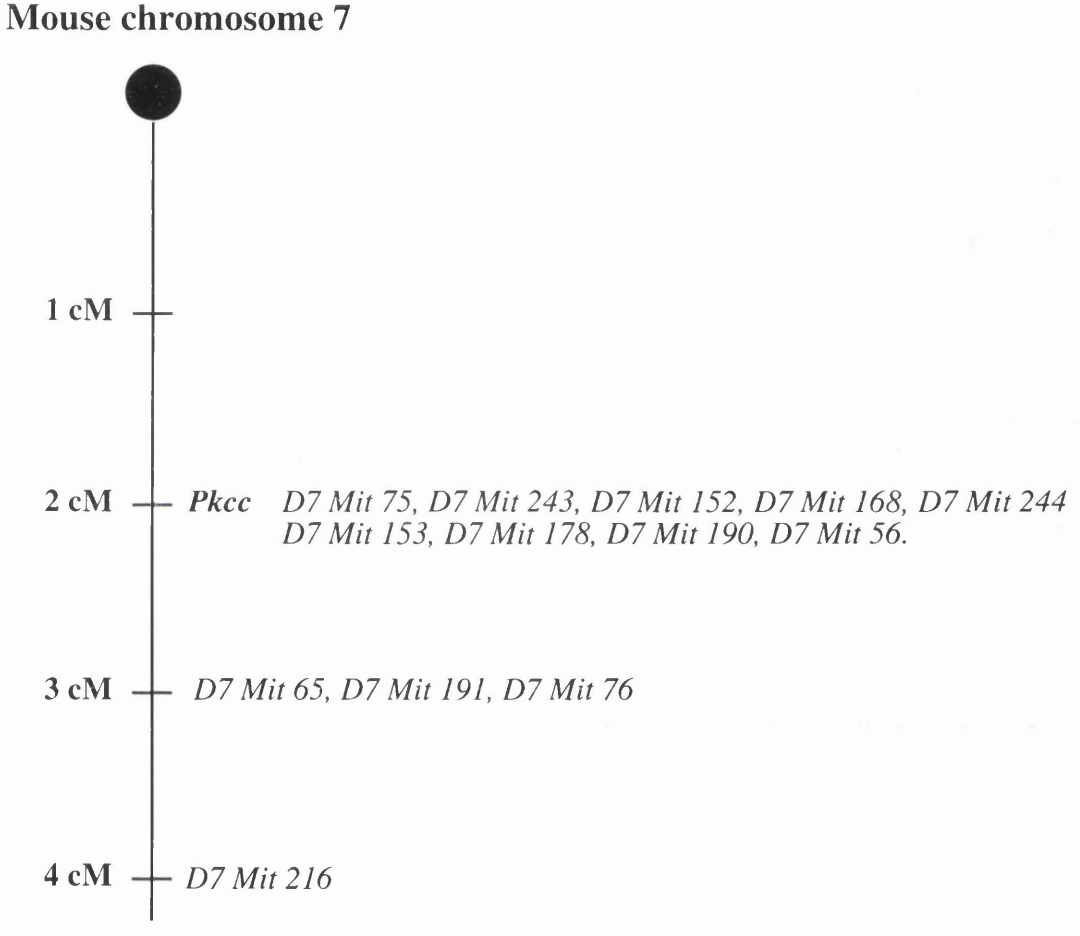

Figure 4.3 Genetic map was taken from the Mouse Genome Database (MGD) (June, 1996) showing the position of mouse markers used, in relation to Pkcc. The centromere is indicated by the black circle.

The mouse markers were initially tested on genomic DNA from different mouse strains to ascertain if the correct allele size for each strain was obtained. The markers were then used in a PCR reaction containing rat genomic DNA from the three rat strains used in this study. Of the thirteen markers tested, 4 produced single bands from rat DNA, however, none showed a polymorphism on 4% agarose gels (Figure 4.4). Tests carried out on 6%

acrylamide gels also failed to display a polymorphism (Figure 4.5). Only three markers gave no PCR product on rat, the remaining six primer pairs produced multiple products.

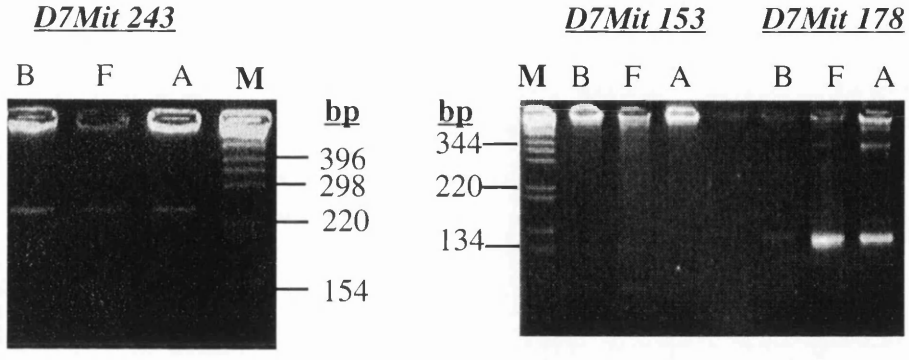

Figure 4.4 Example of mouse microsatellite markers used in PCR from rat genomic DNA from the three rat strains BN, F344 and AS/AGU. *D7Mit 243* and *D7Mit 178* gave single products. *D7Mit 153* produced no product. No strain difference was obtained on 4% Metaphor gels. The marker (M) was a 1 kb ladder.

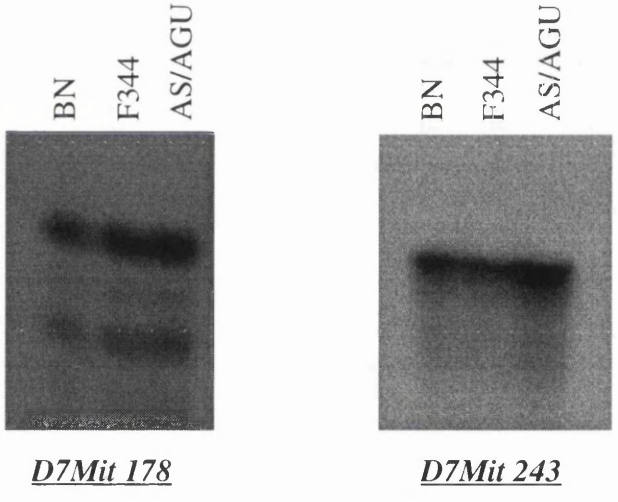

Figure 4.5 Mouse primers *D7Mit 243* and *178* tested on rat genomic DNA. All three rat strains (BN, F344 and AS/AGU) were amplified and resolved on 6% acrylamide. Again no strain difference was obtained

The mouse markers *D7Mit 178 and D7Mit 243* produced clear products of 150 and 250 bp when tested on rat DNA (Figure 4.4 and 4.5). SSCP analysis was carried out with both of these markers but again no strain difference was observed (Figure 4.6). The results obtained from tests of the mouse primers on rat genomic DNA are shown in Table 4.3.

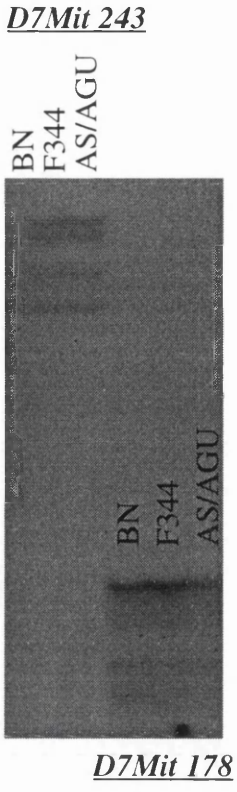

Figure 4.6 SSCP analysis carried out with the mouse primers *D7Mit 243* and *178* on the three rat strains. No polymorphism was observed.

Mouse marker	PCR from rat	Product size in rat	Strain difference
D7Mit 75	No product	-	-
D7Mit 243	Single product	250 bp	No
D7Mit 168	No product	-	-
D7Mit 152	Single product	~ 398 bp	No
D7Mit 153	No product	-	-
D7Mit 178	Single product	150 bp	No
D7Mit 76	Multiple products	Major band 100 bp	No
D7Mit 190	Two products	~ 135 bp	No
D7Mit 56	Single product	130 bp	No
D7Mit 65	Multiple products	Major band 130 bp	No
D7Mit 191	Multiple products	No major product	No
D7Mit 244	Multiple products	No major product	No

Table 4.3 Summary of PCR reactions carried out with mouse genetic markers on rat genomic DNA from the strains BN, F344 and AS/AGU

The marker *D7Mit* 178 produced the strongest signal in a PCR reaction and this marker was used to screen the rat P1 library in an attempt to isolate a P1 clone containing this marker. A PCR product approximately 20 bp larger than the BN positive control was obtained from superpool 61 (Figure 4.7).

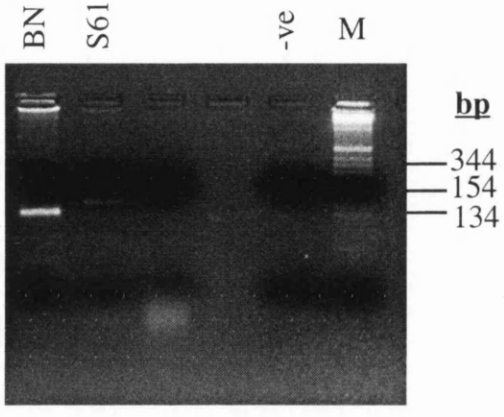

Figure 4.7 PCR carried out with the primers *D7Mit 178* . PCR on rat genomic DNA (BN) and from P1 library pool number 61 (S61) from the P1 library. The gel shows the length polymorphism between the three products. The marker (M) was a 1 kb ladder.

Sequence analysis of the PCR products from mouse genomic DNA, BN genomic DNA and the product from superpool 61, all showed a (GT) microsatellite, with very little flanking unique sequence (Figure 4.8). This indicates that the mouse primers are indeed producing the same product in rat as in mouse, which unfortunately displays a strain difference between the rat strains SD (used to prepare the P1 library) and BN, but not between the three rat strains currently under study.

```
                  10        20        30        40        50        60
                   |         |         |         |         |         |
Contig#     CNNNNNNCNNGNGTGTGTGTGTGTGTGTGTGTGTGTGTGTGTGTGTGNNNNNNTGTGTGNNNNNN
Mouse       CXCCGXXCGTGTGTGTGTGTGTGTGTGTGTGTGTGTGTGTGTGTGTGCACGCATGTGTGCACGCA
Rat         CT---C-----------------CXTAGGCAAAAAGGGGTGTGTGTGTGTG------TGTGTG------
S61         CC---XACAAGGGTGTGTGTGTGTGTGTGTGTGTGTGTGTGTGTGTGTG------TGTGTG------

           70        80        90       100       110       120       130
            |         |         |         |         |         |         |
Contig# 1   TGTGTGTGTACANNTGTATGCCCNNNNNNNNTGTGCGTGTGAGACNNNNTGTANGTBGGGCTCTAGGGT
Mouse       TGTGTGTGTACACTTGTATGCCCTGTGTTTGTGTGTGTGTGAGACGCTGTGTACGTGGGGGTCTAGGGT
Rat         TGTGTGTGTACA--TGTATGTCC--------TGTGCGTGTGTGAC----TGTA-GTTGGGCTCTAGGGT
S61         TGTGTGTGTACA--TGTACCCCC--------TGCGCGTGTGAGAG----TGTA-TTCGCGCCCGAGGGA

           140       150       160
            |         |         |
Contig# 1   AAAAATACGCAAGGGGCACACAAAA
Mouse       AAAGATACGCAAGGGGCCCACA
Rat         AAAAATATGCAAGTGGCACACAAAA
S61         AAAAACACGCCAGGGGCACACAAA
```

Figure 4.8 Sequence alignment of PCR products produced from *D7Mit 178*. Products from mouse genomic DNA (strain C57/BL6), rat genomic DNA (BN) and the P1 superpool number 61 (SD). Dashes indicate a different or absent base.

4.3 Discussion

The object of much of this work was the identification of new genetic markers to map the *agu* gene. SSCP was utilised in this study, however, from the 17 markers tested no polymorphism was observed using this method. This is probably due to the fact that rat strains are quite homogeneous and do not display as many strain differences as is seen between *Mus spretus* and *Mus musculus*. Also the region tested for strain difference is very small, PCR products were generally smaller than 300 bp, and it was unlikely that a polymorphism would be detected in this small length of sequence. It would have been preferable to screen large areas of rat sequence for polymorphisms.

The mouse primers used to identify polymorphisms in rat also showed a low level of polymorphism. The fact that approximately 30% of the primers actually produced a PCR product from rat genomic DNA was promising and showed that in some cases mouse primers could be used for mapping in rat. Again the markers were non-polymorphic between our rat strains; however, only one PCR product was sequenced to confirm that the product contained microsatellite sequence. The mouse primer pair *D7Mit178* produced the correct sized PCR product from rat genomic DNA, which unfortunately was non-informative in our rat strains. This primer pair was used to screen the rat P1 library and a product observed in library pool number 61. Sequence analysis showed that both the products from mouse and rat genomic DNA contained a (GT) microsatellite. Unfortunately the unique sequence surrounding the microsatellite was not long enough to

determine absolutely if the two PCR products were the same. Approximately 400 colonies were screened from this superpool but a colony could not be identified which contained this marker. Unfortunately, there was not enough time to complete this work and further developments occurred which made it less important.

Chapter 5

Mapping the *agu* locus to within <1 cM

5.1 Introduction

Mapping of GU10 placed GRIK5 approximately 5 cM centromere distal from the *agu* gene. This work, along with other mapping studies defined a smaller genetic interval containing *agu*, defining an interval further centromere proximal (Szpirer *et.al.*, 1997), than was originally thought. To date the marker mapped closest to *agu* was R191 (Serikawa *et. al.*, 1992), mapping approximately 4.9 ± 0.5 cM centromere proximal. The publication in 1996 of the Gu *et.al.* rat chromosome 1 map lead to the investigation of new markers mapped close to R191 e.g. D1Mco1, D1Mco2 etc. and also markers previously thought to be further from *agu* e.g. R158 (Figure 5.1).

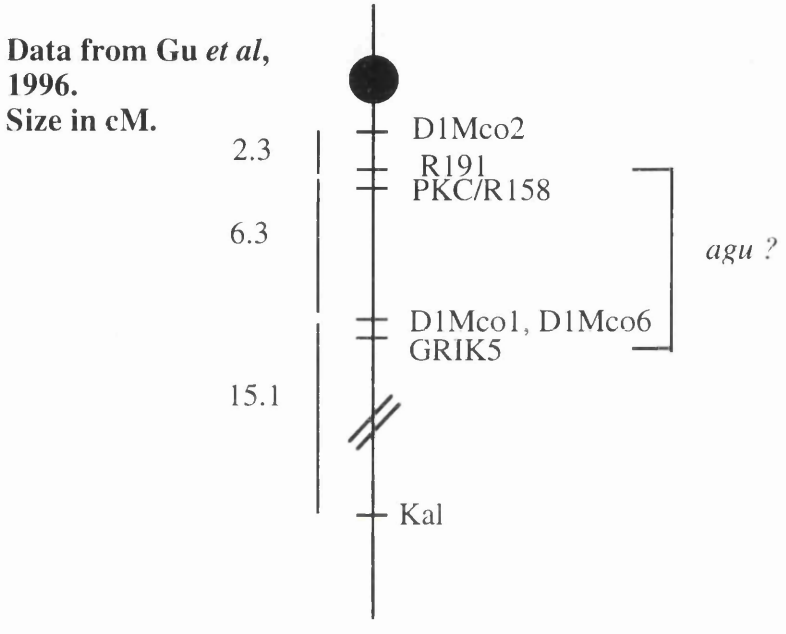

Figure 5.1 Genetic map of rat chromosome 1 published by Gu *et.al.*, 1996. Only the top section is shown. The black circle represents the centromere.

5.2 Results

5.2.1 Establishing a defined genetic interval

It was clearly useful to establish a sub-set of backcross progeny which were recombinant within a defined interval containing *agu*. This would allow any new markers which were identified to be mapped quickly relative to *agu* on a smaller number of animals, rather than on the four thousand progeny constituting the two backcross (BN X AS/AGU and F344 X AS/AGU). This would also provide identification of cross-over events which had occurred within this region in some backcross progeny and would be of assistance in the future during physical mapping. Markers were identified from both backcrosses which spanned an interval containing *agu*. The marker D1Mgh7 (Jacob *et.al.*, 1995) PCR

products display a strain difference, the AS/AGU allele is larger than the BN. D1Mgh7 was mapped in the BN X AS/AGU backcross (Figure 5.2).

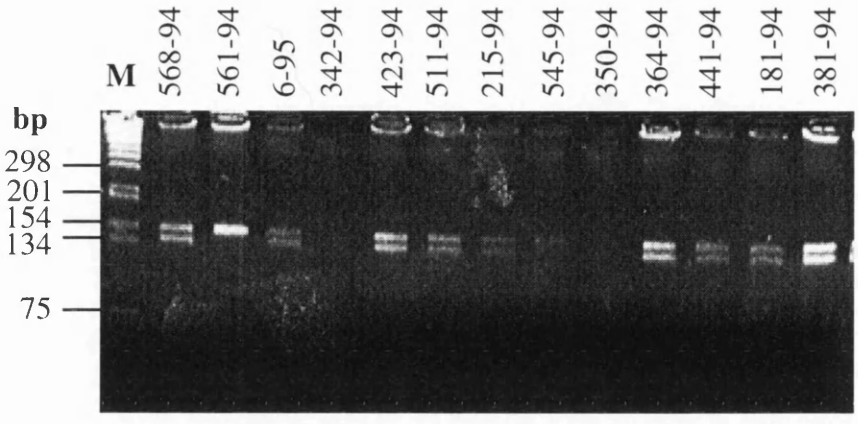

Figure 5.2 Example of genotyping carried out on backcross progeny from the BN X AS/AGU backcross with marker D1Mgh7. The PCR products were resolved on 4% Metaphor gels at 125V for 4 hours. An example of a heterozygote and a homozygote animal are shown in the first two lanes. Numbers corresponding to each animal is given above. The marker (M) was a 1 kb ladder.

324 backcross progeny were genotyped with this marker and 70 proved to be recombinant between the *agu* and the D1Mgh7 loci, placing the marker 23.1 ±2.3 cM from the *agu* mutation using the Kosambi estimate of map distance (Kosambi, 1944). A marker identified flanking *agu* on the other side (D1Mit1; Jacob *et.al.*, 1995)] had previously been mapped by M.B. Duran Alonso (Duran Alonso, 1998) to 5.5 ± 1.1 cM from *agu*. This defined a region of 30 cM in the BN X AS/AGU backcross in which recombinant progeny were selected (Figure 5.3). The two closest markers in the F344 backcross were GU10 (Chapter 3, Section 3.2.5) and R191 (Serikawa *et.al.*, 1992). R191 was originally mapped by Mr. A. McCallion, 4.5 ± 0.5 cM from *agu*. Along with GU10, this gave a region for selection of recombinant animals of around 10 cM in the F344 backcross. Miss M.B. Duran Alonso (Duran Alonso, 1998) was responsible for identifying the recombinant panel of animals and showed that the markers R191 and GU10 and D1Mit1 and D1Mgh7 could be multiplexed in the PCR reaction and the allelic products reliably resolved on agarose, allowing the fast and efficient identification of recombinant animals.

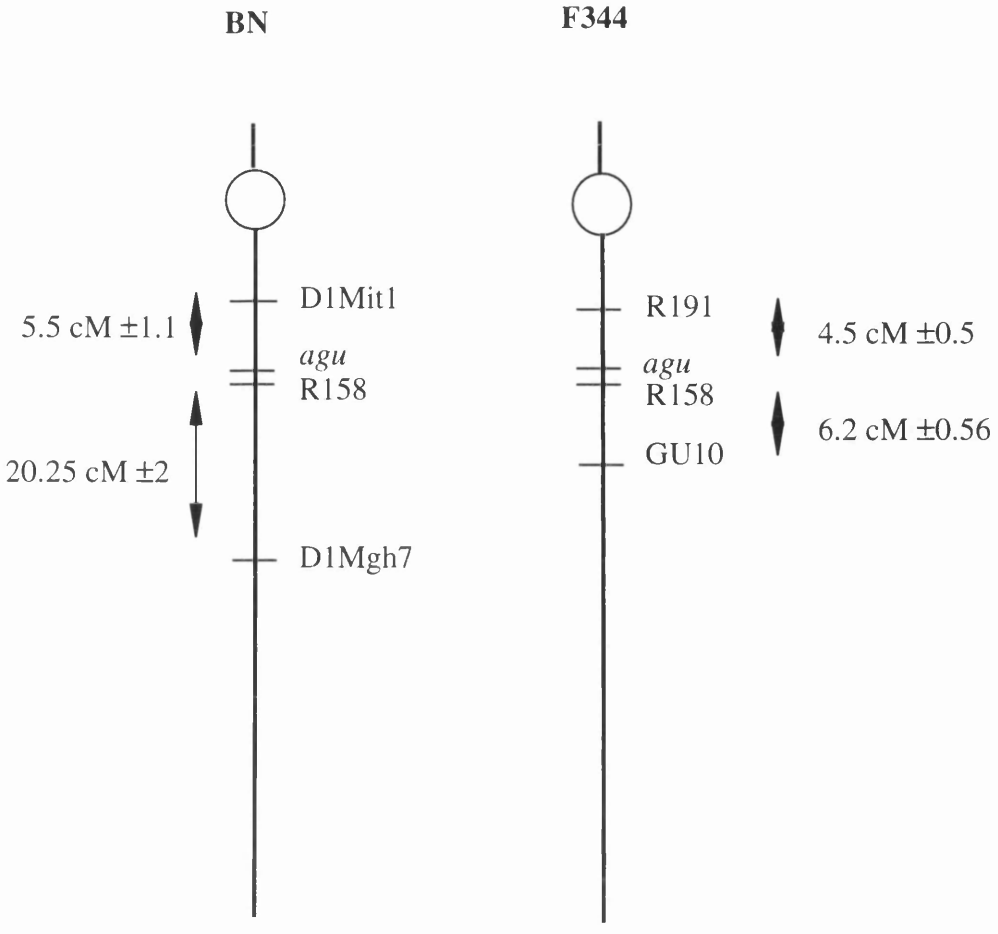

Figure 5.3 The region of genome selected to contain recombination events. The diagram illustrates the genetic markers used to establish panels of backcross progeny recombinant in the interval containing *agu*. The two backcrosses BN X AS/AGU and F344 X AS/AGU are labelled BN and F344.

5.2.2 Mapping R158

Further investigation of the genetic interval identified a new set of markers for study. One of these was R158 (Serikawa *et.al.,* 1992). Gu and colleagues (Gu *et.al.*, 1996) also described the mapping of this marker and reported a strain variation between AS and BN (AS<BN). When a test was carried out with R158, there proved to be a strain difference between the three strains used in the backcrosses, with the microsatellite being two bases (1 repeat unit) shorter in AS/AGU than in F344 and BN (Figure 5.4). The panels of recombinant animals which had been established from both backcrosses (Section 5.1) were genotyped with the marker R158. (Table 5.1)

F344 backcross		BN backcross	
Rec. panel	**Total progeny**	**Rec. panel**	**Total progeny**
185	1800	102	400

Table 5.1. Summary of backcross progeny contained within the recombinant panels (as of 21/2/98).

The 287 animals in the panels derived from 1800 F344 X AS/AGU and 400 BN X AS/AGU backcross progeny. Of all 287 animals recombinant within the selected interval, one animal from the BN X AS/AGU backcross was identified to be recombinant between R158 and *agu* (Animal number : 66-95). Another three animals from the F344 X AS/AGU backcross were found to have two recombination events between the flanking markers and also had a recombination event between the *agu* locus and R158 (Animal numbers : 280-96, 252-96 and F401-96).

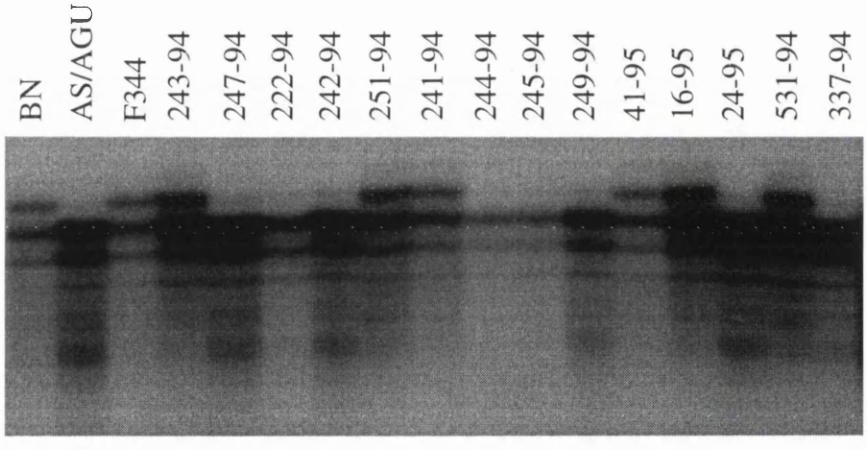

Figure 5.4 An example of genotyping BN X AS/AGU backcross progeny with R158. The radio-actively-labelled PCR products were resolved on 6% acrylamide gels for 3 hours at 60 W. The parental strains are shown in the first three lanes and the backcross progeny in the remainder. The numbers above the gel correspond to individual animal numbers.

In total, from the two backcrosses, six animals were identified which appeared to have two recombination events between the flanking markers (Table 5.2). This was considered high for the small distances tested. Therefore, a PCR test was established to test if the DNA was derived from the correct animal. This test would be useful in establishing errors, either during DNA isolation or PCR.

Animal no.	BN 531-94	F 401-95	F 251-96	F252-96	F279-96	F 280-96
Marker 1	1	2	2	1	2	1
agu	2	1	1	2	1	2
R158	2	2	1	1	1	1
Marker 2	1	2	2	1	2	1

Table 5.2 Haplotypes of animals identified to have two recombination events in the interval selected. 1 = homozygote; 2 = heterozygote. Marker 1 is D1Mit 1 in the BN X AS/AGU backcross and R191 in the F344 X AS/AGU backcross. Marker 2 is D1Mgh7 in the BN X AS/AGU backcross and GU10 in the F344 X AS/AGU backcross.

Therefore, PCR primers were designed to specifically amplify the sex determining region Y gene (SRY) from the Y chromosome (Griffiths *et.al.*, 1993). The sequence encoding the *Rattus norvegicus* SRY gene was retrieved from the database (Accession numbers: Z26907 and X89730) and PCR primers were designed to the sequence (Figure 5.5).

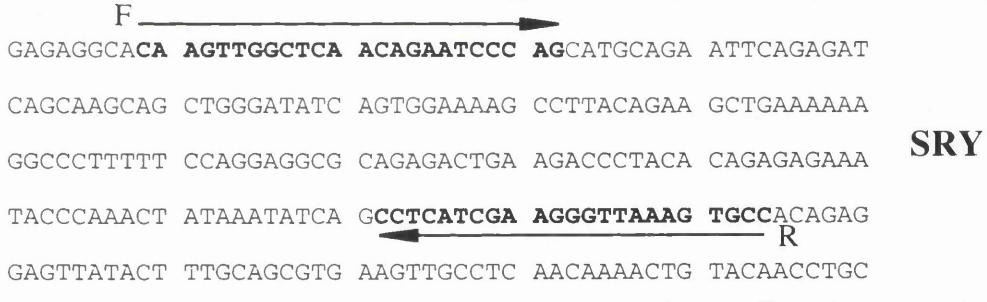

Figure 5.5 PCR test for the SRY gene. PCR primers shown in bold were designed to amplify the rat Y chromosome to detect male-derived tissue.

The primers were firstly tested on a set of animals for which the sex was known and the primers were shown to be specific for the Y chromosome. The animals shown to be recombinant with R158 (Table 5.2) were tested using the primers and the sex of these animals was correct (Figure 5.6). However, the animals containing two cross-over events within the interval had sequential numbers and had therefore been maintained within the same cage. As only animals of the same sex were maintained in cages together it was unlikely that this test could establish errors during spleen and DNA isolation in these animals. One recombinant event between *agu* and R158 was identified in animal 66-95 from the BN X AS/AGU backcross. This typing was verified by re-isolating DNA for this animal and repeating the genotyping with R158. The flanking markers also displayed

the expected haplotype, and the position of the cross-over used to position *agu*, relative to R158.

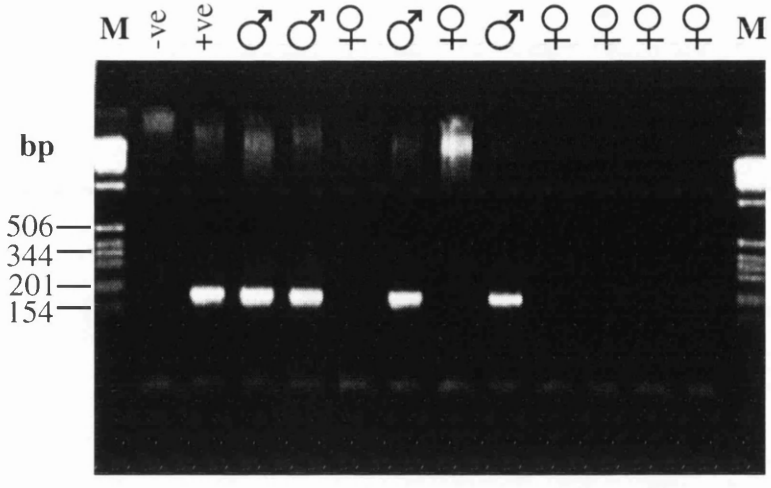

Figure 5.6 Animals recombinant for R158 typed with SRY to determine the sex of each animal. A -ve control containing DNA from a female F344 animal was included and a positive containing DNA from a male F344 animal. The marker (M) was a 1 kb ladder.

5.3 Discussion

The identification of backcross progeny which are recombinant within a defined interval provides a useful panel of animals which can be studied with new markers identified in future. This will reduce both the time and effort required for genotyping all backcross progeny. It will also establish a set of cross-over events which have occurred within this interval, which will be a useful tool in the fine genetic mapping of the region before the isolation of candidate cDNAs.

In total, six double recombination events and one single were detected between R158 and *agu*. Three animals from the F344 backcross appeared to be recombinant; however these animals were also recombinant for both markers flanking *agu*. The numbers of these animals were sequential which indicates the possibility of an error. Unfortunately the test devised to check for errors was unable to verify if these were correct, as animals of the same sex are maintained together in cages. Therefore, any mix up between these animals could not be established. As DNA was re-isolated from the spleens thought to correspond to these animals and the R158 typing was unchanged, it is thought that these animals represent errors which occurred during the removal of the animal's spleen, possibly in the labelling of tubes; further work with new markers should determine this.

Therefore, at this time only one animal, 66-95, was considered to show a true recombination event between R158 and *agu*, placing R158 less than 0.1 cM from *agu*. This small distance makes a chromosome walk from a genomic clone containing R158 a feasible option.

Chapter 6

Establishing a genomic clone-based contig surrounding R158.

6.1 Introduction

The new genetic marker R158 was identified by Serikawa *et. al.*, (1992) during a sequence database search for microsatellites within the rat genome. The marker consists of an $(AC)_{26}$ repeat contained within the 3' UTR of the gene encoding protein kinase C gamma (PKC type I/PKC-γ) (Figure 6.1). This marker has been utilised by various groups for mapping purposes and was useful as an anchor point within our map, when comparing it to published genetic maps. It also displayed a strain difference in the length of the microsatellite between F344, BN and AS/AGU rat strains (F344=BN>AS/AGU) and was used for mapping the *agu* mutation in both backcrosses (Chapter 5).

The *agu* locus had been mapped to less than 0.1 cM (approximately 100 kb) from R158. There are no absolute cut-offs for determining what level of linkage is necessary before positional cloning is attempted. However, in general in mouse, linkage has been tighter than 1 cM. Therefore, it was reasonable to consider creating a clone-based physical map of a genetic interval which is larger than the distance estimated by linkage analysis. A contig of approximately 1 Mb would prove useful. This will take into account errors from genetic mapping and because the cM to megabase (Mb) ratio is not constant throughout the genome. To identify if a contig contains the agu locus, markers at each end of the contig would be isolated and used to map the position of the *agu* gene. This would be easily carried out on the panel of backcross progeny recombinant within this interval (Chapter 5, Section 5.1).

Construction of a physical map involves the identification of overlapping genomic clones within a given region, to form a contig. This involves isolation of a clone containing the closest marker, in this case R158, identifying the ends of the cloned insert in this clone and using this sequence to screen the genomic library from which the clone was originally isolated. This will identify further clones which hopefully overlap the original but extend further into novel regions. To achieve this both ends of the clone must be sequenced and used in a screen of the genomic library.

6.2 Results

6.2.1 Investigation of the PKCγ gene.

As previously mentioned the marker R158 is contained within the 3' UTR of the gene encoding the γ isoform of protein kinase C (PKCγ or PKC type I). This isoform is expressed solely in the neurons of the brain and the spinal cord (Saito *et.al.*, 1988). The rat PKCγ cDNA was cloned in 1986 by Knopf *et.al.* (1986). PCR primers were designed within the 3' and 5' UTRs (named K3 and K5, respectively) of the gene to amplify short

probes for hybridisation, to enable assays to be carried out to detect both ends of the gene on genomic clones (Fig 6.1. and 6.2.). The PCR product from the marker R158 could not be used for probing as it was a microsatellite repeat and therefore not specific enough to allow probing. The PCR primers for both UTRs were designed using the computer programme MacVector. The primers from the 5' UTR were designed to the sequence from Chen *et.al.*, 1990 (Accession number: M55417 and J05664) and the 3' UTR sequence was taken from Ono *et.al.*, 1986 (Accession number: X07287).

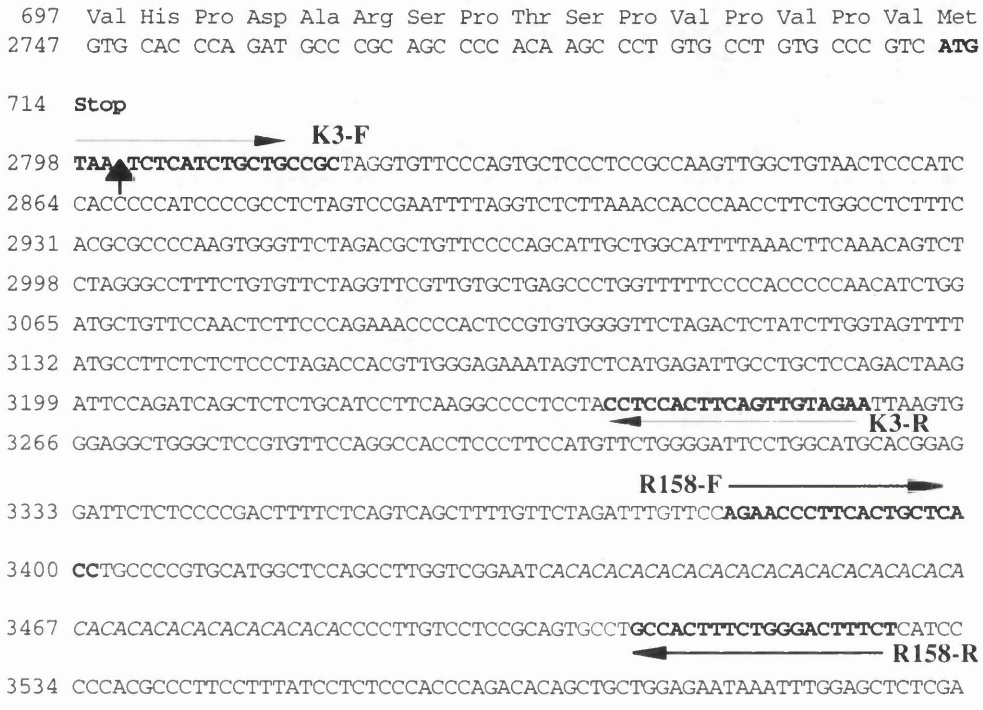

Figure 6.1 PCR primers designed to the 3' UTR of the rat PKC-γ gene. The PCR primers are shown in bold and are indicated by arrows. The stop codon for the gene is indicated by a vertical arrow. The PCR primers specifying the marker R158 are also shown in bold, with the microsatellite in italics.

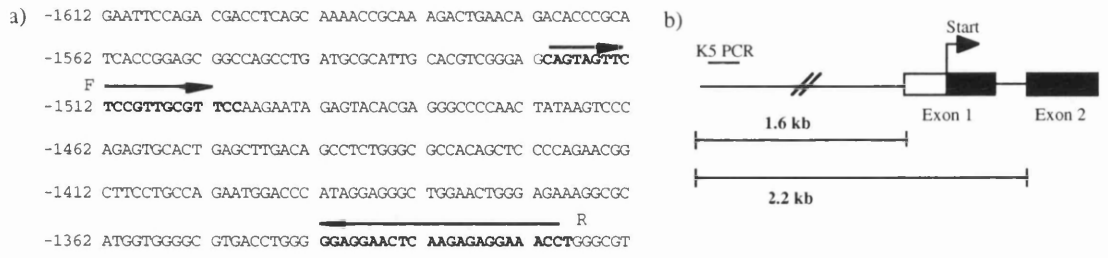

Figure 6.2 Position of marker K5. a) PCR primers for K5 (shown in bold and indicated by arrows) were designed to a region of the 5' UTR of PKC-γ to allow probing for this end of the gene. Co-ordinates are taken from a sequence alignment of the rat mRNA and exon 1. b) Schematic diagram indicating where the K5 PCR product lies within the PKC-γ gene.

6.2.2 Investigation of the P1 library.

The P1 library was kindly provided by Dr.R.MacDonald of the University of Texas, and had been utilised extensively by our group in the isolation of microsatellite markers from the 10 cM region initially identified to contain *agu*. A summary is given in Table 6.1 of P1 clones selected by PCR for containing genes or genetic markers from the interval of rat chromosome 1 thought to contain the *agu* locus. The table shows the 13 P1 clones isolated to date, thus far there have been no cases of absent clones from the library. The P1 library has shown good coverage of the rat genome, to date.

6.2.3 Screening the P1 library for overlapping P1 clones.

A P1 clone (clone K) was isolated by PCR from the P1 library superpool 39, using the genetic marker R158, by Dr. P. Shiels. The clone ends of the P1 clone were sequenced with both the SP6 and T7 primers. Sequence was obtained from the SP6 end of the cloning site and PCR primers (KSP6) specified to a region of this sequence. Dr. D. Donald sub-cloned the P1 clone K, identified a sub-clone containing the T7 end of the cloning site and designed PCR primers (KT7) to this sequence.

Marker/Gene used in screen	P1 clone identified	Investigator	Superpool number
GRIK5	Yes	Nicola Craig	49
ATPL	Yes	Nicola Craig	65
Ferritin light chain	Yes	Dr.P.Shiels	39
Cyp 2A3	Yes	Dr.P.Shiels	-
R158	Yes	Paul Shiels	39
D7 Mit178	Superpool identified	Nicola Craig	61
D1 Mcol	Yes	Miss M.B. Duran Alonso	37
SCNIB	Yes	Miss M.B.Duran Alonso	56
Bgp2	Superpool identified	Mrs.M.Gardiner	13
Cea 1	Yes	Mr.M.Canhan	23
Cea 2	Yes	Mr.M.Canhan	17
Cea 3	Yes	Mr.M.Canhan	62
Cea 4	Yes	Mr.M.Canhan	46

Table 6.1 Summary of P1 clones isolated from the library to date.

The primers KSP6 and KT7 were used to screen the P1 library to try to identify clones which overlap the original P1 clone K, containing the marker R158. When primer pair KSP6 was used to screen lysates of the P1 library pools, no product of the correct size (140 bp) was obtained from the library pool lysates. However a PCR product 20 bp larger was observed in certain superpools e.g. 11, 50 and 79 (Figure 6.3). This indicated the KSP6 primers were not sufficiently specific. The sequence obtained from the SP6 end of clone K was investigated using the RepeatMasker programme which screens DNA sequences for interspersed repeats known to exist in mammalian genomes and the forward primer from KSP6 was homologous to a Short Interspersed Repeat Element (SINE/Alu) repeat in rat (Figure 6.4) (Batzer *et.al.*, 1996). This indicated that during the design of the primers, they were not sufficiently investigated for the presence of line element sequence.

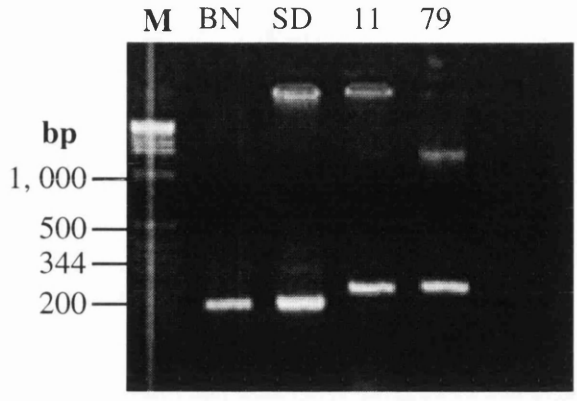

Figure 6.3 PCR screen of the P1 library with the primers specifying KSP6. Lanes BN and SD are positive controls containing Brown Norway and Sprague Dawley rat genomic DNA. PCR signals from superpools 11 and 79 are shown. The marker (M) was a 1 kb ladder.

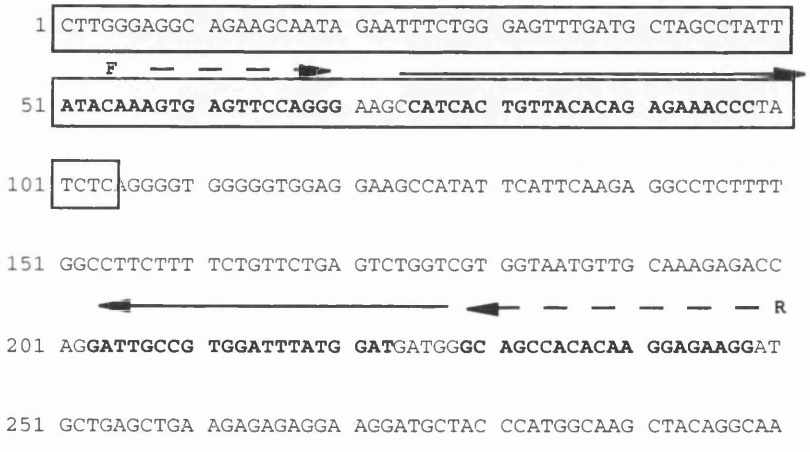

Figure 6.4 Sequence identified at the SP6 end of P1 clone K. The SINE/Alu element is boxed. The primer pairs KSP6 and KSP62 are shown in bold and are indicated by dashed and plain arrows, respectively. The SINE/Alu sequence was a standard repeat element supplied by the RepeatMasker programme.

Figure 6.5 Sequence alignment over 104 bp of sequence from the SP6 end of clone K (top line), aligned to a standard SINE/Alu repeat element from the RepeatMasker program (bottom line). The sequences are 81% homologous. Forward primers for KSP6 and KSP62 are indicated by dashed and plain lines, respectively.

A region of sequence from the SP6 end of K showed 81% homology with this repeat (Figure 6.5), therefore the PCR primers may be amplifying SINE/Alu repeat elements from elsewhere within the rat genome. Prior to receiving this data new primers were designed to another region of this sequence (Figure 6.4). This new primer pair (KSP62) also showed homology to the SINE/Alu element but was less homologous when compared to KSP6 (Figure 6.5). A PCR reaction with KSP62 showed only a single band from genomic DNA and the primers were used in a screen of 150 of the library pool lysates. However, no bands were observed.

6.2.4 Screening the P1 library for clones containing KSP6 and KT7.

No PCR signal was obtained from either the KSP6/KSP62 or KT7 PCR assays on the P1 library. PCR assays had been carried out on lysates made from the library pools and these could at times produce faint PCR signals. Lysates were tested over a period of time by Dr. M.B. Duran Alonso (Duran Alonso, 1998) and the signal achieved from the PCR reaction was seen to reduce over time, presumably as the DNA in the lysates decayed. It was essential that a walk could be extended from P1 clone K using the P1 library and this required reliance on the negative results obtained so far from screens with KT7/KSP6. We reasoned that DNA isolated from the P1 superpools would provide a more reliable template and would allow a greater confidence in the assay. Producing library pool DNA may also allow us to combine superpools into megapools to allow a reduction in time and reagents taken to screen the library.

The 209 superpools from the library were therefore plated onto agar plates containing kanamycin and sucrose. Colonies were plated to achieve 95% confidence of including any particular sequence, using the formula derived by Clarke and Carbon (1976). Colonies were washed from the plates and DNA isolated from the bacterial cell pellet.

PCR tests were carried out for 8 genes and markers previously isolated from the P1 library, to assess coverage of the DNA from the library and utility of the megapool system. The coverage of the library as far as could be tested appeared intact and the megapool system was successful. A PCR test was carried out for the P1 clone containing the gene encoding ATPL (the isolation of which is described in Chapter 3). The DNA isolated from superpool 65 and a megapool of 10 superpools, containing superpool 65 were tested with the primer pair NCA, for the ATPL gene. Both tests showed PCR products of the correct size and the level of signal obtained from the library pool DNA was comparable to that seen for the positive control, genomic DNA (Figure 6.6). The megapool containing library pool 65 also produced a strong positive signal, with approximately 25% of the signal strength in a duplicate test. Another test was carried out with the primer pair GU103 for the gene GRIK5 on library pool 49 and the megapool containing it. A similar result was observed. Other tests were carried out for the gene encoding Cea 3 (for which PCR primers were provided by Mr.M. Canhan and the SSR marker GU14 (primers provided by Dr. M. Alonso) (Figure 6.6).

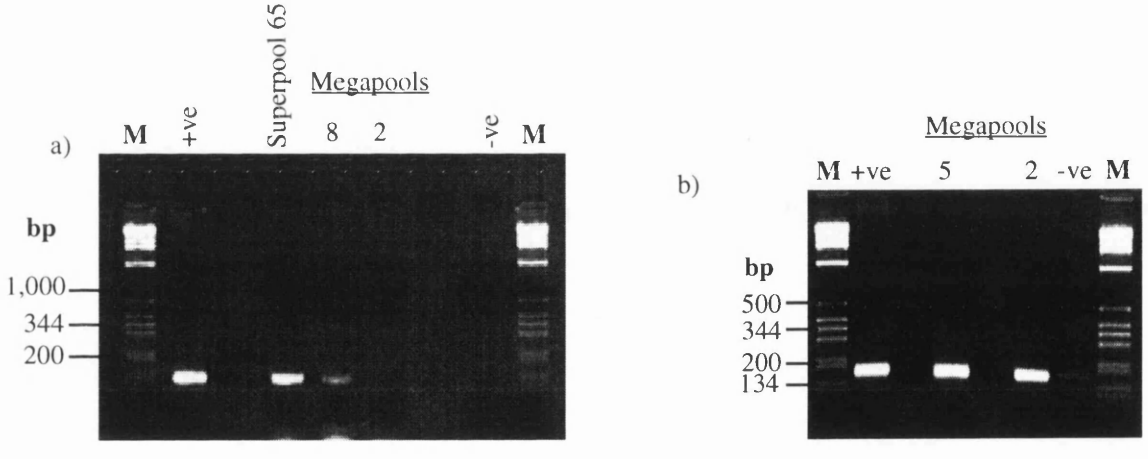

Figure 6.6 PCR assay for ATPL and GU14 on DNA isolated from P1 superpools. a) Superpool 65 was the pool from which ATPL was isolated. Megapool 8 is made up of nine other superpools plus 65. Megapool 2 contains 10 other superpools. b) The megapools 5 and 2 both contain superpool 37, from which the P1 clone was isolated, and both gave a strong positive signal. The marker (M) was a 1 kb ladder.

DNA isolated from the P1 superpools produced better quality, reproducible PCR results and coverage of the library as far as could be tested with 8 genes and markers was complete. The tests also showed that DNA isolated from the library pools, could be combined into groups of ten to produce megapools which will reduce screening time in future work.

The P1 library megapools and the individual library pool DNAs were screened with KSP62 (Figure 6.7). Again no positive signal was obtained. Primer pair R158, originally used to isolate the P1 clone K gave a positive result in megapool 15, containing positive library pool 39. A screen of the library megapool and library pool DNA carried out by Dr. D. Donald also produced no signals for the PCR primers KT7.

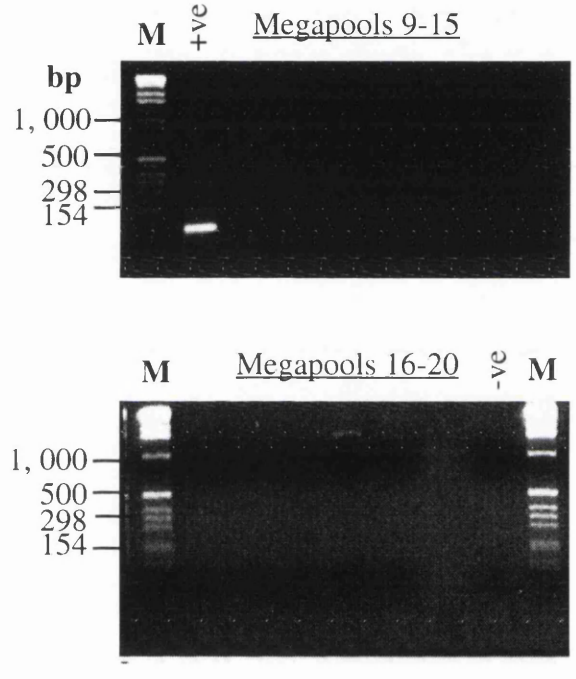

Figure 6.7 Screen of the P1 library megapools with the primers KSP62. Megapools 9-20 are tested, no positive was observed. The positive control contains BN genomic DNA and the negative, no DNA. The marker (M) is 1 kb ladder.

The results of screening the P1 library with KSP6, KT7 and R158 indicated that there were no P1 clones within the library which overlap the original P1 clone, K at these sequences. This indicates that there is a gap in the coverage of the P1 library at this point, possibly indicating that DNA from this region is more difficult to clone, either because of sequence present or lack of restriction enzyme sites. The coverage of the library from other areas tested indicates that in general the coverage of the library is good. Work carried out by Southard-Smith (1994) suggested that the coverage of the rat genome by the library was at least two fold, therefore it appears that this region of DNA is not so well represented within this library.

The isolation of DNA from the P1 library superpools and subsequent screening allowed reliance on the negative results obtained in screening for ends of P1 clone K. The DNA is now stored also as megapools to allow more efficient screening of the entire library which may prove useful in the future.

6.3 Investigation of a new rat YAC library.

A rat Yeast Artificial Chromosome (YAC) library from Research Genetics became available in April, 1997. The construction of the YAC library was described in Cai *et. al.*, (1997). The YAC library is contained within 67 superpools of DNA which are screened by PCR (Green and Olson, 1990). After the identification of positive superpools, the address of the clone within the superpool is determined by carrying out a further 28 PCR reactions, which identify a row and column within a particular library plate.

The YAC library was screened by PCR using the marker R158. From the sixty-seven superpools, seven positive signals were obtained (superpools 4, 14, 18, 23, 31, 45, and 66) (Figure 6.8). The subsequent 28 PCR reactions were carried out for each superpool resulting in seven YAC clone addresses. The YAC clones (527 F9, 181 G12, 109 D1, 26 F1, 355 E3, 143 G9 and 243 B6) were purchased from Research Genetics.

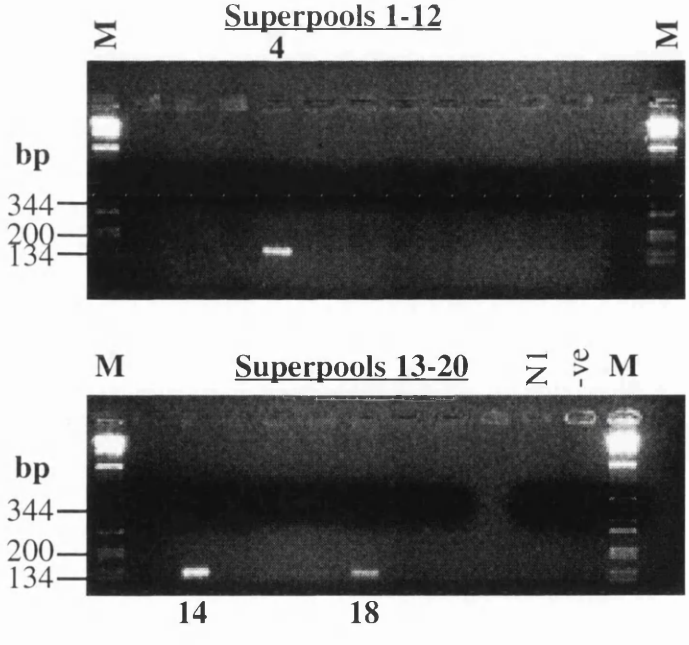

Figure 6.8 A PCR screen of the YAC superpools 1-20 with R158. The negative control (-ve) contains no DNA, the other negative control (N1) contains yeast genomic DNA. The marker (M) was 1 kb ladder.

The YAC clones were plated onto YPD plates (minimal medium) and single colonies dissolved in distilled water to make lysates, to allow identification of the correct YAC clone by PCR analysis with marker R158. YAC clones were resolved on contour-clamped homogenous electric field (CHEF) gels and yeast DNA was isolated from cells in agarose plugs to reduce shearing (Schwartz and Cantor, 1984). YAC clones were grown in YPD culture media to produce agarose plugs and resolved on a CHEF gel (Figure 6.9). However, the yield of YAC DNA was low. It was difficult to observe on CHEF gels and a weak hybridisation signal was obtained (Figure 6.10). It was suggested that YAC clones produce better DNA when grown in the medium AHC, which is a complete medium for growing the yeast strain AB1380 while still selecting for the YAC clone (Brownstein *et.al.*, 1989). The YAC clones were grown in AHC medium and a greater concentration of YAC clone DNA was observed (Figure 6.10).

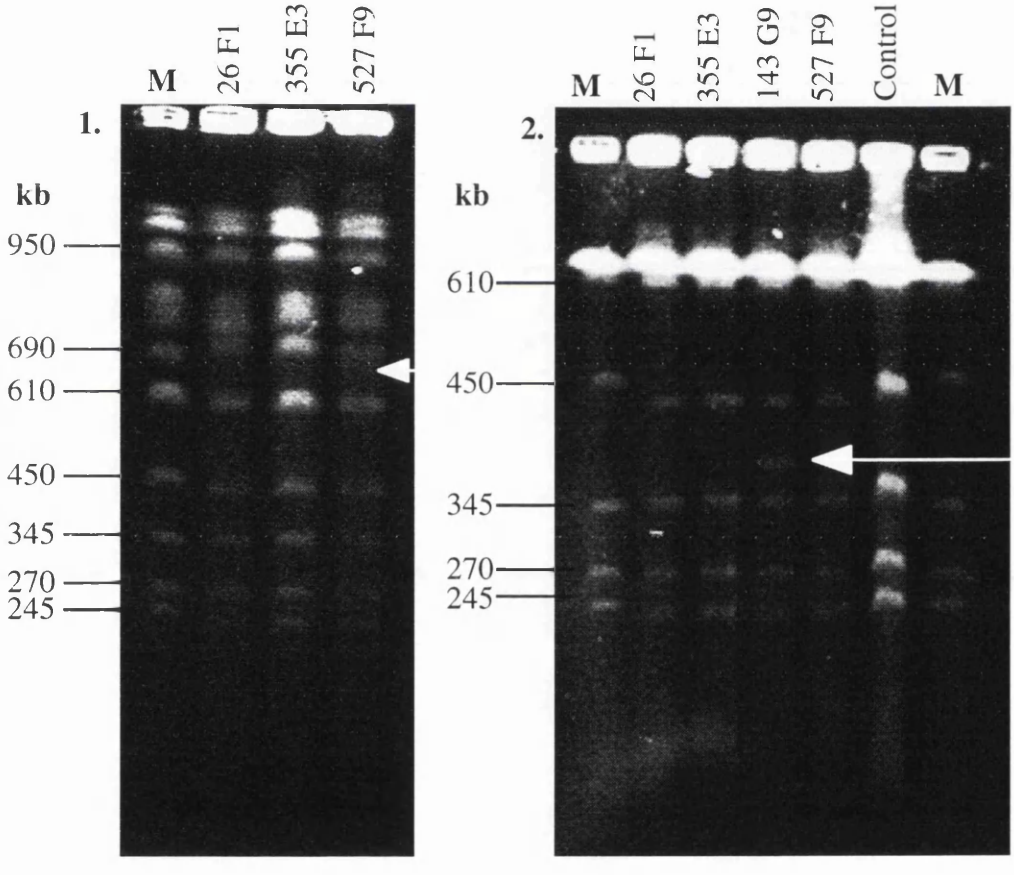

Figure 6.9 Resolution of YAC clones on CHEF gels. The marker (M) is a yeast chromosome ladder from Promega. Bands corresponding to YAC clones 527 F9 and 143 G9 are indicated by arrows, at 680 and 400 kb respectively. The remaining YAC clones are difficult to see because of the yeast chromosomes. Gels (1) and (2) were electrophoresised as follows; 1% Seaplaque GTG gels in 0.5X TBE at 14°C for 20 and 22 hours respectively, with switch times of 30-30 secs and 20-84 secs. The gels were electrophoresised at 6V/cm.

Following electrophoresis of the YAC clones on CHEF gels, the DNA was transferred from the gel to nitrocellulose by Southern blotting. These filters were then probed with the PCR probes K5 and K3 (Figure 6.1 and 6.2) from the 5' and 3' UTR of the rat PKCγ gene, respectively (Section 6.1). This allowed estimation of the size of each YAC clone (Table 6.2) and also allowed identification of overlaps between YAC clones and the original P1 clone, K. The average size of YAC clones reported in the library was 700 kb; the average for the 5 YAC clones tested was 626 kb, very similar to that reported for the library.

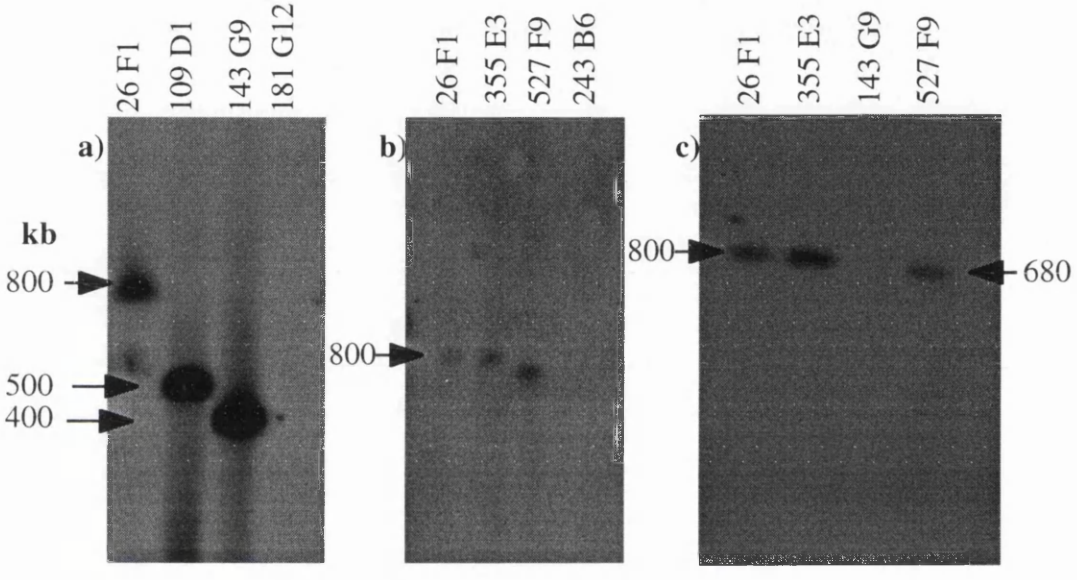

Figure 6.10 Southern blots of YAC clones resolved on CHEF gels.
The blots (a) and (b) were probed concurrently to allow comparison between YPD and AHC medium. (a) YAC clones from cultures grown in AHC medium, blotted and probed with the K3 probe. (b) YAC clones from cultures grown in YPD medium, blotted and probed with the K3 probe. (c) YAC clones from cultures grown in YPD medium, blotted and probed with the K5 probe.

Clone	181 G12	109 D1	26 F1	243 B6	355 E3	527 F9	143 G9
Size	?	500 kb	800 kb	?	750 kb	680 kb	400 kb

Table 6.2 Summary of YAC clone sizes (in kb) as estimated from Southern blots probed with K5 and K3 probes. The size of 181 G12 could not be determined as this clone was shown not to contain either the K3 or the K5 sequence by PCR.

PCR tests were carried out on all of the YAC clones for the presence of sequence identified from the original P1 clone K. These tests involved the ends of the P1 clone (KT7 and KSP6) and SSR markers isolated from K (K100, K106 and K66). This allowed elucidation of the overlap between clones and provided information on the overlap of the YAC clones and the P1 clone K. DNA can be isolated easily for this purpose from the YAC clones by lysing the cells and precipitating the DNA, as shearing of the DNA is not a consideration. Figure 6.11 shows an example of one of these tests.

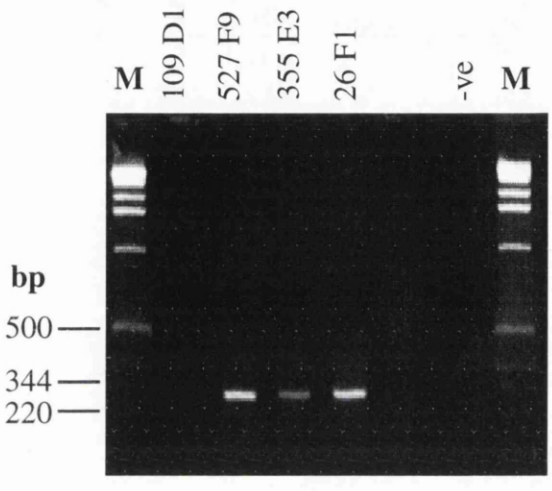

Figure 6.11 Example of a PCR test carried out on YAC DNA, using the marker KT7. The negative control contains no DNA. The YAC clones 527 F9, 355 E3 and 26 F1 are positive and clone 109 D1 is negative. The marker (M) was a 1 kb ladder.

The PCR and hybridisation allowed a putative contig to be established with the YAC clones and P1 clone K (a summary of the results are given in Table 6.3 and Figure 6.12). The grouping of markers on the YAC clones allowed an orientation for markers within clone K.

YAC	KSP62	K100	K106	K3	R158	K5	K66	KT7
109 D1	-	-	-	+	+	-	-	-
181 G12	-	-	-	-	+	-	-	-
26 F1	-	-	-	+	+	+	+	+
243 B6	+	+	+	-	+	-	-	-
527 F9	+	+	+	+	+	+	+	+
355 E3	+	+	+	+	+	+	+	+
143 G9	+	+	-	+	+	-	-	-

Table 6.3 PCR results from YAC clones tested with markers from P1 clone K.

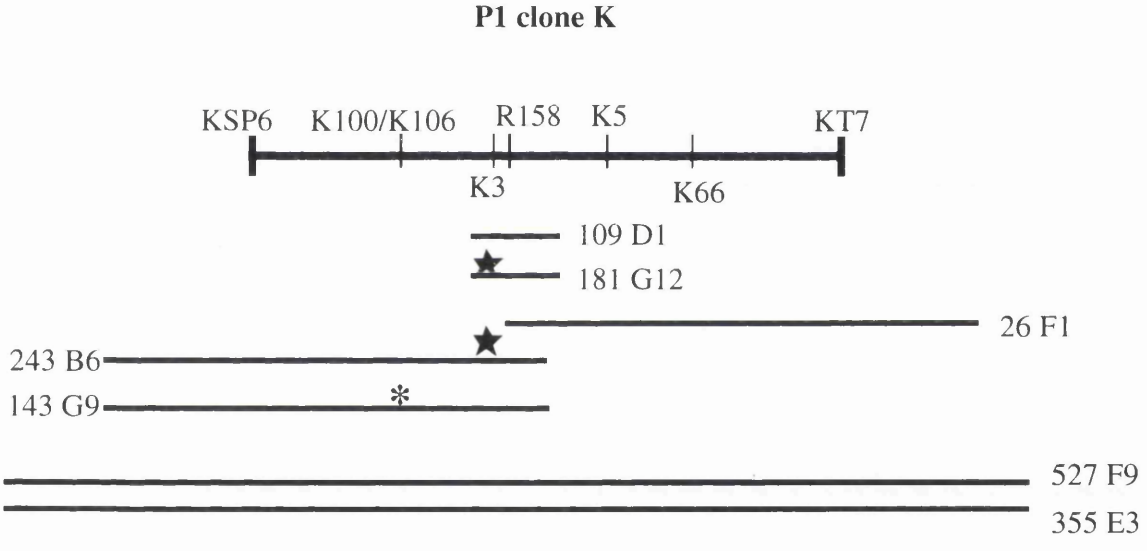

* Indicates a deletion of the marker K106 from the YAC clone 143 G9.

★ Indicates a deletion of the marker K3 from the clones 243 B6 and 181 G12.

Figure 6.12 Establishing a putative contig of YAC clones using markers from the P1 clone K.

6.4. Identification of over-lapping genomic clones from a PAC library.

Contigs containing YAC clones are often difficult to construct because of problems associated with YAC cloning e.g. chimaerism, difficulty in isolating DNA and deletions of inserts. A more popular approach is to screen genomic libraries of clones containing smaller inserts (P1, BACs, PACs and cosmids) and to order and characterise these. A new rat P1 artificial chromosome (PAC) library (Ioannou *et.al.*, 1994) became available in April 1997, which was ideal for our purposes. It combines all of the advantages of the P1 library; large insert size, between 100-300 kb, easy preparation of clone DNA, clone stability and high cloning efficiency with a convenient screening system. The library has been arrayed into 384 well microtiter plates and placed onto nylon high density hybridisation filters for screening by probe hybridisation. This allows a quick and easy identification of a clone address. The PAC library from BAC/PAC (Roswell Park Center, www site: http://bacpac.med.buffalo.edu.) resources was gridded, as a set of duplicate clones, on filters for probing by hybridisation.

The PCR product, K5 (from the 5' UTR of the rat gene encoding PKCγ), was band isolated, radioactively-labelled by random-priming and used as a probe on a genomic Southern blot of rat DNA. This allowed me to check for the presence of any repetitive element within the probe. The probe produced one band and was used to screen the PAC library filters. *E.coli* DNA was also radioactively-labelled to the same specific activity as K5 and added at 1/10 the activity of the K5 probe to allow background grid colonies to be lightly labelled. An adequate image of the background grid of colonies was essential to orientate filters and identify the address of positive clones (some examples are given in Fig. 6.13). Five positive PAC clones were identified from the library with the K5 probe: 603 C15, 542 G19, 365 J2, 437 C18 and 539 G6 (Figure 6.13).

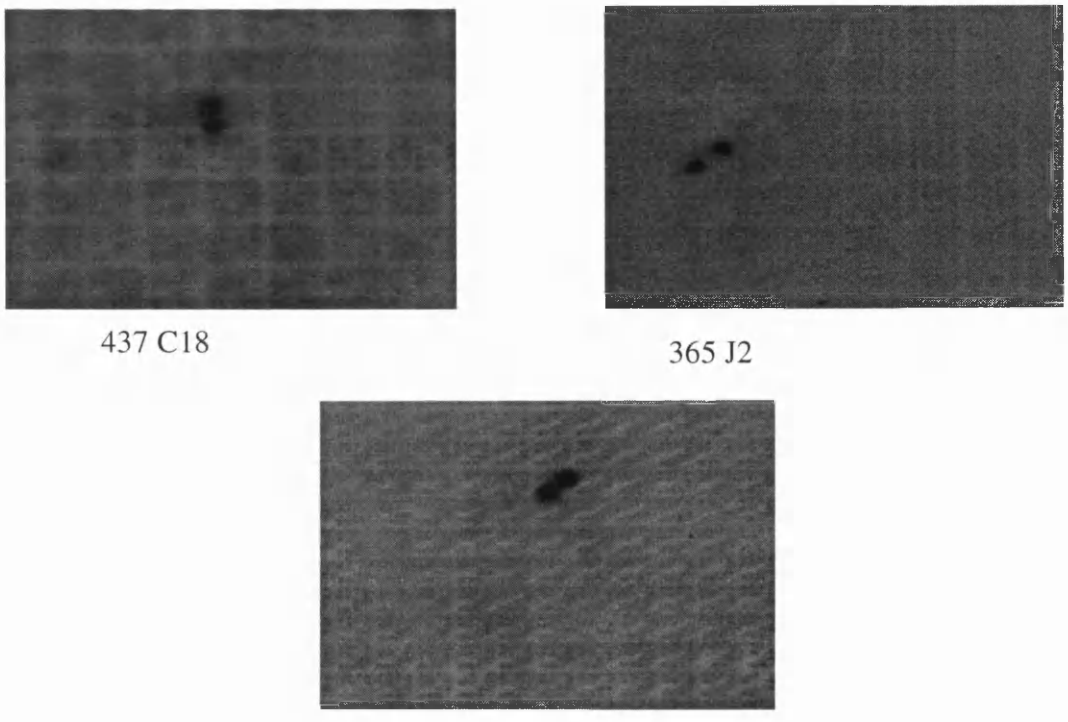

Figure 6.13 Identification of PAC clones from the library probed with the K5 probe. The background grid is lightly labelled with *E.coli* DNA. Five positive clones were identified from this screen. Duplicate signals were seen for each colony (as shown above).

DNA was isolated from each of the PAC clones using phenol/chloroform extraction, as for the P1 clones. The PAC DNA was partially digested using *Sau* 3A and ligated into pUC 18. The resulting colonies were screened with SP6 and T7 radioactively labelled oligonucleotides to identify the sub-clones containing the end fragments of the PAC clones. Sub-clone 106 contained the T7 end of PAC clone 542 G19 and was used as a probe to isolate overlapping PAC clones and extend a contig.

DNA isolated from sub-clone 106 was digested to excise PAC vector sequence and a 0.9 kb band (Figure 6.14) was identified from 106 which produced a single band in genomic Southern blots. The PAC library was screened with this fragment ; three new positive clones in addition to the original PAC clones identified which had been identified with the K5 probe. The new PAC clones were: 582 G16, 462 P14 and 419 M14. They were confirmed to overlap 542 G19 by probing with the 0.9 kb band digested from sub-clone 106 used to screen the library and an independent probe using another fragment of 1.1 kb digested from sub-clone 106.

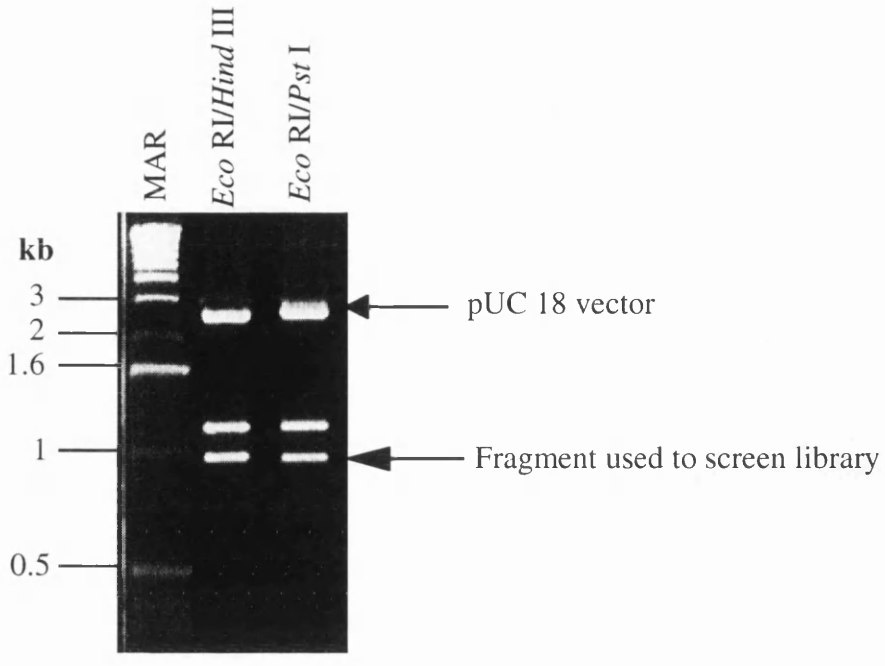

Figure 6.14 Restriction analysis of subclone 106. The large arrow indicates the fragment identified for screening the PAC library. The smaller arrow indicates the pUC18 vector band. The other band shown (1.1 kb) was used to confirm that the clones identified were correct.

A 2.3 kb *Bgl* II fragment identified from PAC 542 G19 contained the SP6 end of this clone. This was sub-cloned into pUC 18 and sequenced using the SP6 primer. The 2.3 kb *Bgl* II fragment also contained a dinucleotide (CA) repeat unit of 22 repeats and PCR primers were designed to amplify this repeat (GU20 Forward and Reverse) (Figure 6.15). Rat strains BN, F344 and AS/AGU were screened for a strain variation in the size of the PCR product from GU20 by Miss M.B. Duran Alonso; no length variation was observed between the rat strains BN, F344 and AS/AGU. A strain difference was observed between the rat strains DA and AS/AGU.

Another region of presumably unique sequence within the clone was amplified with the PAC 542 G19 SP6 F and R primers to enable screening of the PAC library (542 G19 SP6 F and R) (Figure 6.15). A radioactively-labelled PCR product from the 542 G19 SP6 forward and reverse primers gave a single band on a genomic Southern blot (Figure 6.16) which identified 4 new PAC clones from the library ; 429 O2, 434 L2, 372 C17 and 399 G7. Only PAC 542 G19, of those previously isolated, hybridised with this probe.

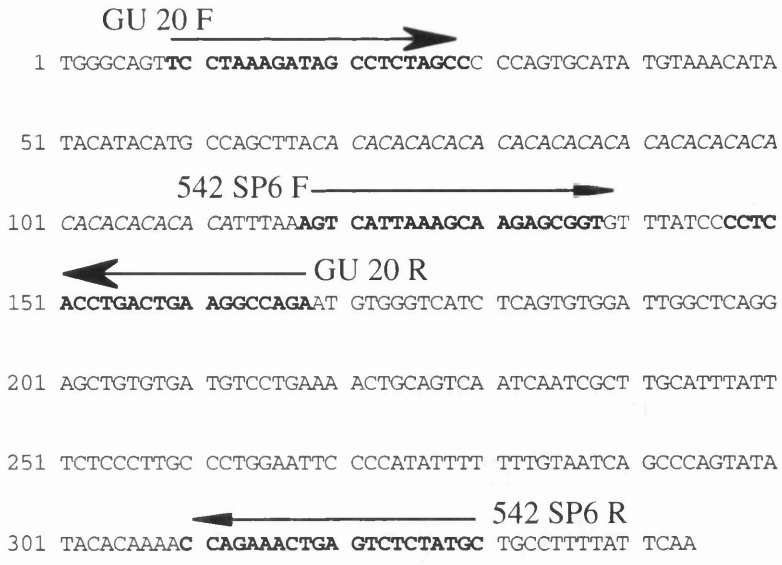

Figure 6.15 Sequence obtained from the SP6 end of the PAC clone 542 G19. The repeat unit is shown in italics. The primers designed are shown in bold and indicated by arrows.

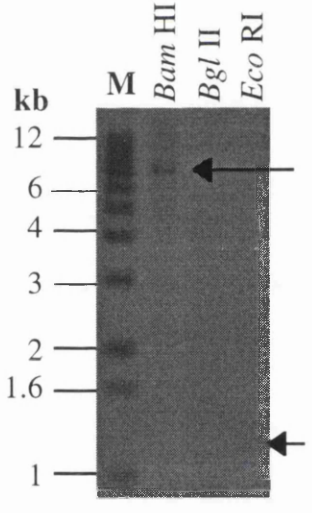

Figure 6.16 Rat genomic Southern blot probed with the PAC 542 G19 SP6 end PCR product. Only one band is seen in each restriction digest on the blot.

6.5 Discussion

To date one P1, twelve PAC and seven YAC clones have been isolated using markers identified close to R158. These genomic clones were assayed by PCR and hybridisation to determine clone overlap and to create a contig (Craig *et.al.*, 1997). The YAC clones were previously tested with the SSR markers from P1 clone K, and the ends of PAC clone 542 G19 were used to probe the YAC clones, and markers from the P1 clone K were also tested on the PAC clones (Table 6.4). The degree of shared DNA markers between the PAC and YAC clones has been established (Figure 6.17).

	KSP6	K100	K106	K3	R158	K5	K66	KT7
				YAC	Clones			
109 D1	-	-	-	+*	+	-	-	-
181 G12	-	-	-	-*	+	-	-	-
243 B6	+	+	+	-*	+	-*	-	-
143 G9	+	+	-	+*	+	-*	-	-
26 F1	-	-	-	+*	+	+*	+	+
355 E3	+	+	+	+*	+	+*	+	+
527 F9	+	+	+	+*	+	+*	+	+
				PAC	Clones			
542 G12	+*	+*	+	n.t.	+	+*	+	+*
365 J2	-*	+*	+	n.t.	+	+*	+	+*
603 C15	+*	+	+	n.t.	+	+*	+	+*
582 G16	-	+	+	-	-	-	-	-
462 P14	-	-	-	-	-	-	-	-
419 M14	-	+	+	-	-	-	-	-
372 C17	-	-	-	-	-	-	-	-
429 O2	+	+	+	+	+	+	+	+

Table 6.4 Summary of tests with markers from the genomic region containing R158 on the YAC and PAC genomic clones. *indicates the test carried out was by hybridisation. n.t. indicates where a test was not carried out. PCR test on the PAC clones for markers from K were carried out by Dr. M.B. Duran Alonso.

There are a few anomalies within the contig construct:

(1) The YAC clone 26 F1 is approximately 800 kb in length by Southern blotting (Table 6.2) but does not appear to contain either the SP6 or T7 ends of the PAC clone 542 G12 indicating that this YAC clone may be chimaeric, as the distance from R158 to these two markers is probably less than 200 kb.

(2) The YAC clone 243 B6 has a deletion of the sequence for marker K3 and contains the sequence for SP6 end of the PAC 542 G19 when it is expected to contain the T7 end. (The orientation of the 542 G19 clone was established because of markers K100 and K106 found in PAC clones isolated using the T7 end of the clone (582 G16 and 419 M14).

(3) YAC clone 143 G9 appears to have deletions not only for K106 but also the SP6 end of 542 G19.

YAC clones 355 E3 and 527 F9, however, appear to contain most of the markers tested and do not appear to contain any rearrangements or deletions, thus far. These YAC clones are also 750 and 680 kb in length, respectively and will cover a large area of contig established using PAC clones. At present these YAC clones are the most interesting for study and should be tested further to assay clone stability and integrity.

One of the YAC clones 181 G12 appeared only to contain the DNA containing the marker R158 for which the library was screened. This YAC clone may have been a false positive, an error which may have arisen during either screening of the YAC library or during selection for positive YAC clones from plates, possibly because of PCR contamination. The YAC clone 109 D1 contained only markers R158 and K3, approximately 70 kb apart, but this YAC clone is 500 kb in size as estimated by probing with the K3 probe. This indicated that this clone may be a chimera which probably arose by co-cloning of DNA fragments from two disparate genomic locations. The level of chimearism within this library was estimated at 20-30% by Cai *et.al.*, 1997 and to date our evidence for chimearism is one clone from six, giving an estimate of 16% for the clones isolated with R158. However, this was not an exhaustive study of the clones and if further work is to be carried out on these clones this will have to be investigated in detail.

The YAC clones 143 G9 and 243 B6 appear to lack DNA corresponding to the markers K106 and K3 respectively. These may reflect small deletions of sequence from the YAC clones. This is the case for YAC 243 B6; marker K3 is approximately 70 kb from R158, the marker used to isolate the YAC clones, yet this clone has the DNA sequence corresponding to R158 but not K3. This may indicate that these clones are unstable, a problem estimated to occur in 1-2% of YAC clones (Wada *et.al.*, 1994). The YAC clones

26 F1, 527 F9 and 355 E3 however, appear to have an intact insert for the markers tested so far.

Twenty genomic clones have been isolated to have markers close to the *agu* locus and have been used to establish a genomic contig spanning at least 750 kb. A contig of PAC clones extending in both directions from the original P1 clone (K) has been established. New microsatellite markers are currently being isolated by Dr.M.B. Duran Alonso to establish the orientation of *agu* with respect to R158 within the contig. Mapping of the new markers will also establish the genetic distance "walked" from R158. The physical distance can also be determined by restriction mapping.

At this time no further work was carried out on the YAC clones isolated. The problems associated with YAC clones have been well documented e.g. chimaerism, instability and rearrangements, particular problems for physical mapping. Therefore the YAC clones will only be used should a problem occur with PAC clones e.g. chimaerism or in the absence of PAC clones. However, results so far obtained from the PAC library indicate that coverage of the library is good. The YAC clones isolated in this study have not been tested exhaustively for chimearism etc. but appear to show between 30-40% chimaerism. The level reported by Cai *et.al.* (1997) for the library was 20-30% so the level we observe is slightly higher than expected. PAC clones are now being routinely used within this study. DNA can be easily isolated from clones and thus far no problems have been encountered with instability. The levels of chimaerism in these clones is so far untested but there have been no reports of this occurring.

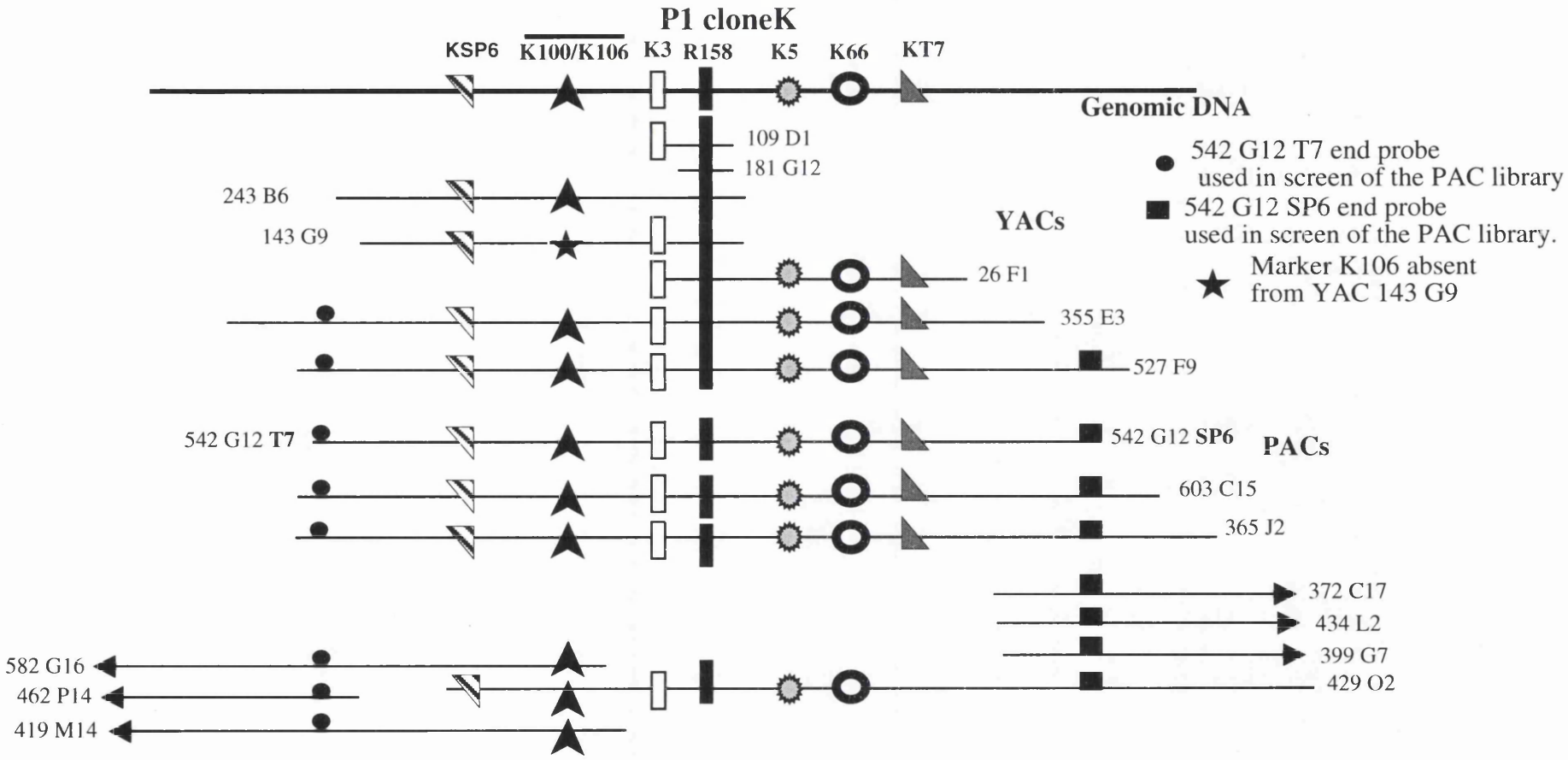

Figure 6.17. Genomic contig established using YAC, PAC and P1 clones. The length and extent of overlap between clones has not been accurately determined.

Chapter 7

Discussion

7.1 Progress Review

The goals of my research as outlined in Section 1.8 were the identification of new genetic markers to allow fine mapping of the *agu* gene in a genetic interval and the establishment of a genomic clone based contig of this region. The identification of new genetic markers from P1 clones was carried out and in the case of D1GU10 produced a marker which has been useful in the fine mapping of the region containing *agu* and in the establishment of a panel of recombinant backcross progeny. These backcross progeny will prove to be useful in the investigation of cross-over events which have occurred within this region which should further define the interval for investigation. It is unfortunate that some of the other markers identified proved to be non-informative within the rat strain AS/AGU, F344 and BN, but this problem has been addressed (Section 7.4.3.1). A genomic contig of twenty genomic clones spanning approximately 750 kb has been established which will hopefully contain the *agu* gene. However, further investigation of this contig must be carried out to establish the coverage of these clones and rule out any problems e.g. chimaeric clones and deletions. Therefore, the two major goal have been achieved.

7.2 Utilisation of rat genomic libraries

Three rat genomic libraries were utilised during the positional cloning phase of this project; a P1 library (Southard-Smith *et.al.*, 1994), a PAC library and a YAC library (Cai *et.al.*, 1997). Initial work involving the isolation of clones carried out with the P1 library was difficult and the system of work established is not ideal. Isolation of P1 clones from superpools was time consuming and not always successful. Also when a walk was attempted from the original P1 clone, K, no overlapping clones were identified (Chapter 6). Therefore it was fortuitous that within a short space of time after this was confirmed two new genomic rat libraries became available. Work carried out using the YAC library has been important, seven YAC clones were isolated using the marker R158. However, working with YAC clones presents some problems, the major one being the difficulty in isolating intact DNA not containing any host DNA. YACs also present problems involving rearrangements and chimaerism (Green *et.al.*, 1991). However, the YAC clones isolated still have a role to play in the construction of a contig containing *agu*. Their large insert size makes them ideal for cloning large segments of genome. In future studies, they will be confirmed as being non-chimaeric and then used as a frame-work against which all new clones can be confirmed to be contained within the contig.

The library most heavily utilised was the PAC library, the major reason being that the cloned DNA within the PAC clones is large but isolation of DNA from PAC clones is still simple, quick and inexpensive. This allows a far greater range of investigations on the clones to be carried out. This resulted in the PAC library being used to walk in either

direction from one of the original PAC clones isolated. The method of screening the library is fast and efficient, allowing a rapid pace of walking, even though smaller steps are being taken when compared to YAC clones. For these reasons the PAC library is now being used to construct a contig across the region thought to contain *agu*, and it is hoped that once this region has been mapped both physically and genetically, the PAC clones will eventually be used to isolate cDNAs encoded by genes contained on the PACs.

7.3 Evidence for the role of the *agu* gene from phenotypic analysis

The number of possible candidate proteins which could contain the *agu* mutation are huge and range from enzymes involved in dopamine synthesis and metabolism e.g. MAO-B, tyrosine hydroxylase and the dopamine receptor, to proteins involved in oxidative stress e.g. ferritin light chain, glutathione and SOD. However, a number of candidate genes which could contain the mutation are suggested by the altered pharmacology produced in the AS/AGU rat. In a previous study, dopamine levels in striatal micropunch samples from AS/AGU rats, deficits only occurred after 6 months of age (Campbell *et.al.*, 1997), when there was a 30% loss, compared with controls. However, in further studies, carried out using microdialysis and HPLC analysis (Campbell *et.al.*, 1998), extracellular levels of dopamine in the dorsal caudate-putamen of conscious animals were markedly reduced to only 10-20% of control levels at all three ages selected (3, 6 and 9 months). Conversely, levels of DOPAC were 2-4 times higher in AS/AGU than in AS animals (Campbell *et.al.*, 1998).

It is unclear if this loss in extracellular dopamine is due to the loss of dopaminergic neurons in these animals. For example, at 6 months of age the AS/AGU rat displays no detectable loss of whole tissue dopamine when compared to controls (Campbell *et.al.*, 1997). However, when extracellular levels of dopamine are measured there is a massive decrease at 3 months of age (Campbell *et.al.*, 1998), in the absence of a detectable loss of whole tissue dopamine. This could be a result of over compensation by cells which are still functioning for their non-functioning neighbours. It is likely, therefore, that the loss of extracellular dopamine is not simply the result of the loss of dopaminergic neurons.

The high extracellular concentration of the metabolite DOPAC relative to that of dopamine is normally observed in studies of rats and is thought to reflect the high re-uptake and metabolic capacity of nerve terminals. As this was also the case in tests on the AS/AGU rat, it indicates that there is no major deficit in uptake and metabolism of dopamine in these animals (Campbell *et.al.*, 1998). However, the elevated levels of the metabolite DOPAC (2.5 - 5 fold) in AS/AGU animals, when compared to controls, are very interesting. This evidence may indicate that the primary defect is in dopamine release in the AS/AGU animal.

Suggestions that the *agu* mutation leads to a defect in the release of dopamine from presynaptic nerve terminals provides many other considerations. As discussed previously (Chapter 1, Section 1.1.3) the number of proteins which appear to be involved in the release of neurotransmitters is huge. Therefore, the number of possible candidate genes is large (Section 7.4.2.2).

Not only does the suggestion of a defect in the release of dopamine in the AS/AGU rat suggest candidate genes, it may also indicate a mechanism by which cell death within the substantia nigra occurs. If dopamine produced by a neuron is not released, what are the consequences? Although the cause of PD is still unknown, oxidative stress has been implicated as a pathogenic factor. According to this so called "free radical hypothesis", the degeneration of the nigro-striatal system in PD is related to the relatively high exposure of these neurons to reactive oxygen species (ROS).

Oxidative stress in PD may arise from the metabolism of dopamine itself by both chemical and enzymatic mechanisms. The autoxidation of dopamine leads to the production of semiquinones, which are themselves toxic and may also lead to the generation of reactive oxygen species (Olanow, 1990). The semiquinone cascade leads to polymerisation and the formation of neuromelanin which may also act as a ROS, although there is no evidence that increased dopamine oxidation or melanin formation occurs in individuals who develop PD.

Perhaps more important is the enzymatic metabolism of dopamine, which leads not only to the deaminated metabolites homovanillic acid (HVA) and 3,4-dihydroxyphenylacetic (DOPAC) but also to the generation of hydrogen peroxide (H_2O_2). Every dopamine molecule deaminated produces one molecule of hydrogen peroxide (H_2O_2). Based on this observation, a theoretical scheme for the excess formation of the oxidant species, H_2O_2, and $OH^{\bullet}$ formation has been devised (Jenner and Olanow, 1996). Increased dopamine turnover in the early stages of PD might generate excessive H_2O_2, which would normally be inactivated by glutathione (GSH) in a reaction catalysed by glutathione peroxidase. However, if the GSH system were impaired or deficient, H_2O_2 might be converted by the iron-mediating Fenton reaction to form highly reactive $OH^{\bullet}$, so initiating lipid peroxidation and cell death (Jenner and Olanow, 1996). Indeed, the experimental elevation of dopamine turnover can lead to increased oxidative stress as determined by a rise in the formation of oxidised glutathione (Spina and Cohen, 1989).

To prevent breakdown of dopamine before it's release from presynaptic endings, the transmitter is taken up and stored in presynaptic granules (vesicles). Excessive dopamine within the cell may not be packaged into vesicles due to the fact that this packaging is carried out by a receptor (VMAT) and is thus limited by the numbers of receptors available

at any given time. Excessive dopamine in the presynaptic neuron may lead to an increased turnover of dopamine being deaminated by monoamine oxidase, a by-product of which is hydrogen peroxide, which can produce free radicals and can contribute to oxidative stress. To evoke increased presynaptic turnover of dopamine, Spina and Cohen (1989) used the drug reserpine, which prevents the storage of dopamine in neuronal transmitter vesicles by interfering with the transport of dopamine into the vesicles (through VMAT). As a result, the metabolism of dopamine by mitochondrial MAO-A is increased. Levels of glutathione disulphide (GSSG) were greatly increased, indicating that the rate of production of hydrogen peroxide evoked by reserpine was sufficient to override the cellular mechanism for reducing GSSG. Therefore, an increased amount of presynaptic metabolism of dopamine can lead to a detectable alteration in the redox status of dopamine terminals (Spina and Cohen, 1989). A persistent oxidative stress, coupled to significant loss of GSH, may promote a faster than normal rate of neuronal senescence.

Another piece of evidence which substantiates this theory is the injection of L-Dopa into AS/AGU rats. Injection of L-Dopa appears to reduce the severity of the phenotype produced by the *agu* mutation, as displayed by an increase in performance in the locomotion and balance tests (A.Payne, personal communication). Dopamine (DA) synthesised from L-Dopa is not packaged into synaptic vesicles, different to native dopamine. Studies suggest that most of the DA formed from L-Dopa remains in the cytoplasm and is not stored in the vesicles (Melamed, 1992). The DA produced from L-Dopa is then not released by the classical transmitter release pathway, but is probably released from the cell by diffusion. Likewise, the normal negative feedback mechanisms regulating DA synthesis and release appear to be absent in the case of L-Dopa derived dopamine (Melamed 1992; Ponzio *et.al.*, 1983). As the injection of L-Dopa is seen to reduce the severity of the AS/AGU phenotype, the dopamine produced may be overriding the reduction of released dopamine from the neuron.

The *agu* mutation may lead to a reduction in the amount of dopamine released from neurons in the caudate putamen. This would have several consequences; increased dopamine turnover within the cell would lead to the production of free radicals which could lead to cell death. Another consequence of reduction of released dopamine would be on the negative feedback loop which regulates the synthesis of dopamine. If reduced amounts dopamine are being released this will not signal to the cell to limit the synthesis of new dopamine. The cell will then be producing larger amounts of dopamine than would be normal which would then have to be metabolised leading to further production of free radicals. Also as the dopamine producing cells die, the neighbouring surviving cells will increase their production of dopamine to compensate for the loss, leading to the production of excess free radicals within these cells.

7.4 Identification of the *agu* gene

7.4.1 Strategies involved in gene identification

There a many ways of identifying the gene which contains the *agu* mutation but the following strategies appear to be the most likely approach. The first stage of the investigation is to rule out any candidate genes. These can be divided into two categories; those implicated by their genetic map location and those implicated by clues derived from the phenotype analysis. These candidate genes can be eliminated in many ways e.g. Northern blot analysis of RNA transcripts, probing of genomic clones with probes derived from these genes and if they are present, direct sequencing within the AS and AS/AGU rat strains.

If this approach does not identify a gene containing the *agu* mutation the next step would involve the fine mapping of the interval containing the gene to identify the smallest genetic region, defined by cross-over events, which contains the gene. This region can then be investigated for expressed genes by various methods (Section 7.4.3.2).

7.4.2 Identification of genes which are candidates to contain the agu mutation

As previously detailed (Section 7.4.1) there are two approaches to identifying candidate genes for this project; candidates based on genetic data and from phenotypic analysis.

7.4.2.1 Candidates based on genetic data

Genetic mapping of the marker R158 (Section 5.2) very close to *agu* allowed a small interval of the rat genome to be investigated in detail. Investigation of this interval can therefore be carried out to identify novel genes within this genomic region. Also genes which have previously been mapped to this genetic interval in rat could be considered candidate genes and must be excluded from future study.

A major candidate gene suggested by the current mapping data, was the gene encoding protein kinase C type 1 (PKC-γ). The marker R158 (Serikawa *et.al.*, 1992) was contained within the 3' UTR of the gene encoding PKC-γ (Section 6.1), and mapping of this marker positioned it to within 100 kb of the *agu* locus. However, this figure is only a very crude estimation from genetic mapping, as only one definite recombinant animal has been identified between the marker and *agu*. Also the exact size of the gene encoding PKC-γ in rat is unknown, it is a possibility therefore that this gene could contain the *agu* mutation. PKC is present in high concentrations in neuronal tissues and has been implicated in a variety of neuronal functions including signal transduction, modulation of

ion channel activity and synaptic transmission. The γ-subspecies of PKC appears to be expressed solely in the brain and spinal cord, and is particularly concentrated in the rat brain in the hippocampus, cerebellum, cerebral cortex and amygdaloid complex (Ono *et.al.*, 1988 and Yoshihara *et.al.*, 1991)). Subcellular localisation studies indicate that PKC-γ is present primarily in the soma and dendritic processes of neurons (Huang *et.al.*, 1988).

PKC-γ deficient mice were created in 1993 (Abeliovich *et.al*, 1993a) and have been used in the study of memory and long-term potentiation. It is interesting to compare the phenotype of these mice to the AS/AGU rat, if the gene encoding PKC-γ is considered as a candidate gene. These mice were reported to show no gross anatomical abnormalities of the brain, and as this work was focused on the hippocampus and cerebellum (Abeliovich *et.al*, 1993b) it is unlikely that fine anatomical studies were carried out e.g. investigation of the substantia nigra. The mutant mice were mildly ataxic and showed a decreased effect of ethanol on behaviours and they were demonstrated to be defective in motor co-ordination but were fully capable of motor learning (Chen *et.al.*, 1995). However, as these mice displayed unusual, persistent multiple innervation of Purkinje cells by climbing fibres (Kano *et.al.*, 1995), the authors proposed this as the primary cause of the motor discoordination (Chen *et.al.*, 1995). It is difficult to compare these mice to the AS/AGU rat as similar tests and investigations have not been carried out, however, there is one similarity e.g. mild ataxia. The authors do not detail the progression of this ataxia or indeed when it becomes observable.

Evidence suggests that phosphorylation of the dopamine transporter (DAT) is controlled by PKC, and reduction in DAT phosphorylation leads to increased dopamine transport (Vaughan *et.al.*, 1997). If the *agu* mutation is contained within PKC-γ, then it is feasible that a reduction in PKC-γ brought about by the mutation could lead to reduced phosphorylation of DAT, producing increased dopamine transport from the synaptic cleft into the cell This may lead to decreased extracellular dopamine and increased metabolites of dopamine, after the action of MAO, as observed in the AS/AGU rat.

However, the γ isoform of PKC seems to be localised in the postsynaptic side of the glutamatergic synapse (Kose *et.al.*, 1988) but has not been localised within the dopamine synapse. PKC-γ may be involved in long-term potentiation (LTP) and long-term depression (LTD), possibly involved in storage of information in the brain (Tanaka and Nishizuka, 1994). The γ isoform is therefore thought of as a likely candidate for involvement in postsynaptic regulation of glutamate receptors (Tanaka and Nishizuka, 1994). However, PKC-γ may still have a role to play in presynaptic processes. PKC-γ therefore still proves a very interesting candidate gene and one which must be ruled out before a thorough investigation of novel candidate genes is carried out.

Another major candidate gene identified by work carried out by Polymeropoulos and colleagues (Polymeropoulos *et.al.*, 1997) was the gene encoding α-synuclein. As discussed in Chapter 1 the gene encoding α-synuclein was shown to contain a missense mutation that segregated with PD in the large Contursi kindred (Polymeropoulos *et.al.*, 1997) and was also found in three additional PD families of Greek origin. The mechanism by which this mutation leads to PD is largely unknown and there is relatively little known about the protein itself. However, α-synuclein immunostaining can be observed in Lewy bodies of idiopathic PD and diffuse Lewy body disease patients and it is thought that the mutation within the protein may promote the aggregation of α-synuclein into filaments, resulting in the formation of Lewy bodies (Spillantini *et.al.*, 1997).

Synuclein was first isolated by an expression screen of a *Torpedo* electric lobe cDNA library using an anti-serum against purified synaptic vesicles (Maroteaux *et.al.*, 1988). In *Torpedo* and rat the gene encodes a protein comprised largely of 11 amino acid repeat units, and is expressed only in neurons with immunoreactivity localised to synaptic vesicles within the presynaptic nerve terminal and a region of the nuclear envelope. Two observations gave rise to the hypothesis that synuclein was associated with synaptic vesicles: the first, that the gene was initially identified in an expression screen using a serum antibody generated against purified cholinergic synaptic vesicles. The second, EM localisation of synuclein fusion protein antibody staining in the vicinity of synaptic vesicles (Maroteaux *et.al.*, 1988). Experiments also suggest that one form of the synuclein protein appears to be associated with the synaptosomal membrane (Maroteaux and Scheller, 1991) and may be inserted into the membrane after post translational modification.

Since the protein structure predicted from the analysis of cDNA clones most likely ruled out an enzymatic role for synuclein in nerve cells, it was postulated that the function of the protein was a functional or structural one (Maroteaux *et.al.*, 1988). The repeats within the protein contain a conserved core which is also found in the *rho* gene family (Maroteaux *et.al.*, 1988) which may indicate a role in cell signalling. Also the localisation of synuclein to the synaptic vesicles could indicate a role in the trafficking, docking and membrane fusion of synaptic vesicles. Synuclein expression co-localises with neurons using phosphoinositol (PI) and phospholipase C (PLC) as second messengers, and the form of synuclein associated with the synaptosomal membrane can be induced to return to the soluble form by phosphotidylinositol specific PLC. It is possible that activation of PLC after neuronal stimulation leads to solubilisation of synucleins, thus implicating synucleins in synaptic vesicles release and/or recycling (Maroteaux and Scheller, 1991). It is interesting that NCAP, a peptide fragment of α-synuclein, is an unusual protein in that it adopts an extended, non-globular conformation known as a "natively unfolded" random coil, *in vitro*. Such random coil domains promote protein-protein interactions and make

the protein amyloidogenic *in vitro* (Weinreb *et.al.*, 1996). As previously detailed Chapter 1 the synaptic vesicle release system is comprised of many protein-protein interactions.

The discovery that α-synuclein, when mutated, predisposes with high probability to the development of PD in families with autosomal dominant disease, suggest that a structural abnormality of this protein, either by changing conformation or altering normal proteolytic processing, may be the initiating event for protein aggregation. Why this mutation gives rise to nerve cell death primarily within the substantia nigra is a question which remains unanswered.

α-synuclein represents a strong candidate for the gene containing the *agu* mutation. Synuclein is localised to the presynaptic nerve terminal, the area of the cell where the *agu* protein is thought to act (Section 7.3). Synuclein is associated with synaptic vesicles and is thought to play a role in trafficking, docking or membrane fusion of vesicles. There is, however, one major piece of evidence to suggest that α-synuclein is not the gene containing the *agu* mutation. The region of human chromosome thought to contain the *agu* mutation, by synteny with rat is chromosome 19q13.4 and α-synuclein was shown to map to chromosome 4q21-q23 (Polymeropoulos *et.al.*, 1996). However, there is a possibility that rearrangements have occurred within the human genome to breakdown the region of synteny. Also there may be as yet unidentified/un-mapped members of the synuclein gene family which may be contained in the correct region of rat chromosome 1. In fact, Southern blot analysis of rat genomic DNA indicated that there are at least three rat synuclein family members (Maroteaux and Scheller, 1991).

Another strong candidate gene suggested by genetic mapping data is synaptotagmin 3 (*Syt3*) which maps to within 1.2 cM of the gene encoding PKCγ on mouse chromosome 7 (Stubbs *et.al.*, 1996), the region syntenic to rat chromosome 1 which contains the *agu* gene. As detailed in Section 1.2.2 synaptotagmins are likely to function as Ca^{2+} sensors at the site of neurotransmitter exocytosis and are likely to trigger the final stage of the fusion of vesicles to the synaptic membrane. Therefore, the genetic location of synaptotagmin 3 and the action of the protein makes this a strong candidate gene (Section 7.4.2.2).

PKC-γ, α-synuclein and synaptotagmin 3 are all good candidates for the *agu* gene and will have to be eliminated before future studies are carried out.

7.4.2.2 Candidate genes identified from phenotypic analysis

The pharmacology presented in the AS/AGU rat (Section 7.3) suggests that the *agu* mutation leads to a reduction in the amount of dopamine being released from the presynaptic membrane. Neurosecretion is a complex, multistep process involving vesicle

biogenesis, neurotransmitter packaging, vesicle translocation and Ca^{2+} dependent vesicle fusion with the plasma membrane (Section 1.2.2). Proteins which are involved at any one of these steps could be considered a candidate to contain the *agu* mutation. As anticipated for a highly regulated, multistep pathway, the concerted action of a large number of gene products is required for neurosecretion. Genetic screens in *C.elegans* identified approximately 30 genes with presynaptic functions (Miller *et.al.*, 1996). There are at least 50 proteins currently known to be essential for trafficking in the exocytotic pathway in neurons (Martin, 1997) (Table 7.1). They could all be considered candidates to contain the *agu* mutation.

Translocation, cytoskeletal anchorage, recruitment of vesicles	**Vesicle proteins with uncharacterised roles**	**Unknown site of action**	**C. elegans genes**	**ATP-dependent priming**	**Late stages prior to fusion**
kinesins,rab3s 14-3-3s,actin, myosin II ,myosin light chain kinase, scinderin, synapsins, CaM kinase II, rabphillin	synaptophysin synaptoporin SV2s, SCAMPs, synaptogyrin, $pp60^{src}$, cysteine string proteins	Rab3s, rabphillin, RabGDI, MSS4, Doc-2, Hrs-2, unc-41p, unc-18p (munc18, nSec1, rop), unc-13p, aex-3p, rSec6, annexins, GAP-43, neurexins, VAP-33	ric-1, ric-6 ric-7, ric-8 unc-10, unc-26, unc-7	PtdIns transfer proteins (PEP3), PtdIns 4-kinase, PtdIns4P-kinase (PEP1), NSFs, α/β/γ-SNAP	synaptobrevins, syntaxins, SNAP-25s, synaptotagmins, CAPs.

Table 7.1 Proteins involved in regulated exocytosis in the neuron. The protein types are given as a heading to each column. Many of these proteins, indicated by plurals, are encoded by multiple genes. PtdIns = phosphatidylinositol phosphate. Adapted from Miller (1997).

Both α-synuclein and synaptotagmin 3 fall into this category of candidate genes as well as those from genetic mapping, as they are also suggested by the phenotype of the AS/AGU rat (Section 7.3). α-synuclein represents a strong candidate for the gene containing the

agu mutation. Synuclein is localised to the presynaptic nerve terminal, the area of the cell where the *agu* protein is thought to act (Section 7.3). Synuclein is associated with synaptic vesicles and is thought to play a role in protein interactions in trafficking, docking or membrane fusion of vesicles (Maroteaux and Scheller, 1991). Another good example is syntaxin; *Drosophila* with mutations in syntaxin reveal a complete absence of both evoked and spontaneous neurotransmitter release. Ultrastructural studies of syntaxin mutants show that vesicles appear normally docked at the active zone and that there is a significant increase in the number of docked vesicles (Broadie *et.al.*, 1995). This suggests that in syntaxin mutants the absence of syntaxin impairs the ability of vesicles to undergo fusion.

7.4.3 Identification of the agu gene by genetic and physical mapping

If the above strategies do not identify the *agu* gene, then the conventional process of positional cloning will be instigated. There are two distinct steps within this final process; they are the definition of a precise genetic region containing the *agu* mutation, followed by investigation of genes expressed in this region.

The precise definition of the genetic region contained on a contig involves the detailed mapping of that contig with closely-linked genetic markers. To achieve this aim new microsatellite markers will be isolated from clones contained in the contig (as detailed in Chapter 3). Once these markers have been identified they can be used to map cross-over events which have occurred within the recombinant panel of backcross progeny established in Section 5.2.2. This will further refine the region for investigation. This will also allow the determination of the direction in which the chromosome walk should be carried out i.e. towards *agu*, by positioning *agu* on one side of the contig.

7.4.3.1 Establishing a new backcross with AS/AGU and DA

To achieve the fine mapping of a genetic interval a number of informative microsatellite markers must be identified. Some problems have been encountered in identifying informative markers in the rat strains used in this study (F344, BN and AS/AGU). Genetic map construction is significantly more difficult in the rat, than in the mouse in one important respect: genetic mapping in the mouse can exploit artificial laboratory crosses with different species that have SSLP polymorphism rates with laboratory strains of about 90%, rather than intraspecific crosses in which the polymorphism rate is only about 50% (Jacobs *et.al.*, 1995). An excellent example, is in the case of the interspecific backcross generated using *M.musculus* and *M.spretus*, utilised in our laboratory for mapping SSCPs (McCallion, 1997), where strain variations were found in > 90% of PCR products tested from the 3' UTR of mouse genes. A complete barrier to gene flow existed between the house mouse (*M.musculus*) and the aboriginal strain (*M.spretus*), two populations with

overlapping ranges which do not breed - the definition of a species. However, in 1978, Bonhomme and his colleagues (Bonhomme *et.al.*, 1978) reported the finding that *M.spretus* males and laboratory strain females could be bred in captivity to produce viable offspring of both sexes. Because similarly genetically unrelated rat strains are not available, only about half of the SSRs isolated are informative in any given mapping cross.

Initial analysis of polymorphism rates between the strains BN and F344 indicated an average of 68% across the genome (Shiels *et.al.*, 1995), and AS/AGU differed from BN, F344 and PVG at 62%, 47% and 43% respectively. Strain BN has previously been shown to have the highest genetic divergence from all other inbred strains (Canzian, 1997). However, there was concern with the low rates of strain variation in PCR products containing novel SSR markers identified from P1 clones; no strain differences were observed in PCR products from eight SSR markers from the region surrounding P1 clone K (Section 6.3, markers K100, K106 etc.). To allow fine mapping of the interval surrounding *agu*, contained in the genomic contig, a large number of informative markers must be identified from this region.

A project mapping markers on rat chromosome 1 was carried out by Ding and colleagues (Ding *et.al.*, 1996) which utilised a rat cross between the inbred rat strains DA/Bkl and F344/Hsd. Polymorphism rates for SSR markers between the strains F344, LEW, BN and DA were assessed and polymorphism rates between F344/DA and BN/DA were 72.5% and 77.5%, respectively for 40 markers tested. Markers reported by Ding and colleagues within the interval thought to contain *agu* were tested and proved to be non-informative between our rat strains (Canham, 1997). Three markers from 11 tested which were not polymorphic between the rat strains AS/AGU, F344 and BN, showed a polymorphism between DA and AS/AGU (*D1Arb33* = Cea1, *Cgm4* = Cea4, Ding *et.al.*, 1996). However, strain DA was not informative when compared to AS/AGU for markers D1GU10 (Chapter 3) and D1Mgh7 (Chapter 5 and Jacobs *et.al.*, 1995) which were utilised in the present study.

A new backcross has been initiated between the strains DA and AS/AGU with progeny expected in February 1998. Although this backcross may not necessarily produce a higher polymorphism rate when compared to AS/AGU, it will still provide another rat strain in which microsatellite markers can be investigated for strain variation. It is hoped that this backcross will prove useful in fine mapping of the <1 cM region thought to contain *agu*, which entails the isolation and mapping of a large number of informative SSR markers from the interval.

7.4.3.2 Expressed gene identification

Once this fine genetic mapping of the interval has been achieved and the *agu* gene has been identified to be contained on as few clones as possible then the process of expressed gene identification can be carried out. This can be carried out by two main processes; cDNA hybrid selection and exon trapping.

Once a region of genomic DNA cloned has been shown to contain the *agu* locus by fine mapping of the interval, an investigation will be carried out to identify candidate genes contained within this interval. Many techniques have been utilised to aid in the identification of transcribed sequences from particular genomic regions e.g. identification of CpG islands, zoo blots, screening cDNA libraries with genomic clones, direct sequencing and using genomic clones to identify a transcript in RNA on a Northern blot.

However, in recent years two techniques have become established as the most efficient and simple ways of identifying transcribed sequences from genomic regions. The first strategy was devised by Duyk *et.al.*, (1990) and further developed by Buckler *et.al.* (1991) and involves the identification of exons from random pieces of genomic DNA and is known as exon trapping. In summary, genomic DNA is cloned into a vector that contains functional splice donor and acceptor sites and the clones are then propagated in *E.coli* and then transfected into COS cells. When the cloned DNA contains an exon, splicing occurs between the vector and the genomic DNA, RNA is then isolated from the cells, cDNA is synthesised and amplified using primers to the vector. A unique DNA fragment is therefore obtained where correct splicing has occurred. Theoretically this procedure should identify all internal exons from a region of interest and has been applied with good results (Chen *et.al.*, 1996). However, it is technically complex and as it simply requires the presence of splice donor and acceptor sites, false positives can be encountered.

Recently, techniques which involve direct cDNA selection or "hybrid selection" have been devised. These methods employ the sensitivity of PCR with the specific selection of cDNAs by hybridisation to large genomic regions. This was first devised by Lovett *et.al.* (1991) and involves the hybridisation of an entire cDNA pool to an immobilised genomic clone. Genomic clone DNA was isolated, digested and immobilised onto nylon filter discs. cDNA inserts were amplified from an oligo d(T) cDNA library using primers designed to the library vector. The amplified inserts were preblocked with sheared total human DNA, yeast DNA and pBR322 DNA, this reduced non-specific hybridisation of repetitive elements, yeast and vector sequences. The blocked cDNA was then hybridised in solution with the filter containing the genomic DNA. Non-specific hybrids were removed, selected cDNAs were eluted, amplified with the primers used to amplify the

cDNA at the onset and either cloned into a phage vector or subjected to further selection. More recently the technique has been improved by introducing better blocking efficiency, hybridisation in solution to better control hybridisation conditions and biotin/streptavidin capture on magnetic beads (Parimoo *et.al.*, 1991, Korn *et.al.*, 1992 and Morgan *et.al.*, 1994). The initial experiments were carried out using YAC genomic clones but the technique has been adapted to the use of P1, PAC, BAC and cosmid clones.

There are several advantages to hybrid selection: first it is rapidly carried out, second this method tends to normalise the frequency of the transcripts encoded by the genomic clone and has greater enrichment factors for rare transcripts than abundant ones. The abundant cDNAs will quickly saturate their genomic target, leaving the majority of cDNAs in solution. Thus the net result should be an approximate normalisation of the abundant cDNAs downwards and the low abundance transcripts upwards. Since the isolation of rare cDNAs is as important as the isolation of abundant ones, enrichment of these is a great advantage of this technique, as opposed to screening conventional libraries which may not even contain these transcripts. Third, it is more robust than screening with labelled probes and has a much higher signal to noise ratio mainly because it is easier to quench sequences by blocking to prevent non-specific hybridisation. Finally, it is also less sensitive to the size of the clone used for selection. Cosmid, BAC or P1 DNA is better than YAC DNA because it is less prone to deletions, chimaerism and is readily separated from *E.coli* DNA.

There are a few limitations to hybrid selection: firstly, it is not suitable for retrieving complete coding sequences for genes, rather it provides a route to finding expressed sequence tags (ESTs) which can be used as probes to isolate the gene. Thus, screening a library is probably a second step in the process. Secondly, there is a problem with the co-selection of pseudogenes, either transcribed or non-transcribed. Thirdly, it is limited when the transcription pattern of the gene of interest is unknown; cDNA from many different tissues or developmental stages may have to be tested.

The improvements in the cDNA hybrid selection method make this technique a rapid and feasible way of isolating transcribed sequences from genomic clones thought to contain the *agu* locus. This could be carried out with PAC clones currently under investigation. The sequencing of cDNAs encoded by the genomic interval under investigation would allow the identification of candidate genes for *agu*, which could then be sequenced in the rat strains AS and AS/AGU and the gene sequence compared to identify the mutation in AS/AGU.

7.5 Future work - Do mutations in the *agu* gene lead to PD in man?

The obvious goal of the project is the identification of the gene containing the *agu* mutation. Once this has been established it is important to ascertain if this gene has any involvement in human Parkinson's disease. This is vital because not only could it provide an insight into susceptibility to PD, but could also validate the AS/AGU rat as a genetic model of human PD, a tool currently lacking in this field of research.

An assessment will have to be carried out if the *agu* gene is implicated in human PD. This should be a relatively simple task with probably no need for complicated linkage studies. Once the gene sequence has been identified in rat and then in man, the gene can be sequenced in many of the PD families identified (for example; Maragnore *et.al.*, 1991, Golbe *et.al.*, 1996, Denson *et.al.*, 1997) to ascertain if any mutation is present in the affected individuals in these families.

Preliminary work has already been carried out on the involvement of the *agu* gene in human PD. When a region of human chromosome 19 was identified to contain the *agu* gene by nature of synteny with rat, genetic markers flanking this region were tested for linkage to PD in the large Contursi kindred, the kindred which was recently identified to contain a mutation in the α-synuclein gene thought to contribute to PD. No linkage was found between the markers and PD in this family (R.G. Sutcliffe, personal communication). However, this family is seen as a good example of early-onset families with PD characterised by a highly penetrant, autosomal dominant inheritance. These families account for only a small proportion of familial cases of PD and the majority of cases of PD are sporadic. Therefore, the *agu* gene may not be involved in PD within this family but may prove to be important in other PD families and sporadic cases. Also the protein produced from the agu gene may not itself produce human PD but may nevertheless, still be involved in the pathological process and is therefore still important. In either case the AS/AGU rat still provides a good model in which to study the pathology of neurodegeneration.

7.6 Concluding remarks

There still remains much work to be carried out before the gene containing the *agu* mutation can be identified, although many candidate genes have been suggested. Future work would involve the exclusion of these candidate genes as the *agu* gene. If this is successful and all candidates have been eliminated, then identification of transcribed sequences from cloned DNA will be carried out, presumably using cDNA hybrid selection. The cDNAs can then be sequenced to again identify candidate genes, which can

be sequenced in AS and AS/AGU to identify the *agu* mutation. To ascertain that the gene thought to contain the mutation is in fact the one mutated in AS/AGU, the gene can be introduced back into these rats to "rescue" the phenotype.

When the mutation has been identified sequencing can be carried out in man to ascertain the involvement of the *agu* gene in human PD. If this is confirmed then the AS/AGU rat could be used a model of human PD, and could be utilised in the elucidation of new treatment procedures and novel drugs to reduce the effects of Parkinson's disease.

References

Abeliovich, A., Chen, C., Goda, Y., Silva, A.J., Stevens, C.F. and Tonegawa, S. (1993 a). Modified hippocampal long-term potentiation in PKCγ-mutant mice. *Cell*, **75**, 1253-1262.

Abeliovich, A., Paylor, R., Chen, C., Kim, J.J., Wehner, J.M. and Tonegawa, S. (1993 b). PKCγ mutant mice exhibit mild deficits in spatial and contextual learning. *Cell*, **75**, 1263-1271.

Adams, J.D.Jr. and Odunze, I.N. (1991). Biochemical mechanisms of 1-methyl-4-phenyl-1,2,5,6,-tetrahydropyridine toxicity. *Biocemical Pharmacology*, **41**, 1099-1105.

Agúndez, J.A.G., Jiménez-Jiménez, F.J., Luengo, A., Bernal, M.L., Molina, J.A., Ayuso, L., Vázquez, A., Parra, J., Duarte, J., Coria, F., Ladero, J.M., Alvarez, J.C. and Benítez, J. (1995) Association between the oxidative polymorphism and early onset of Parkinson's disease. *Clinical Pharmacology and Therapeutics*, **57**, 291-298.

Albin, R.L., Young, A.B. and Penney, J.B. (1989). The functional anatomy of basal ganglia disorders. *Trends in Neurosciences*, **12**, 366-375.

Altschul, S.F., Gish, W., Miller, W., Myers, E.W. and Lipman, D.J. (1990). Basic local alignment search tool. *Journal of Molecular Biology*, **215**, 403-410.

Avramopoulos, D., Chakravarti, A. and Antonarakis, S.E. (1993). DNA polymorphisms in the 3' untranslated region of genes on human chromosome 21. *Genomics*, **15**, 98-102.

Balk, J., Picetti, R., Saiardl, A., Thirlet, G., Dierich, A., Depaulis, A., Le Meur, M. and Borrell, E. (1995). Parkinsonian-like locomotor impairment in mice lacking dopamine D2 receptors. *Nature*, **377**, 424-428.

Bandmann, O., Davis, M.B., Marsden, C.D. and Wood, N.W. (1996). The human homolog of the weaver mouse gene in familial and sporadic Parkinson's disease. *Neuroscience*, **72**, 877-879.

Barbeau, A., Roy, M., Paris, S., Cloutier, T., Plasse, L. and Poirier, J. (1985). Ecogenetics of Parkinson's disease : 4-hydroxylation of debrisoquine. *The Lancet*, Nov 30, 1213-1216.

Batzer, M.A., Deininger, P.L., Hellmann-Blumberg, U., Jurka, J., Labuda, D., Rubin, C.M., Schmid, C.W., Zietkiewicz, E. and Zuckerkandl, E. (1996). Standardised nomenclature for Alu repeats. *Journal of Molecular Evolution*, **42**, 3-6.

Beckmann, J.S. and Weber, J.L. (1992). Survey of human and rat microsatellites. *Genomics*, **12**, 627-631.

Beckstead, R.M., Domesick, V.B. and Nauta, W.J.H. (1979). Efferent connections of the substantia nigra and ventral tegemental area in the rat. *Brain Research*, **175**, 191-217.

Ben-Schachar, D. and Youdim, M.B.H. (1991). Intranigral iron injection induces behavioral and biochemical "parkinsonism" in rats. *Journal of Neurochemistry*, **57**, 2133-2135.

Bezard, E., Dovero, S., Bioulac, B. and Gross, C.E. (1997). Kinetics of nigral degeneration in a chronic model of MPTP-treated mice. *Neuroscience Letters*, **234**, 47-50.

Birnboim, H.C. and Doly, J. (1979). A rapid alkaline extraction procedure for screening recombinant plasmid DNA. *Nucleic Acids Research*, **7**, 1513-1523.

Bonhomme, F., Martin, S. and Thaler, L. (1978). Hybridation en laboratiore de *Mus musculus* L. et *Mus spretus* Lataste. *Experientia*, **34**, 1140-1141.

Booth, R.G., Castagnoli, N. and Rollema, H. (1989). Intracerebral microdialysis neurotoxicity studires of quinoline and isoquinoline derivatives related to MPTP/MPP^+. *Neuroscience Letters*, **100**, 306-312.

Bradford, H.F. (1986). Chemical Neurobiology: An introduction to neurochemistry, W.H. Freeman and Company New York.

Broadie, K. Prokop, A., Bellen, H.J., O'Kane, C.J., Schulze, K.L. and Sweeney, S.T. (1995). Syntaxin and synaptobrevin function downstream of vesicle docking in *Drosophila. Neuron*, **15**, 663-673.

Brown, A., J., P., Leibold, E., A., Munro, H., N. (1983) Isolation of cDNA clones for the light subunit of rat liver ferritin : Evidence that the light subunit is encoded by a multigene family. *Proceedings of the National Academy of Science of the USA.*, **80**, 1265-1269.

Brown, M.D., Shoffner, J.M., Kim, Y.L., Jun, A.S., Graham, B.H., Cabell, M.F., Gurley, D.S. and Wallace, D.C. (1996). Mitochondrial-DNA sequence-analysis of 4 Alzheimers-disease and Parkinsons-disease patients. *American Journal of Medical Genetics*, **61**, 283-289.

Brownstein, B.H., Silverman, G.A., Little, R.D., Burke, D.T., Korsmeyer, S.J., Schlessinger, D. and Olson, M.V. (1989). Isolation of single-copy human genes from a library of yeast artificial chromsome clones. *Science*, **244**, 1348-1351.

Buclker, A.J., Chang, D.D., Graw, S.L., Brook, J.D., Haber, D.A., Sharp, P.A. and Housman, D.E. (1991). Exon amplification - A strategy to isolate mammalian genes based on RNA splicing. *Proceedings of the National Academy of Science of the USA.*, **88**, 4005-4009.

Burn, D.J., Mark, M.H., Playford, E.D., Maraganore, D.M., Zimmerman, T.R., Duvoisin, R.C., Harding, A.E., Marsden, C.D. and Brooks, D.J. (1992). Parkinson's disease in twins studied with ^{18}F-dopa and positron emission tomography. *Neurology*, **42**, 1894-1900.

Burns, R.S., Chiveh, C.C., Markey, S.P., Ebert, M.H., Jacobowitz, D.M. and Kopin, I.J. (1983). A primate model of parkinsonism - selective destruction of dopaminergic-neurons in the pars compacta of the substantia nigra by N-methyl-4-phenyl-1,2,3,6-tetrahydropyridine. *Proceedings of the National Academy of Sciences of the USA*, **80**, 4546-4550.

Cai, L., Schalkwyk, L.C., Schoeberlein-Stehli, A., Zee, R.Y.L., Smith, A., Haaf, T., Georges, M., Lehrach, H. and Lindpainter, K.(1997). Construction and characterisation of a 10-genome equivalent yeast artificial chromosome library for the laboratory rat, Rattus norvegicus. *Genomics*, **39**, 385-392.

Campbell, J.M., Payne, A.P., Gilmore, D.P., Byrne, J.E., Russell, D., McCadey, J., Clarke, D.J., Davies, R.W. and Sutcliffe, R.G. (1996). Neostriatal dopamine and locomotor abnormalities due to the Albino Swiss rat *agu* mutation. *Neuroscience Letters*, **213**, 173-176.

Campbell, J.M., Payne, A.P., Gilmore, D.P., Russell, D., McCadey, J., Clarke, D.J., Branton, R., Davies, R.W. and Sutcliffe, R.G. (1997). Age changes in dopamine levels in the corpus striatum of Albino Swiss (AS) and AS/AGU mutant rats. *Neuroscience Letter*s, **239**, 54-56.

Campbell, J.M., Gilmore, D.P., Russell, D., Growney, C.A., Favor, G., Weir, J., Stone, T.W. and Payne, A.P. (1998). Extracellular levels of dopamine and its metabolite DOPAC measured by microdialysis in the corpus striatum of conscious AS/AGU mutant rats. *Neuroscience*, in press.

Canham, M. (1997). Genetic mapping studies of the rat *agu* gene. University of Glasgow, MSc. Thesis.

Canzian, F. (1997). Phylogenetics of the laboratory rat *Rattus norvegicus*. *Genome Research*, **7**, 262-267.

Caskey, J. H. (1983). Human ferritin gene is assigned to chromosome 19. *Proceedings of the National Academy of Sciences of the USA.*, **80**, 482-486.

Cavanna, J.S., Greenfield, A.J., Johnson, K.J., Marks, A.R., Nadal-Ginard, B. and Brown, S.D.M. (1990). Establishment of the mouse chromosome 7 region with homology to the Myotonic dystrophy region of human chromosome 19q. *Genomics*, **7**, 12-18.

Chen, K., Widen, S.G., Wilson, S.H. and Huang, K. (1990). Characterisation of the 5'-flanking region of the rat protein kinase C γ gene. *Journal of Biological Chemistry*, **265**, 19961-19965.

Chen, C., Kano, M., Abeliovich, A., Chen, L., Bao, S., Kim, J.J., Hashimoto, K., Thompson, R.F. and Tonegawa, S. (1995). Impaired motor co-ordination correlates with persistent multiple climbing fiber innervation in PKCγ-mutant mice. *Cell*, **83**, 1233-1242.

Chen, H., Chrast, R., Rossier, C., Morris, M.A., Lalioti, M.D., Antonarakis, S.E. (1996). Cloning of 559 potential exons of genes of human-chromosome-21 by exon trapping. *Genome Research*, **6**, 747-760.

Clarke, D.J. and Payne, A.P. (1994). Neuroanatomical characterisation of a new mutant rat with dopamine depletion in the substantia nigra. *European Journal of Neuroscience*, **6**, 885-888.

Clarke, L. and Carbon, J. (1976). A colony bank containing synthetic Col E1 hybrid plasmids representative of the entire *E.coli* genome. *Cell*, **9**, 91-99.

Collins, F.S. (1992). Positional cloning: Let's not call it reverse anymore. *Nature Genetics*, **1**, 3-6.

Connor, J.R., Snyder, B.S., Arosio, P., Loeffler, D.A. and LeWitt, P. (1995). A quantitative analysis of isoferritins in select regions of aged, Parkinsonian and Alzheimer's diseased brains. *Journal of Neurochemistry*, **65**, 717-724.

Craig, N.J., Shiels, P., Donald, D., Duran Alonson, M.B., Payne, A.P., Sutcliffe, R.G. and Davies, R.W. (1997). Genetic and physical mapping of the *agu* mutation. *Society for Neuroscience*, Abstracts **23**; Part 2, pg.1873, Abstract 728.3.

Cross, S.H. and Little, P.F.R. (1986). A cosmid vector for systematic chromosome walking. *Gene*, **49**, 9-22.

Davey, G., Tipton, K.F. and Murphy, M.P. (1992). Uptake and accumulation of MPP^+ by rat liver mitochondria measured using an ion-selective electrode. *Biochemical Journal*, **288**, 439-443.

Davis, R.W., Thomas, M., Cameron, J., St. John, T.P., Scherer, S. and Padgett, R.A. (1980). Rapid DNA isolations for enzymatic and hybridisation analysis. *Methods In Enzymology*, **65,** 404-411.

Denson, M.A., Wszolek, Z.K., Pfeiffer, R.F., Wszolek, E.K., Paschall, T.M. and McComb, R.D. (1997). Familial Parkinsonism, dementia, and Lewy body disease: Study of family G. *Annals of Neurology*, **42**, 638-643.

Dexter, D.T., Wells, F.R., Lees, A.J., Agid, F., Jenner, P. and Marsden, C.D. (1989). Increased nigral iron content and alterations in other metal-ions occurring in the brain in Parkinson's disease. *Journal of Neurochemistry*, **52**, 1830-1836.

Diederich, N., Hilger, C.H., Goetz, C.G., Keipes, M., Hentges, F. and Metz, H.(1995) CYP 2D6 mutant alleles and sporadic Parkinson's disease in a carefully defined population. *Annals of Neurology*, **38**, 300.

Ding, Y, Remmers, E.F., Du Y., Longman R.E., Goldmuntz, E.A., Hongbin, Z., Shigeru, K., Cannon, G.W., Griffiths, M.M., and Wilder, R.L. (1996). Genetic maps of polymorphic DNA loci on rat chromosome 1. *Genomics*, **36**, 320-327.

Duran Alonso, M.B. (1997). Genetic mapping of the rat *agu* gene. University of Glasgow, PhD Thesis.

Duvoisin, R.C., Eldridge, R., Williams, A., Nutt, J. and Calne, D. (1981). Twin study of Parkinson disease. *Neurology*, **31**, 77-80.

Duvoisin, R.C. (1992). The genetic etiology of Parkinson's disease. A review of the evidence. *Neurologia*, **7**, 223-229.

Duyk, G.M., Kim, S.W., Myers, R.M. and Cox, D.R. (1990). Exon trapping - A genetic screen to identify candidate transcribed sequences in cloned mammalian genomic DNA. *Proceeding of the National Academy of Science of the USA.*, **87**, 8995-8999.

Dwork, A.J. , Balmaceda, C., Fazzini, E.A., MacCollin, M. Côté, L. and Fahn, S. (1993). Dominantly inherited parkinsonism : Neuropathology of a new form. *Neurology*, **43**, 69-74.

Elsworth, J.D. and Roth, R.H. (1997). Dopamine synthesis, uptake, metabolism and receptors: Relevance to gene therapy of Parkinson's disease. *Experimental Neurology*, **144**, 4-9.

Feldman, R.S., Meyer, J.S. and Quenzer, L.F. (1996). Principles of Neuropsychopharmacology, Sinauer Associates Inc, Publishers. Chapter 20.

Filie, J.D., Buckler, C.E. and Kozak, C.A. (1998). Genetic mapping of the mouse ferritin light chain gene and 11 pseudogenes on 11 mouse chromosomes. *Mammalian Genome*, **9**, 111-113.

Forno, L.S. (1996). Neuropathology of Parkinson's disease. *Journal of Neuropathology and Experimental Neurology*, **55**, 259-272.

Gaspar, P., Jelloun, N.B. and Febvret, A. (1994). Sparing of the dopaminergic neurons containing calbindin-D_{28k} and of the dopaminergic mesocortical projections in weaver mutant mice. *Neuroscience*, **61**, 293-305.

Gauguier, D., Froguel, P., Parent, V., Bernard, C., Bihoreau, M.T., Portha, B., James, M.R., Penicaud, L., Lathrop, M. and Ktorza, A. (1996). Chromosomal mapping of genentic loci associated with non-insulin dependent diabetes in the GK rat. *Nature*, **12**, 38-43.

Geppert, M., Goda, Y., Hammer, R.E., Li, C., Rosahl, T.W., Stevens, C.F. and Südhof, T.C. (1994). Synaptotagmin I: A major Ca^{2+} sensor for transmitter release at a central synapse.*Cell*, **79**, 717-727.

Gerfen, C.R. and Engber, T.M. (1992). Molecular neuroanatomic mechanisms of Parkinson's disease: A proposed therapeutic approach. *Neurologic Clinics*, **10**:2, 435-449.

Gerfen, C.R. (1992). The neostriatal mosaic:multiple levels of comparmental organisation. *Trends in Neurosciences*, **15**, 133-138.

Gerlach, M., Benshachar, D., Riederer, P. and Youdim, M.B.H. (1994). Altered brain metabolism of iron as a cause of neurodegenerative disease. *Journal of Neurochemistry*, **63**, 793-807.

Gerlach, M., Riederer, P. and Youdim, M.B.H. (1996). Molecular mechanisms for neurodegeneration: Synergism between reactive oxygen species, calcium and excitotoxic amino acids. *Advances in Neurology*, **69**, 177-194.

Gibb, W.R.G. and Lees, A.J. (1994). Anatomy, pigmentation, ventral and dorsal subpopulations of the substantia nigra, and differential cell death in Parkinson's disease. *Journal of Neurology, Neurosurgery and Psychiatry*, **54**, 388-395.

Gibb, W.R.G. (1992). Neuropathology of Parkinson's disease and related syndromes. *Neurologic Clinics*, **10**:2, 361-376.

Glinka, Y. and Youdim, M.B.H. (1995). Inhibition of mitochondrial complexes I and IV by 6-hydroxydopamine. *European Journal of Environmental Toxicology and Pharmacology Section*, **295**, 329-332.

Golbe, L.I. (1993). The genetics of Parkinson's disease. *Reviews in the Neurosciences*, **4**, 1-16.

Golbe, L.I., Iorio, G.D., Sanges, G., Lazzarini, A.M., La Sala, S., Bonavita, V. and Duvoisin, R.C. (1996). Clinical genetic analysis of Parkinson's disease in the Contrusi kindred. *Annals of Neurology*, **40**, 767-775.

Goldowitz, D. and Smeyne, R.J. (1995). Tune into the weaver channel. *Nature Genetics*, **11**, 107-109.

Gorell, J.M., Ordidge, R.J., Brown, G.G., Deniau, J.C., Buderer, N.M. and Helpern, J.A. (1995). Increased iron-related MRI contrast in the substantia nigra in Parkinson's disease. *Neurology*, **45**, 1138-1143.

Green, E.D. and Olson, M.V. (1990). Systematic screening of yeast artificial chromosome libraries by use of the polymerase chain reaction. *Proceedings of the National Academy of Science of the USA*. **87**, 1213-1217.

Green, E.D., Riethman, H.C., Dutchik, J.E. and Olson, M.V. (1991). Detection and characterisation of chimeric yeast artificial-chromosome clones. *Genomics*, **11**, 658-669.

Griffiths, R. and Tiwari, B. (1993). Primers for the differential amplification of the sex-determining region Y-gene in a range of mammal species. *Molecular Ecology*, **6**, 405-406.

Gu, L., Dene, H., Deng, A.Y., Hoebee, B., Bihoreau, M., James, M. and Rapp, J.P. (1996). Genetic mapping of two blood pressure quantitative trait loci on rat chromosome 1. *Journal of Clinical Investigation*, **97**, 777-788.

Haldi, M.L., Lim, P., Kaphingst, K., Akella, U., Whang, J. and Lander, E.S. (1997). Construction of a large-insert yeast artificial chromosome library of the rat genome. *Mammalian Genome*, **8**, 284.

Hasebe, M., Hanada, H., Moriyama, Y., Maeda, M. and Futai, M. (1992). Vacuolar type H^+-ATPase genes : Presence of four genes including pseudogenes for the 16 kDa proteolipid subunit in the human genome. *Biochemical and Biophysical Research Communications*, **183**, 856-863.

Heikkila, R.E., Hess, A. and Duvoisin, R.C. (1984). Dopaminergic neurotoxicity of 1-methyl-4-phenyl-1,2,5,6,-tetrahydropyridine in mice. *Science*, **224**, 1451-1453.

Heikkila, R.E., Manzino, L., Cabbat, F.S. and Duvoisin, R.C. (1984). Protection against the dopaminergic neurotoxicity of 1-methyl-4-phenyl-1,2,5,6,-tetrahydropyridine by monoamine-oxidase inhibitors. *Nature*, **311**, 467-469.

Hessler, N.A., Shirke, A.M. and Malinow, R. (1993). The probability of neurotransmitter release at a mammalian central synapse. *Nature*, **366**, 569-572.

Hessler, N.A., Shirke, A.M. and Malinow, R. (1993). The probablility of transmitter release at a mammalian central synapse. *Nature*, **366**, 569-572.

Hikosaka, O. and Wurtz, R.H. (1983). Visual and oculomotor functions of monkey substantia nigra pars reticlata .4. relation of substantia nigra to superior colliculus. *Journal of Neurophysiology*, **49**, 1285-1301.

Hino, O., Testa, J., Buetow, K.H., Taguchi, T., Zhou, J.-Y., Bremer, M. et al. (1993). Universal mapping probes and the origin of human chromosome 3. *Proceedings of the National Academy of Science of the USA*, **90**, 730-734.

Hirsch, E.C., Brandel, J-P.,Galle, P., Javoy-Agid, F., Agid, Y. (1991). Iron and aluminium increase in the substantia nigra of patients with Parkinson's disease: An X-ray microanalysis. *Journal of Neurochemistry*, **56**, 446-451.

Ho, S.L., Kapadi, A.L., Ramsden, D.B. and Williams, A.C. (1995). An allelic association study of monoamine oxidase B in Parkinson's disease. *Annals of Neurology*, **37**, 403-405.

Hotamisligil, G.S., Girmen, A.S., Fink, J.S., Tivol, E., Shalish, C., Trofatter, J., Baenziger, J., Diamond, S., Markham, C. and Sullivan, J. (1994). Hereditary variations in monoamine oxidase as a risk factor for Parkinson's disease. *Movement Disorders*, **9**, 305-310.

Huang, F.L., Yoshida, Y., Nakabayashi, H., Young, W.S. and Huang, K.P. (1988). Immunocytochemical localisation of protein kinase C isozymes in rat brain. *Journal of Neuroscience*, **8**, 4734-4744.

Ioannou, P., Amemiya, C.T., Garnes, J., Kroisel, P.M., Shizuya, H., Chen, C., Batzer, M.A. and Jong, P.J. (1994). A new bacteriophage P1-derived vector for the propagation of large human DNA fragments. *Nature Genetics*, **6**, 84-89.

Iwai, A., Yoshimoto, M., Masliah, E. and Saitoh, T. (1995). Non-A-beta component of Alzeimers-disease amyloid (NAC) is amyloidogenic. *Biochemistry*, **34**, 10139-10145.

Iwai, A., Masliah, E., Yoshimoto, M., Ge, N.F., Flanagan, L., Desilva, H.A.R., Kittel, A. and Saitoh, T. (1995). The precursor protein of non-A-beta component of Alzheimers-disease amyloid is a presynaptic protein of the central nervous system. *Neuron*, **14**, 467-475.

Jacob, H.J., Brown, D.M., Bunker, R.K., Daly, M.J., Dzau, V.J., Goodman, A., Koike, G., Kren, V., Kurtz, T., Lernmark, A., Levan, G., Mao, Y., Pettersson, A., Pravenec, M., Simon, J.S., Szpirer, C., Szpirer, J., Trolliet, M.R., Winer, E.S. and Lander, E.S. (1995). A genetic linkage map of the laboratory rat, *Rattus norvegicus*. *Nature Genetics*, **9**, 63-69.

Javitch, J.A., D'Amato, R.J., Strittmatter, S.M. and Snyder, S.H. (1985). Parkinsonism-inducing neurotoxin, *N*-methyl-4-phenly-1,2,3,6- tetrahydropyridine: Uptake of the metabolite *N*-methyl-4-phenylpyridine by dopamine neurons explains selective toxicity. *Proceeding of the National Academy of Science of the USA*, **82**, 2173-2177.

Jenner, P.G. (1992). Oxidative stress as a cause of Parkinson's disease. Neurodegeneration, pg.1-20. Academic press Ltd.

Jenner, P. and Olanow, C.W. (1996). Oxidatve stress and the pathogenesis of Parkinson's disease. *Neurology*, **47** (Suppl 3), S161-S170.

Johnson, W.G. (1991). Genetic suscepitbilty to Parkinson's disease. *Geriatrics*, **46** (Supplement 1), 52-59.

Kano, M., Hashimoto, K., Chen, C., Abeliovich, A., Aiba, A., Kurihara, H., Watanabe, M., Inoue, Y. and Tonegawa, S. (1995). Impaired synapse elimination during cerebellar development in PKCγ mutant mice. *Cell*, **83**, 1223-1231.

Kimmerly, W.J., Kyle, A.L., Lustre, V.M., Martin, C.H. and Palazzolo, M.J. (1994). Direct sequencing of terminal regions of genomic P1 clones : A general strategy for the design of sequence-tagged site markers. *Genetic Analysis, Techniques and Applications*, **11**, 117-128.

Kish, S.J., Shannak, K. and Hornykiewicz, O. (1988). Uneven pattern of dopamine loss in the striatum of patients with idiopathic Parkinsons-disease - Pathophysiologic and clinical implications. *New England Journal of Medicine*, **318**, 876-880.

Knopf, J.L., Lee, M.H., Sultzman, L.A., Kriz, R.W., Loomis, C.R., Hewick, R.M. and Bell, R.M. (1986). Cloning and expression of multiple Protein Kinase C cDNAs. *Cell*, **46**, 491-502.

Kondo, Y., Mori, M., Kuramoto, T., Yamada, J. and Beckmann, J.S. (1993). DNA segments mapped by reciprocal use of microsatellite primers between mouse and rat. *Mammalian Genome*, **4**, 571-576.

Kosambi, D.D. (1994). The estimation of map distances from recombination values. *Annuals of Eugenics*, **12**, 172-175.

Kumar, R., Agarwal, A.K. and Seth, P.K. (1995). Free radical-generated neurotoxicity of 6-hydroxydopamine. *Journal of Neurochemistry*, **64**, 1703-1707.

Lam, A., Campbell, J.M., Bennett, N.K., Payne, A.P., Davies, R.W., Sutcliffe, R.G. amd McCulloch, J. Local cerebral glucose utilisation in the AS/AGU rat; A mutant with movement disorders. *European Journal of Neurobiology* (submitted).

Lane, J.D., Nadi, N.S., McBride, W.J., Apriso, M.H. and Kusano, K. (1977). Contents of serotonin, norepineephrine and dopamine in the cerebrum of the "staggerer", "weaver" and "nervous" neurologically mutant mice. *Journal of Neurochemistry*, **29**, 349-350.

Langston, J.W., Ballard, P., Tetrud, J.W. and Irwin, I. (1983). Chronic Parkinsonism in humans due to a product of Meperidine-analog synthesis. *Science*, **219**, 979-980.

Langston, J.W. (1996). The etiology of Parkinson's disease with emphasis on the MPTP story. *Neurology*, **47** (Suppl.3.), S153-S160.

Lanièce, P., Le Hir, H., Bodeau-Péan, S. Charon, Y., Valentin, L., Thermes, C., Mallet, J. and Dumas, S. (1996). A novel rat tyrosine hydroxylase mRNA species generated by alternative splicing. *Journal of Neurochemistry*, **66**, 1819-1825.

Lazzarini, A.M., Myers, R.H., Zimmerman, T.R., Mark, M.H., Golbe, L.I., Sage, J.I., Johnson, W.G. and Duvoisin, R.C. (1994). A clinical genetic study of Parkinson's disease : Evidence for dominant transmission. *Neurology*, **44**, 499-506.

Le Bourdellès, B., Horellou, P., Le Caer, J.P., Denèfle, P., Latta, M., Haavik, J., Guibert, B., Mayaux, J.F. and Mallet, J. (1991). Phosphorylation of human recombinant tyrosine hydroxylase isoforms 1 and 2: An additional phosphorylated residue in isoform 2, generated through alternative splicing. *Journal of Biological Chemistry*, **266**, 17124-17130.

Lesch, K.P., Balling, U., Seeman, M., Teufel, A., Bengel, D., Heils, A., Godeck, P. and Riederer, P. (1997). Molecular heterogeneity of neurotransporters: Implications for neurodegeneration. *Journal of Neural Transmission* - Supplement, **49**, 155-167.

Lovett, M., Kere, J.H. and Hinton, L.M. (1991). Direct selection - A method for the isolation of cDNAs encoded by large genomic regions. *Proceedings of the National Academy of Sciences of the USA*, **88**, 9628-9632.

Makino, Y., Tasaki, Y., Ohta, S. and Hirobe, M. (1990). Confirmation of the enantiomers of 1-methyl-1,2,3,4,-tetrahydroisoquinoline in the mouse brain and foods applying gas-chromatography, mass-spectrometry with neagtive-ion chemical ionization. *Biomedical and Environmental Mass spectrometry*, **19**, 415-419.

Makino, Y. Ohta, S., Tasaki, Y., Tachikawa, O., Kashiwasake, M. and Hirobe, M. (1990). A novel and neurotoxic tetrahydroisoquinoline derivative in vivo - formation of 1,3-dimethyl-1,2,3,4-tetrahydroisoquinoline, a condensation product of amphetamines, in brains of rats under chronic ethanol treatment. *Journal of Neurochemistry*, **55**, 963-969.

Makowski, E.C. and Ordonez, L.A. (1981). Behavioral alterations induced by formaldehyde-derived tertahydroisoquinolones. *Pahrmocology, Biochemistry and Behaviour*, **14**, 639-643.

Malo, D., Gros, P., Bergmann, A., Trask, B., Mohrenweiser, H.W., Canfield, V.A. and Levenson, R. (1993). Genes encoding the H, K-ATPase alpha and Na, K-ATPase alpha 3 subunits are linked on mouse chromsome 7 and human chromosome 19. *Mammalian Genome*, **4**, 644-649.

Maraganore, D.M., Harding, A.E. and Marsden, C.D. (1991). A clinical and genetic study of familial Parkinson's disease. *Movement Disorders*, **8**, 205-211.

Marder, K., Tang, M.X., Mejia, H., Alfaro, B., Cote, L., Louis, E., Groves, J. and Mayeux, R. (1996). Risk of Parkinson's disease among first degree relatives - A community-based study. *Neurology*, **47**, 155-160.

Maroteaux, L., Campanelli, J.T. and Scheller, R.H. (1988). Synuclein: A neuron-specific protein localized to the nucleus and presynaptic nerve terminal. *Journal of Neuroscience*, **8**, 2804-2815.

Maroteuax, L. and Scheller, R.H. (1991). The rat brain synucleuins; A family of proteins transiently associated with neuronal membrane. *Molecular Brain Research*, **11**, 335-343.

Martin, T.F.J. (1997). Stages of regulated exocytosis. *Trends in Cell Biology*, **7**, 271-276.

Marttila, R.J., Kaprio, J., Koskenvuo, M. and Rinne, U.K. (1988). Parkinson's disease in a nationwide twin cohort. *Neurology*, **38**, 1217-1219.

Maroteaux, L., Campanelli, J.T. and Scheller, R.H. (1988). Synuclein: A neuron-specific protein localized to the nucleus and presynaptic nerve terminal. *Journal of Neuroscience*, **8**, 2804-2815.

Maroteaux, L. and Scheller, R.H. (1991). The rat synucleins; family of proteins transiently associated with neuronal membrane. *Molecular Brain Research*, **11**, 335-343.

McCallion, A.S. (1997). Characterisation and genetic mapping of genes with potential involvement in neurodenerative disease. PhD thesis, University of Glasgow.

Melamed, E. (1992). Biochemical and functional differences between dopamine formed from endogenous tyrosine and exogenous L-Dopa in nigrostriatal dopaminergic neurons. *Neurochemistry International*, **20**, SS, S115-S117.

Miller, K.G., Alfonso, A., Nguyen, M., Crowell, J.A., Johnson, C.D. and Rand, J.B. (1996). A genetic selection for Caenorhabditis-elegans synaptic transmission mutants. *Proceedings of the National Academy of Sciences USA.*, **93**, 12593-12598.

Mizuno, Y., Ohta, S., Tanaka, M., Takamiya, S., Suzuki, K., Sato, T., Oya, H., Ozawa, T. and Kagawa, Y. (1989). Deficiences in Complex I subunits of the respiratory chain in Parkinson's disease. *Biochemical and Biophysical Research Communications*, **163**, 1450-1455.

Nezu, J., Motojima, K, Tamura, H. and Ohkuma, S. (1992). Molecular cloning of a rat liver cDNA encoding the 16 kDa subunit of vacuolar H^+-ATPases : Organellar and tissue distribution of 16 kDa proteolipids. *Journal of Biochemistry*, **112**, 212-219.

Nussbaum, R.L. and Polymeropoulos, M.H. (1997). Genetics of Parkinson's disease. *Human Molecular Genetics*, **6**, 1687-1691.

Oestreicher, E., Sengstock, G.J., Riederer, P., Olanow, C.W., Dunn, A.J. and Arendash, G.W. (1994). Degeneration of nigrostriatal dopaminergic neurons increases

iron within the substantia nigra: a histochemical and neurochemical study. *Brain Research*, **660**, 8-18.

Olanow, C.W. (1990). Oxidation reactions in Parkinson's disease. *Neurology*, **40**, 32-37.

Ono, Y., Kurokawa, T., Kawahara, K., Nishimura, O. and Marumoto, R. (1986). Cloning of rat brain protein kinase C complementary DNA. *FEBS Letters*, **203**, 111-115.

Orita, M., Iwahana, H., Kanazawa, H., Hayashi, K., and Sekiya, T. (1989). Detection of polymorphisms of human DNA by gel electrophoresis as single-strand conformation polymorphisms. *Proceedings of the National Academy of Science of the USA*, **86**, 2766-2770.

Parimoo, S., Patanjali, S.R., Shukla, H., Chaplin, D.D. and Weissman, S. M. (1991). cDNA selection : Efficient PCR approach for the selection of cDNAs encoded in large chromosomal DNA fragments. *Proceedings of the National Academy of Science of the USA*, **88**, 9623-9627.

Patel, N., Cox, D.R., Bhat, D., Faham, M., Myers, R.M. and Peterson, A.S. (1995). A potassium channel mutation in weaver mice implicates membrane excitability in granule cell differentiation. *Nature Genetics*, **11**, 126-129.

Payami, H., Bernard, S., Larsen, K., Kaye, J. and Nutt, J. (1995). Genetic anticipation in Parkinson's disease. *Neurology*, **45**, 135-138.

Perry, T.L., Godin, D.V. and Hansen, S. (1982). Parkinson's disease: a disorder due to nigral glutathione deficiency. *Neuroscience Letters*, **33**, 305-310.

Pierce, J.C. and Sternberg, N.L. (1992). Using bacteriophage P1 system to clone high molecular weight genomic DNA. *Methods in Enzymology*, **216**, 549-574.

Pierce, J.C., Stauer, B. and Sternberg, N.L. (1992). A positive selection vector for cloning high molecular weight DNA by the bacteriophage P1 system: Improved cloning efficacy. *Proceedings of the National Academy of Science of the USA.*, **89**, 2056-2060.

Polymeropoulos, M.H., Higgins,J.J., Golbe, L.I., Johnson, W.G., Ide, S.E., Iorio, G. D., Sanges, G., Stenroos, E.S., Pho, L.T., Schaffer, A.A., Lazzarini, A.M.,

Nussbaum, R.L. and Duvoisin, R. C. (1996). Mapping of a gene for Parkinson's disease to chromosome 4q21-q23. *Science*, **274**, 1197-1199.

Polymeropoulos, M.H., Lavedan, C., Leroy, E., Ide, S.E., Dehejia, A., Dutra, A., Pike, B., Root, H., Rubenstein, J., Boyer, R., Stenroos, E.S., Chandrasekharappa, S., Athanassiadou, A., Papapetropoulos, T., Johnson, W.G., Lazzarini, A.M., Duvoisin, R.C., Iorio, G.D., Golbe, L.I. and Nussbaum, R.L. (1997). Mutation in the α-Synuclein gene identified in families with Parkinson's disease. *Science*, 276, 2045-2047.

Pollanen, M.S. Bergeron, C. and Weyer, L. (1992). Detergent-insoluble cortical Lewy body fibrils share epitopes with neurofilament and tau. *Journal of Neurochemistry*, **58**, 1953-1956.

Ponzio, F., Achilli, G., Perego, C., Rinaldi, G. and Algeri, S. (1983). Does acute L-Dopa increase active release of dopamine from dopaminergic-neurons. *Brain Research*, **273**, 45-51.

Raastad, M., Strom, J.F. and Andersen, P. (1992). Putative single quantum and single fiber excitatory postsynaptic currents show similar amplitude range and variability in rat hippocampal slices. *European Journal of Neuroscience*, **4**, 113-117.

Rosenthal, A., Rhee, L., Yadegari, R., Paro, R., Ullrich, A. and Goeddel, D.V. (1987). Structure and nucleotide sequence of a *Drosophila melanogaster* protein kinase C gene. *The EMBO Journal*, **6**, 433-441.

Rosenmund, C., Clements, J.D. and Westbrook, G.L. (1993). Release probability at excitatory synapses on cultured hippocampal neurons. *Biophysical Journal*, **64**, A327.

Saito, N., Kikkawa, U., Nishizuka, Y. and Tanaka, C. (1988). Distribution of protein kinase C-like immunoreactive neurons in rat brain. *Journal of Neuroscience*, **8**, 369-382.

Sakai, K. and Gash, D.M. (1994). Effect of bilateral 6-OHDA lesions of the substantia nigra on locomotor activity in the rat. *Brain Research*, **633**, 144-150.

Sandy, M.S., Armstrong, M., Tanner, C.M. Daly, A.K., Dimonte, D.A., Langston, J.W. and Idle, J.R. (1996). CYP2D6 allelic frequencies in young-onset Parkinson's disease. *Neurology*, **47**, 225-230.

Sambrook, J., Fritsch E.F. and Maniatis, T. (1989). Molecular Cloning-A laboratory manual. Cold Spring Harbour Laboratory Press. 2nd edition.

Scalzi, J.M. and Hozier, J.C. (1998). Comparitive genome mapping : Mouse and rat homologies revealed by fluorescence *in situ* hybridisation. *Genomics*, **47**, 44-51.

Schapira, A.H.V. , Cooper, J.M., Dexter, D., Jenner, P., Clark, J.B. and Marsden, C.D. (1989). Mitochondrial complex I deficiency in Parkinson's disease. *The Lancet*, **1**, 1269.

Schwartz, D.C. and Cantor, C.R. (1984). Separation of yeast chromosome-sized DNAs by Pulsed Field Gradient Gel electrophoresis. *Cell*, **37**, 67-75.

Scott, D.L., Campbell, J.M., McGadey, J., Clarke, D.J., Gilmore, D.P. and Payne, A.P. (1994). Noradrenergic deficits in the locus coeruleus of AS/AGU rats. *European Journal of Neuroscience*, Suppl. **7**, 96.

Seeman, P. and Vantol, H.H.M (1994). Dopamine receptor pharmacology. *Trends in Pharmacological Sciences*, **15**, 264-270.

Sengstock, G.J., Olanow, C.W., Menzies, R.A., Dunn, A.J. and Arendash, G.W. (1993). Infusion of iron into the rat substantia-nigra - Nigral pathology and dose-dependent loss of striatal dopaminergic markers. *Journal of Neuroscience Research*, **35**, 67-82.

Serikawa, T., Kuramoto, T., Hilbert, P., Mori, M., Yamada, J., Dubay, C.J., Lindpainter, K., Ganten, D., Guénet, J., Lathrop, G.M. and Beckmann, J.S. (1992). Rat gene mapping using PCR-analysed microsatellites. *Genetics*, **131**, 701-721.

Shiels, P., Durán Alonso, M.B., Davidson, A.O., Heeley, R.P., Dominiczak, A.F., Payne, A.P., Davies, R.W. and Sutcliffe, R.G. (1995). Optimized protocols for typing 75 microsatellite loci in AS, PVG, F344 and BN rats. *Mammalian Genome*, **6**, 214-215.

Shoffner, J.M., Brown, M.D., Torroni, A., Lott, M.T., Cabell, M.F., Mirra, S.S., Beal, M.F., Yang, C.C., Gearing, M., Salvo, R., Watts, R.L., Juncos, J.L., Hansen, L.A., Crain, B.J., Fayad, M., Reckford, C.L. and Wallace, D.C. (1993). Mitochondrial-DNA variants observed in Alzheimer-disease and Parkinson disease patients. *Genomics*, **1**, 171-184.

Shull, G.E. and Lingrel, J.B. (1986). Molecular cloning of the rat stomach (H^++K^+)-ATPase. *Journal of Biological Chemistry*, **261**, 16788-16791.

Silver, L.M. (1995). Mouse genetics: Concepts and applications. Oxford University Press.

Simckes, A.M., Giambrone, S.A., Dowler, L.L. and White, R.A. (1996). Mapping and characterisation of the vacuolar H(+)ATPase (V-H-ATPase) subunit in mouse. *Pediatric Research* , **39**, 2202.

Singer, T.P., Castagnoli, N. Jr., Ramsay, R.R., Trevor, A.J. (1987). Biochemical events in the development of parkinsonism induced by 1-methyl-4-phenyl-1,2,5,6,-tetrahydropyridine. *Journal of Neurochemistry*, **49**, 1-8.

Slesinger, P.A., Patil, N., Liao, Y.J., Jan, Y.N., Jan, L.Y. and Cox, D.R. (1996). Functional effects of the mouse *weaver* mutation on G protein-gated inwardly rectifying K^+ channels. *Neuron*, **16**, 321-331.

Sofic, E. Paulus, W., Jellinger, K., Riederer, P. and Youdim, M.B.H. (1991). Selective increase of iron in substantia nigra zona compacta of Parkinsonian brains. *Journal of Neurochemistry*, **56**, 978-982,

Sofic, E., Lange, K.W. and Riederer (1992). Reduced and oxidised glutathione in the substantia nigra of patients with Parkinson's disease. *Neuroscience Letters*, **142**, 128-130.

Southard-Smith, M., Pierce, J.C. and MacDonald, R.J. (1994). Physical mapping of the rat tissue kallikrien family in two gene clusters by analysis of P1 bacteriophage clones. *Genomics*, **22**, 404-417.

Spillantini, M.G., Schmidt, M.L., Lee, V.M.-Y., Trojanowski, J.Q., Gakes, R. and Goedert, M. (1997). α-Synuclein in Lewy bodies. *Nature*, **388**, 839-840.

Spina, M.B. and Cohen, G. (1989). Dopamine turnover and glutathione oxidation - Implications for Parkinson's disease. *Proceedings of the National Academy of Sciences of the USA*, **86**, 1398-1400.

Stallings, R.L., Ford, A.F., Nelson, D., Torney, D.C., Hildebrand, C.E. and Moyzis, R.K. (1991). Evolution and distribution of $(GT)_n$ repetitive sequences in mammalian genomes. *Genomics*, **10**, 807-815.

Sternberg, N.L. (1992). Cloning high molecular weight DNA fragments by the bacteriophage P1 system. *Trends in Genetics*, **8**,

Sternberg, N.L., Smoller, D. and Braden, T. (1994). Three new developments in P1 cloning : Increased cloning effeciency, improved clone recovery and a new P1 mouse library. *GATA*, **11**, 171-180.

Stubbs, L., Carver, E.A., Shannon, M.E., Kim, J., Geisler, J., Generoso, E.E., Stanford, B.G., Dunn, W.C., Mohrenweiser, H., Zimmerman, W., Watt, S.M. and Ashworth, L.K. (1996). Detailed comparitive map of human chromosome 19q and related regions of the mouse genome. *Genomics*, **35**, 499-508.

Südhof, T.C. (1995). The synaptic vesicle cycle: a cascade of protein-protein interactions. *Nature*, **375**, 645-653.

Sun, H.S. and Kirkpatrick, B.W. (1996). Exploiting dinucleotide microsatelittes conserved among mammalian species. *Mammalian Genome*, **7**, 128-132.

Sundstrom, E. and Samuelsson, E.B. (1997). Comparison of key steps in 1-methyl-4-phenyl-1,2,4,6-tetrahydrpyridine (MPTP) neurotoxicity in rodents. *Pharmacology and Toxicology*, **81**, 226-231.

Schwartz, D C. and Cantor, C.R. (1984) Seperation of yeast chromosome-sized DNAs by pulsed field gradient gel electrophoresis. *Cell*, **37**, 67-75.

Szpirer, C., Molné, M., Antonacci, R., Jenkins, N. A., Finelli, P., Szpirer, J., Riviere, M., Rocchi, M., Gilbert, D.J., Copeland, N.G. and Gallo,V. (1994). The genes encoding the glutamate receptor subunits KA1 and KA2 (GRIK4 and GRIK5) are located on separate chromosomes in human, mouse and rat. *Proceedings of the National Academy of Science of the USA.*, **91**, 11849-11853.

Szpirer, C., Szpirer, J., Tissir, F., Stephanova, E., Vanvooren, P., Kurtz, T.W., Iwai, N., Inagami, T., Pravenec, M., Kren, V., Klinga-Levan, K. and Levan, G. (1997). Rat chromosome 1: regional localization of seven genes (*Slc9a3*, *Srd5a1*, *Esr*, *Tcp1*, *Grik5*, *Tnnt3*, *Jak2*) and anchoring of the genetic linkage map to the cytogenetic map. *Mammalian Genome*, **8**, 657-660.

Tanaka, Y., Murayama, N., Tsukamoto, K., Mizuno, Y., Sano, A. and Kondo, I. (1993). Genetic susceptibility to the Parkinson disease. *American Journal of Human Genetics*,

Tanaka, C. and Nishizuka, Y. (1994). The protein kinase C family for neuronal signalling. *Annual Review of Neuroscience*, **17**, 551-567.

Tanner, C.M. (1989). The role of environmental neurtoxins in the eitiology of Parkinson's disease. *Trends in Neurosciences*, **12**, 49-54.

Taussig, D., Planté-Bordeneuve, V. and Trassard, O. (1995). Genetic study of dopaminergic transmission in Parkinson's disease. *Neurology*, **45** (Suppl.4), A316.

Tipton, K.F and Singer, T.P. (1993). Adavnces in our understanding of the mechanisms of the neurotoxicity of MPTP and related compounds. *Journal of Neurochemistry*, **61**, 1191-1206.

Triarhou, L.C., Norton, J. and Ghetti, B. (1988). Mesencepahlic dopamine cell deficit involves areas A8, A9 and A10 in weaver mutant mice. *Experimental Brain Research*, **70**, 256-265.

Triggs, W.J. and Willmore, L.J. (1984). *In vivo* lipid peroxidation in rat brain following intracortical Fe2+ injection. *Journal of Neurochemistry*, **42**, 976-980.

Vaughan, R.A., Huff, R.A., Uhl, G.R. and Kuhar, M.J. (1997). Protein kinase C-mediated phosphorylation and functional regulation of dopamine transporters in striatal synptosomes. *Journal of Biological Chemistry*, **272**, 15541-15546.

Wada, M., Abe, K., Okumura, K., Taguchi, H., Kohno, K., Imamoto, F., Schlessinger, D. and Kuwano, M. (1994). *Nucleic Acids Research*, **22**, 1651-1654.

Ward, C.D., Duvoisin, R.C., Ince, S.E., Nutt, J.D., Eldrige, R. and Calne, D.B. (1983). Parkinon's disease in 65 pairs of twins and in a set of quadruplets. *Neurology*, **33**, 815-824.

Watts, R.L. and Mandir, A.S. (1992). The role of motor cortex in the pathophysiology of voluntary movement deficits associated with parkinsonism. *Neurologic Clinics*, **10**:2, 451-469.

Weinreb, P.H., Zhen, W.G., Poon, A.W., Conway, K.A. and Lansbury, P.T. (1996). NACP, a protein implicated in Alzeimers-disease and learning, is natively unfolded. *Biochemistry*, **35**, 13709-13715.

Wilhelmsen, K., Mirel, D., Marder, K., Bernstein, M., Naini, A., Leal, S.M., Cote, L.J., Tang, M.X., Freyer, G , Graziano, J. and Mayeux, R. (1997). Is there a genetic susceptibility locus of Parkinson's disease on chromosome 22q13. Annals of *Neurology*, **41**, 813-817.

Worwood, M., Brook, J.D., Cragg, S.J., Hellkuhl, B., Jones, B.M., Perera, P., Roberts, S.H. and Shaw, D.J. (1985). Assignment of human ferritin genes to chromosomes 11 and chromosome 19q13.3-19qter. *Human Genetics*, **69**, 371-374.

Yamada, J., Kuramoto, T. and Serikawa, T. (1994). A rat genetic linkage map and comparitive maps for mouse or human homologous genes. *Mammalian Genome,* **5**, 63-68

Yoshihara, C., Saito, N., Taniyama, K. and Tanaka, C. (1991). Different localisation of four subspecies of protein kinase C in the rat striatum and substantia nigra. *Journal of Neuroscience*, **11**, 690-700.

Zigmond, M.J., Abercrombie, E.D., Berger, T.W., Grace, A.A. and Stricker, E.M. (1990). Compensations after lesions of central dopaminergic neurons: some clinical and basic implications. *Trends in Neuroscience*, **7**, 290-296.

Zimmerman, T.R., Bhatt, M., Calne, D.B. and Duvoisin, R.C. (1991). Parkinson's disease in monozygotic twins : A follow-up. *Neurology*, **41** (Suppl.1), 255.

Appendices

Appendix 1 - Genotyping of F344 X AS/AGU backcross progeny with the marker GU10.

Animal number	Phenotype	Genotyping with marker GU10 primers	Genotype at the GU10 locus
F115-95	W	2	P
F116-95	W	2	P
F127-95	W	2	P
F143-95	μ	2	**Recombinant**
F154-95	W	2	P
F163-95	μ	1	P
F179-95	W	2	P
F193-95	μ	1	P
F197-95	μ	1	P
F199-95	W	1	**Recombinant**
F200-95	μ	1	P
F256-95	μ	2	**Recombinant**
F257-95	μ	1	P
F258-95	W	2	P
F259-95	μ	1	P
F262-95	μ	1	P
F277-95	μ	1	P
F297-95	W	2	P
F302-95	μ	1	P
F310-95	μ	2	**Recombinant**
F322-95	μ	1	P
F331-95	μ	1	P
F333-95	W	2	P
F344-95	W	2	P
F343-95	W	2	P
F344-95	W	2	P
F348-95	W	2	P
F367-95	μ	1	P
F374-95	W	1	**Recombinant**
F383-95	μ	2	**Recombinant**

F384-95	μ	1	P
F387-95	W	2	P
F389-95	W	2	P
F390-95	μ	1	P
F394-95	W	2	P
F397-95	W	2	P
F438-95	μ	1	P
F440-95	μ	1	P
F441-95	μ	1	P
F442-95	μ	1	P
F443-95	μ	1	P
F444-95	μ	1	P
F446-95	μ	1	P
F448-95	W	2	P
F449-95	W	2	P
F450-95	W	2	P
F451-95	μ	1	P
F453-95	W	2	P
F454-95	W	2	P
F455-95	μ	1	P
F456-95	μ	1	P
F457-95	W	1	**Recombinant**
F458-95	μ	1	P
F459-95	μ	1	P
F460-95	μ	1	P
F465-95	W	2	P
F466-95	μ	1	P
F469-95	μ	1	P
F472-95	W	2	P
F485-95	W	2	P
F486-95	W	2	P
F487-95	W	2	P
F489-95	W	2	P
F490-95	W	2	P
F493-95	W	2	P
F494-95	μ	1	P
F495-95	W	2	P
F498-95	W	2	P

F499-95	μ	1	P
F500-95	W	2	P
F501-95	μ	1	P
F511-95	μ	1	P
F512-95	μ	1	P
F513-95	W	2	P
F514-95	μ	1	P
F515-95	μ	1	P
F516-95	W	2	P
F517-95	W	2	P
F518-95	μ	1	P
F519-95	μ	1	P
F520-95	W	2	P
F525-95	W	2	P
F526-95	W	2	P
F655-95	μ	1	P
F656-95	W	2	P
F657-95	W	2	P
F660-95	W	2	P
F661-95	μ	1	P
F663-95	W	2	P
F664-95	W	2	P
F666-95	W	2	P
F667-95	W	2	P
F668-95	W	2	P
F669-95	W	2	P
F671-95	μ	2	**Recombinant**
F672-95	μ	1	P
F673-95	μ	1	P
F674-95	μ	2	**Recombinant**
F675-95	W	2	P
F676-95	μ	1	P
F677-95	W	2	P
F678-95	μ	1	P
F679-95	W	2	P
F680-95	μ	1	P
F682-95	W	2	P
F683-95	μ	1	P

F684-95	W	2	P
F685-95	μ	1	P
F686-95	W	2	P
F687-95	W	2	P
F692-95	W	2	P
F693-95	W	2	P
F694-95	μ	1	P
F695-95	W	2	P
F696-95	W	2	P
F697-95	W	2	P
F698-95	μ	1	P
F699-95	μ	1	P
F700-95	μ	1	P
F701-95	μ	1	P
F702-95	W	2	P
F703-95	W	2	P
F704-95	W	2	P
F705-95	W	2	P
F706-95	W	2	P
F707-95	μ	1	P
F708-95	W	2	P
F709-95	W	2	P
F710-95	μ	1	P
F711-95	μ	1	P
F712-95	μ	1	P
F729-95	W	2	P
F730-95	W	2	P
F732-95	μ	1	P
F733-95	W	2	P
F734-95	W	2	P
F735-95	W	2	P
F736-95	W	2	P
F738-95	W	2	P
F748-95	W	2	P
F749-95	μ	1	P
F750-95	μ	1	P
F751-95	μ	1	P
F752-95	W	2	P

F753-95	W	2	P
F754-95	W	2	P
F756-95	μ	1	P
F757-95	W	2	P
F774-95	W	2	P
F775-95	W	2	P
F776-95	W	2	P
F777-95	W	2	P
F778-95	W	2	P
F779-95	W	1	**Recombinant**
F781-95	W	1	**Recombinant**
F782-95	W	2	P
F783-95	μ	1	P
F785-95	μ	1	P
F786-95	W	2	P
F795-95	μ	1	P
F796-95	μ	1	P
F797-95	W	2	P
F801-95	W	2	P
F802-95	W	2	P
F803-95	W	2	P
F804-95	W	2	P
F805-95	W	2	P
F806-95	W	2	P
F810-95	μ	2	**Recombinant**
F811-95	μ	1	P
F812-95	W	2	P
F815-95	W	2	P
F822-95	μ	1	P
F823-95	μ	1	P
F824-95	W	2	P
F825-95	μ	1	P
F826-95	μ	1	P
F827-95	W	2	P
F830-95	μ	1	P
F831-95	μ	1	P
F851-95	W	2	P
F852-95	W	2	P

F853-95	W	2	P
F854-95	μ	1	P
F855-95	W	2	P
F857-95	μ	1	P
F859-95	μ	1	P
F860-95	μ	1	P
F862-95	μ	1	P
F863-95	W	2	P
F864-95	W	2	P
F865-95	W	2	P
F866-95	W	2	P
F881-95	W	2	P
F882-95	μ	1	P
F883-95	μ	1	P
F885-95	μ	1	P
F886-95	μ	1	P
F887-95	μ	1	P
F889-95	μ	1	P
F890-95	μ	1	P
F892-95	W	2	P

Table A.1 Genotyping data from marker GU10 with progeny from the F344 X AS/AGU backcross. The first column indicates the animal number, the second the animal phenotype; W = wild type phenotype, μ = indicates the mutant phenotype. The third column indicates the genotyping data from the primers specifiying the GU10 locus; with 2 indicating heterozygote (2 bands) and 1 indicating homozygote (1 band). The final column indicates the genotype of the animal at the GU10 locus with P = parental allele at the locus (no cross-over between the *agu* and the GU10 locus) and Recombinant = indicating a recombinant allele (a cross-over event between the *agu* and the GU10 locus).

Appendix 2 - Genotyping of BN X AS/AGU backcross progeny with the marker D1Mgh7.

Animal number	Phenotype	Genotype at D1Mgh7 locus	Genotype
127-94	W	1	**Recombinant**
128-94	W	1	**Recombinant**
129-94	μ	1	P
130-94	μ	1	P
131-94	μ	1	P
138-94	W	1	**Recombinant**
142-94	W	2	P
143-94	μ	1	P
144-94	W	2	P
145-94	μ	1	P
146-94	μ	2	**Recombinant**
147-94	W	2	P
149-94	W	2	P
150-94	μ	1	P
181-94	W	2	P
183-94	W	2	P
184-94	W	2	P
185-94	W	2	P
186-94	W	2	P
187-94	μ	1	P
188-94	μ	1	P
189-94	W	2	P
190-94	μ	1	P
191-94	W	2	P
193-94	W	2	P
195-94	W	2	P
196-94	W	1	**Recombinant**
197-94	W	2	P
198-94	W	1	**Recombinant**
199-94	W	2	P
200-94	W	1	**Recombinant**
201-94	W	1	**Recombinant**

202-94	μ	1	P
203-94	W	2	P
204-94	μ	1	P
205-95	μ	2	**Recombinant**
206-94	μ	2	**Recombinant**
207-94	μ	1	P
208-94	μ	2	**Recombinant**
209-94	μ	2	**Recombinant**
210-94	W	2	P
212-94	μ	1	P
213-94	μ	1	P
214-94	W	2	P
215-94	W	2	P
216-94	W	1	**Recombinant**
217-94	W	1	**Recombinant**
218-94	W	2	P
219-94	W	2	P
220-94	μ	2	**Recombinant**
222-94	μ	2	**Recombinant**
223-94	μ	1	P
232-94	W	2	P
239-94	μ	1	P
240-94	W	2	P
241-94	W	1	**Recombinant**
242-94	μ	2	**Recombinant**
243-94	W	1	**Recombinant**
244-94	μ	2	**Recombinant**
245-94	μ	2	**Recombinant**
246-94	W	2	P
247-94	μ	2	**Recombinant**
248-94	μ	1	P
249-94	μ	2	**Recombinant**
250-94	μ	1	P
251-94	W	1	**Recombinant**
252-94	W	2	P
253-94	μ	1	P
254-94	μ	1	P
255-94	W	2	P

256-94	W	2	P
257-94	W	2	P
258-94	W	2	P
306-94	μ	1	P
309-94	W	2	P
314-94	μ	1	P
317-94	μ	1	P
325-95	μ	1	P
329-94	μ	1	P
335-94	μ	2	**Recombinant**
336-94	μ	1	P
337-94	μ	1	P
338-94	μ	1	P
339-94	W	2	P
340-94	W	2	P
341-94	μ	1	P
342-94	W	2	P
343-94	W	2	P
344-94	W	2	P
354-94	W	2	P
346-94	W	2	P
347-94	W	2	P
348-94	μ	1	P
349-94	W	2	P
350-94	μ	1	P
351-94	μ	1	P
352-94	W	1	**Recombinant**
364-94	μ	1	P
366-94	μ	2	**Recombinant**
367-94	W	2	P
368-94	μ	1	P
369-94	μ	1	P
370-94	W	2	P
371-94	W	2	P
372-94	W	2	P
373-94	μ	1	P
374-94	μ	1	P
375-94	W	2	P

376-94	W	2	P
377-94	μ	1	P
378-94	W	2	P
379-94	μ	1	P
380-94	W	2	P
381-94	μ	2	**Recombinant**
382-94	μ	1	P
383-94	μ	1	P
384-94	μ	1	P
385-94	μ	1	P
386-94	W	2	P
387-94	W	2	P
388-94	μ	2	**Recombinant**
389-94	W	2	P
418-94	W	2	P
419-94	μ	1	P
420-94	μ	1	P
421-94	W	2	P
422-94	μ	1	P
423-94	μ	2	**Recombinant**
424-94	W	2	P
425-94	W	2	P
426-94	μ	2	**Recombinant**
427-94	μ	1	P
428-94	W	2	P
429-94	W	2	P
430-94	W	2	P
431-94	W	2	P
432-94	μ	2	**Recombinant**
433-94	W	2	P
434-94	W	2	P
436-94	μ	2	**Recombinant**
437-94	W	2	P
438-94	W	2	P
439-94	W	1	**Recombinant**
440-94	W	1	**Recombinant**
441-94	μ	1	P
442-94	μ	1	P

443-94	W	1	**Recombinant**
447-94	μ	2	**Recombinant**
451-94	W	2	P
453-94	μ	1	P
454-94	W	2	P
455-94	W	1	**Recombinant**
456-94	W	2	P
457-94	μ	1	P
458-94	W	2	P
460-94	μ	2	**Recombinant**
461-94	μ	2	**Recombinant**
462-94	μ	1	P
463-94	μ	2	**Recombinant**
464-94	μ	2	**Recombinant**
465-94	μ	1	P
467-94	μ	1	P
469-94	μ	2	**Recombinant**
470-94	μ	1	P
471-94	μ	2	**Recombinant**
473-94	W	2	P
474-94	W	2	P
476-94	W	1	**Recombinant**
511-94	W	2	P
512-94	μ	1	P
513-94	μ	1	P
514-94	μ	1	P
515-94	μ	1	P
516-94	W	1	**Recombinant**
517-94	W	2	P
518-94	W	2	P
519-94	W	2	P
520-94	W	1	**Recombinant**
527-94	W	2	P
528-94	W	2	P
529-94	W	2	P
530-94	W	1	**Recombinant**
531-94	W	1	**Recombinant**
532-94	W	2	P

533-94	μ	1	P
534-94	W	1	**Recombinant**
535-94	W	2	P
536-94	W	2	P
537-94	W	2	P
538-94	W	1	**Recombinant**
539-94	W	2	P
540-94	W	2	P
541-94	W	1	**Recombinant**
542-94	W	2	P
543-94	W	2	P
544-94	μ	1	P
545-95	W	2	P
546-94	W	2	P
547-94	W	2	P
548-94	W	2	P
549-94	μ	1	P
550-94	μ	2	**Recombinant**
551-94	W	2	P
553-94	μ	1	P
554-94	μ	1	P
555-94	W	2	P
556-94	W	2	P
557-94	μ	2	**Recombinant**
558-94	μ	1	P
559-94	μ	1	P
560-94	W	2	P
561-94	μ	2	**Recombinant**
562-94	μ	1	P
563-94	μ	1	P
564-94	μ	1	P
565-94	W	2	P
566-94	W	2	P
567-94	W	2	P
568-94	W	1	**Recombinant**
578-94	W	2	P
579-94	μ	2	**Recombinant**
580-94	W	2	P

581-94	μ	1	P
582-94	μ	2	**Recombinant**
583-94	μ	2	**Recombinant**
584-94	μ	1	P
585-94	W	2	P
586-94	W	2	P
587-94	μ	1	P
588-94	W	1	**Recombinant**
589-94	W	2	P
1-95	W	2	P
3-95	W	2	P
4-95	W	2	P
5-95	W	1	**Recombinant**
6-95	W	1	**Recombinant**
7-95	μ	1	P
8-95	W	2	P
9-95	μ	1	P
10-95	W	2	P
11-95	W	2	P
12-95	μ	1	P
13-95	W	2	P
14-95	W	2	P
15-95	μ	1	P
16-95	W	1	**Recombinant**
17-95	μ	1	P
18-95	μ	1	P
19-95	μ	1	P
22-95	W	2	P
23-95	W	2	P
24-95	μ	1	P
25-95	W	2	P
26-95	μ	1	P
29-95	W	2	P
30-95	μ	1	P
31-95	μ	1	P
32-95	μ	1	P
33-95	μ	1	P
34-95	μ	1	P

35-95	W	2	P
36-95	μ	1	P
37-95	W	2	P
40-95	W	2	P
41-95	W	1	**Recombinant**
49-95	μ	1	P
50-95	μ	1	P
51-95	μ	1	P
52-95	μ	1	P
53-95	μ	1	P
65-95	μ	1	P
66-95	W	1	**Recombinant**
67-95	μ	1	P
68-95	W	2	P
69-95	W	2	P
70-95	μ	1	P
71-95	W	2	P
72-95	W	1	**Recombinant**
80-95	W	2	P
81-95	μ	1	P
82-95	μ	1	P
83-95	μ	1	P
84-95	W	2	P
85-95	W	2	P
86-95	W	2	P
88-95	W	2	P
89-95	μ	1	P
90-95	μ	1	P
91-95	W	2	P
92-95	W	2	P
94-95	W	2	P
209-95	W	2	P
211-95	W	2	P
213-95	μ	1	P
214-95	W	1	**Recombinant**
219-95	W	2	P
220-95	μ	1	P
221-95	μ	1	P

222-95	W	1	**Recombinant**
223-95	W	2	P
224-95	W	1	**Recombinant**
225-95	μ	1	P
226-95	μ	1	P
227-95	W	2	P
228-95	μ	2	**Recombinant**
229-95	μ	1	P
232-95	μ	1	P
234-95	μ	1	P
237-95	μ	1	P
253-95	W	2	P
255-95	μ	1	P

Table A.2 Genotyping data from marker D1Mgh7 with progeny from the BN X AS/AGU backcross. The first column indicates the animal number, the second the animal phenotype; W = wild type phenotype, μ = indicates the mutant phenotype. The third column indicates the genotyping data from the primers specifiying theD1Mgh7 locus; with 2 indicating heterozygote (2 bands) and 1 indicating homozygote (1 band). The final column indicates the genotype of the animal at the D1Mgh7 locus with P = parental allele at the locus (no cross-over between the *agu* and the D1Mgh7 locus) and Recombinant = indicating a recombinant allele (a cross-over event between the *agu* and the D1Mgh7 locus).

Appendix 3 - Genotyping of BN X AS/AGU backcross progeny with the marker F34.

Animal number	Phenotype	Genotype at F34 locus	Genotype
186-94	W	2	P
216-94	W	2	P
218-94	W	1	**Recombinant**
309-94	W	2	P
317-94	μ	1	P
325-94	μ	2	**Recombinant**
329-94	μ	1	P
339-94	W	2	P
341-94	μ	1	P
342-94	W	2	P
344-94	W	2	P
351-94	μ	2	**Recombinant**
369-94	W	2	P
378-94	W	1	**Recombinant**
380-94	W	1	**Recombinant**
385-94	W	2	P
422-94	μ	2	**Recombinant**
424-94	W	2	P
425-94	W	2	P
427-94	μ	1	P
428-94	W	1	**Recombinant**
430-94	W	1	**Recombinant**
431-94	W	1	**Recombinant**
432-94	μ	2	**Recombinant**
433-94	W	2	P
434-95	W	1	**Recombinant**
436-94	μ	2	**Recombinant**
439-94	W	2	P
440-94	W	2	P
443-94	W	1	**Recombinant**
537-94	W	2	P
540-94	W	1	**Recombinant**
80-95	W	2	P

86-95	W	1	**Recombinant**
88-95	W	2	P
90-95	μ	1	P
209-95	W	2	P
211-95	W	1	**Recombinant**
223-95	W	1	**Recombinant**
224-95	W	1	**Recombinant**
226-95	μ	1	P
228-95	μ	1	P
232-95	μ	2	**Recombinant**
237-95	μ	1	P
306-95	μ	1	P
377-95	μ	2	**Recombinant**
383-95	μ	1	P
548-95	W	1	**Recombinant**

Table A.3 Genotyping data from marker F34 with progeny from the BN X AS/AGU backcross. The first column indicates the animal number, the second the animal phenotype; W = wild type phenotype, μ = indicates the mutant phenotype. The third column indicates the genotyping data from the primers specifiying the F34 locus; with 2 indicating heterozygote (2 bands) and 1 indicating homozygote (1 band). The final column indicates the genotype of the animal at the F34 locus with P = parental allele at the locus (no cross-over between the *agu* and the F34 locus) and Recombinant = indicating a recombinant allele (a cross-over event between the *agu* and the F34 locus).